# Dissecting the roles of mTORC1 and mTORC2 in the mouse heart

**INAUGURALDISSERTATION**

zur Erlangung der Würde eines Doktors der Philosophie

vorgelegt der

Philosophisch-Naturwissenschaftlichen Fakultät

der Universität Basel

Von

**Pankaj Shende**

aus Indien

Basel,

Switzerland, 2013

# creative commons

## Namensnennung-Keine kommerzielle Nutzung-Keine Bearbeitung 2.5 Schweiz

---

### Sie dürfen:

das Werk vervielfältigen, verbreiten und öffentlich zugänglich machen

### Zu den folgenden Bedingungen:

**Namensnennung**. Sie müssen den Namen des Autors/Rechteinhabers in der von ihm festgelegten Weise nennen (wodurch aber nicht der Eindruck entstehen darf, Sie oder die Nutzung des Werkes durch Sie würden entlohnt).

**Keine kommerzielle Nutzung**. Dieses Werk darf nicht für kommerzielle Zwecke verwendet werden.

**Keine Bearbeitung**. Dieses Werk darf nicht bearbeitet oder in anderer Weise verändert werden.

- Im Falle einer Verbreitung müssen Sie anderen die Lizenzbedingungen, unter welche dieses Werk fällt, mitteilen. Am Einfachsten ist es, einen Link auf diese Seite einzubinden.

- Jede der vorgenannten Bedingungen kann aufgehoben werden, sofern Sie die Einwilligung des Rechteinhabers dazu erhalten.

- Diese Lizenz lässt die Urheberpersönlichkeitsrechte unberührt.

---

**Genehmigt von der Philosophisch-Naturwissenschaftlichen Fakultät Auf Antrag von**


Prof. Dr. Michael Hall

Prof. Dr. Marijke Brink

Prof. Dr. Christoph Handschin


Basel, 13th December 2011


Prof. Dr. Martin Spiess

Dekan der Philosophisch-Naturwissenschaftlichen Fakultät

"Dedicated to my Aba"

## List of abbreviations

| | |
|---|---|
| 4E-BP1 | eukaryotic initiation factor (eIF) 4E-binding protein 1 |
| α-SA | α-skeletal actin |
| AC9 | adenylyl cyclase 9 |
| AMPK | cAMP-activated protein kinase |
| ANP | atrial natriuretic peptide |
| β-MHC | β-myosin heavy chain |
| BNP | B-type natriueretic peptide |
| BrDU | bromodeoxyuridine |
| DAG | diacylglycerol |
| Deptor | DEP domain-containing mTOR-interacting protein |
| ECM | extracellular matrix |
| eEF-2k | eukaryotic elongation factor 2 kinase |
| eIF4B | eukaryotic elongation factor 4b |
| ENaC | epithelial sodium channel |
| FAT | FRAP, ATM, and TRRAP |
| FATC | FAT C-terminus |
| FKBP12 | FK506-binding protein 12kDa |
| FoxO1/3 | forkhead box O1/3 |
| FRB | FKBP12-rapamycin binding |
| GAP | GTPase-activating protein |
| GPCR | G-protein coupled receptors |
| GSK | glycogen synthase kinase |
| HIF-1α | hypoxia-inducible factor-1α |
| HM | hydrophobic motif |
| Hsp70 | heat shock protein 70 |
| IGF1 | insulin-like growth factor -1 |
| IKK | inhibitor of nuclear factor NFkB kinase (IkB kinase) |
| ILK | integrin-linked kinase |
| IP3 | inositol triphosphate |
| IRES | internal ribosome entry segment |
| mLST8 | mammalian lethal with SEC13 protein 8, also known as GβL |
| mSIN1 | mammalian stress-activated map kinase-interacting protein 1 |
| mTORC1/2 | mTOR complex 1/2 |
| NDRG1 | N-myc downregulated gene 1 |
| NFAT | nuclear factor of activated T cells |
| PDCD4 | programmed cell death 4 |
| PH domain | pleckstrin homology domain |
| PIKK | phosphatidylinositol kinase-related kinase |
| PIP2 | phosphatidylinositol biphosphate |
| PKA | protein kinase |
| PKC | protein kinase C |
| PKG | protein kinase G |
| PLCβ | phospholipase C-β |

| | |
|---|---|
| PRAS40 | proline-rich AKT substrate 40 kDa |
| Protor/PRR5 | protein observed with TOR/prolin-rich repeat protein-5 |
| Raptor | regulatory-associated protein of mTOR |
| RBD | ras-binding domain |
| REDD1 | regulated in development and DNA damage response 1 |
| RGD peptide | arginine-glycine-aspartic acid containing peptide |
| Rheb | ras-homolog enriched in brain |
| Rictor | rapamycin-insensitive companion of mTOR |
| S6K1 | ribosomal protein S6 kinase 1 |
| SERCA2a | sarcoplasmic reticulum $Ca^{2+}$ ATPase |
| SGK | serum and glucocorticoid-induced kinase |
| SKAR | S6K1 aly/REF-like target |
| SRBP1 | sterol regulatory element-binding protein |
| TCTP | translationally controlled tumor protein |
| TM | turn motif |
| TOP | tract of oligopyrimidine |
| TOR | target of rapamycin |
| TSC | tuberous sclerosis complex |
| YY1 | ying-yang 1 |

# Table of Content

# 1. Summary

Mammalian target of rapamycin (mTOR) is an evolutionary conserved serine/threonine kinase that regulates cell growth and metabolism. mTOR occurs in cells in two complexes, termed mTORC1 and mTORC2. This thesis describes investigations into the *in vivo* functions of these two complexes in the mouse heart.

The first part of the thesis focuses on the characterization of the role of mTORC1 in the adult heart. To inactivate mTORC1 for analysis of its cardiac functions, we ablated the mTORC1-specific and essential component raptor selectively and conditionally from cardiomyocytes using cre-loxP recombination. The resulting knockout mice showed decreased cardiac function at 3 weeks after gene deletion, culminating in heart failure and death after 5 weeks. Furthermore, the mice were exposed to voluntary wheel running exercise to trigger physiological cardiac growth, or to pathological stress, which was induced by aortic banding. Increased mortality was observed after exercise. In response to aortic banding, the raptor knockout mice lacked the phase of adaptive hypertrophic growth that normally occurs and went directly into dilated cardiomyopathy. In addition, the raptor knockout mice changed their cardiac mitochondrial gene expression pattern and switched from fatty acids to glucose as their primary source of energy. The decrease in cardiac function was accompanied by increased apoptosis and autophagy along with distorted mitochondrial structure. In conclusion, our findings establish mTORC1 as important regulator of cardiac homeostasis.

The second part of the thesis describes the *in vivo* function of mTORC2 in the heart. We used a similar approach as for mTORC1 to delete the mTORC2-specific component rictor selectively from cardiomyocytes. At baseline, during adulthood, rictor deletion had no effect on cardiac function. Cardiac geometry was normal in the cardiac rictor knockout mice despite the fact that downstream of mTORC2, phosphorylated and total Akt and PKC levels were significantly reduced. In contrast, conditions of pathological stress induced by aortic banding caused decreased cardiac function in the rictor knockout mice. The mice had a phenotype of eccentric

hypertrophy with changed chamber dimensions. Increased fibrosis and apoptosis were accompanied by enhanced reexpression of fetal genes compared to wild-type mice. On the other hand, deletion of rictor during postnatal growth did not show any functional or geometrical changes of the heart. Overall, the data demonstrates that rictor/mTORC2 is important for cardiac function during the adaptation to pathological stress.

# **<u>Introduction</u>**

# 2. Introduction

## 2.1 The heart and heart diseases

*The heart of creatures is the foundation of life, the Prince of all, the Sun of their microcosm, from where all vigor and strength does flow.*

- William Harvey, *De Motu Cordis*, 1628

The first organ to form and function in the embryo is the "Heart". The heart is composed of cardiac myocytes and non-myocytes such as fibroblast, endothelial cells, vascular smooth muscle cells and mast cells along with surrounding extracellular matrix. The basic contractile units of the heart are sarcomeres, arranged in a specific repeated manner to form myofibrils and bundles of such myofibrils constitute cardiomyocytes.[1] Cardiomyocytes are the specialized muscle cells and form the bulk of the heart's mass, where 70-80% of total mass comes from the left ventricular myocytes only. Figure 1 shows the basic anatomy of the heart.
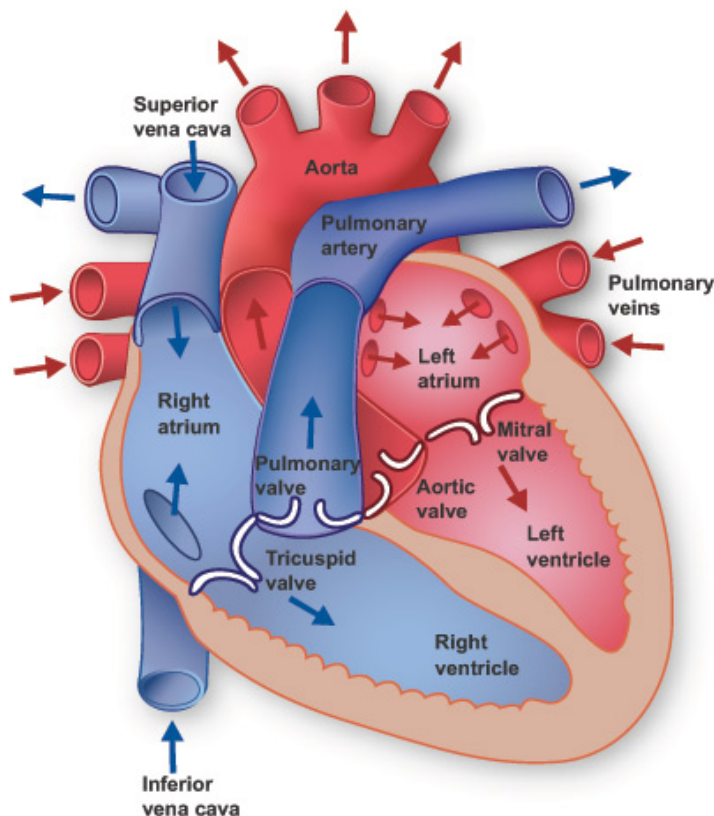


**Figure 1. A schematic representation of anatomical structure of the heart**

The heart has four chambers; the upper two are called right and left atrium whereas the lower two are called right and left ventricle. A muscle wall, called septum, separates the right and left atria as well as

the ventricles from each other. The blue arrows indicate the direction of deoxygenated blood is coming from the body into the right atrium of the heart, which then further ejected by the right ventricle towards the lungs. Oxygenated blood from the lungs, shown by the red arrows, comes first to the left atrium and then to the left ventricle. The left ventricle, the biggest and strongest chamber of the heart, pumps the oxygenated blood to all parts of the body through the circulatory system. (Adapted from, http://www.texasheart.org/HIC/Anatomy/index.cfm).

*The same thing that makes you live can kill you in the end.*

-Neil Young

Cardiovascular disease is the number one cause of death in the industrialized world and it is becoming more and more important, as the numbers of people diagnosed with cardiac dysfunction are increasing. Abnormalities occurring during heart formation due to inherited mutations in cardiac regulatory genes lead to congenital heart diseases. Cardiac malformations are the most common form of birth defect that affects large numbers of newborns every year.[2] Just as the developing heart is highly prone to malfunctions, the adult heart is susceptible to a variety of stimuli arising from different stress conditions, affecting its growth and contractile function. A wide range of stimuli arising from various forms of hemodynamic stress including hypertension, myocardial infarction, valvular dysfunction, or aortic stenosis causes the heart to undergo hypertrophic remodeling. Myocardial hypertrophy is traditionally thought to be a protective mechanism employed by the heart, which in the beginning normalizes ventricular wall tension in case of myocyte injury or myocyte loss. If it persists for a long time, it can lead to diastolic and then systolic dysfunction cumulating to cardiac sudden death.[3, 4]

## 2.1.1 Cardiac hypertrophy: definition and classification

Myocardial hypertrophy, also called cardiac hypertrophy, is one of the most remarkable and important features that permits the heart to adapt in physiological or pathological stress conditions, according to the changes occurring in the hemodynamic load. It is a reactive increase in cardiac size or myocardial mass in response to hemodynamic stress.[5]

Morphogenic changes that occur in heart due to hemodynamic stress are classified according to the nature of the inciting tension such as pressure-overload or volume-overload. A hypertrophied heart is usually concentric, eccentric, or dilated, depending on the ratio of left

ventricular free wall thickness to left ventricular chamber dimensions.[6, 7] An increase in ventricular wall thickness with little or no change in chamber volume is called concentric hypertrophy; an increase in chamber volume with an increase in ventricular wall thickness is called eccentric hypertrophy, whereas no change in wall thickness accompanied by increased chamber volume is called dilated hypertrophy. Note that both in concentric and eccentric hypertrophy there is an increase in cardiac dry mass (reviewed in[8]).
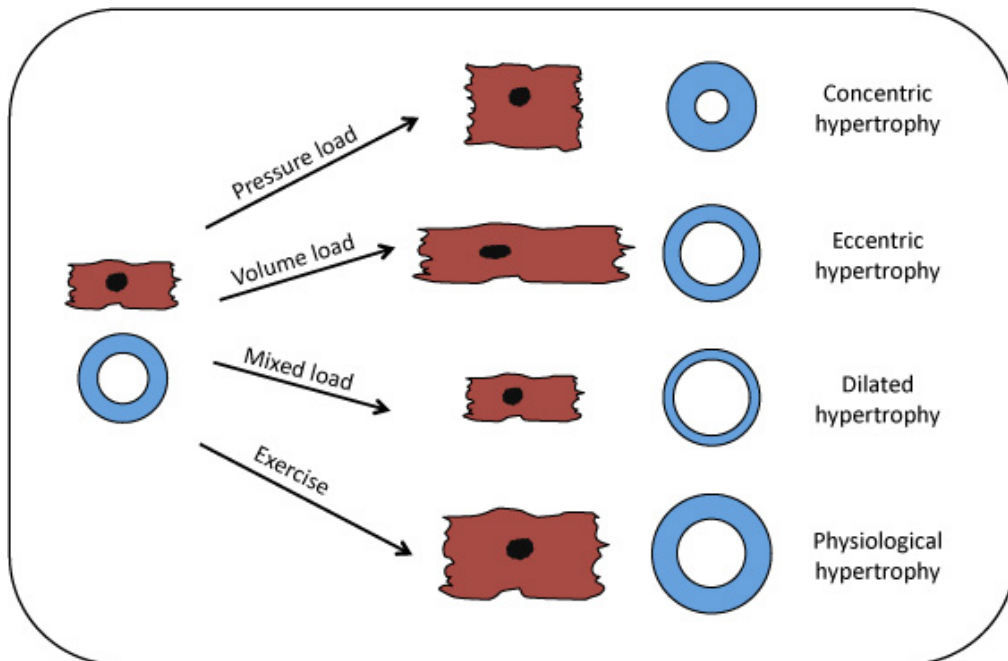


**Figure 2. The four major patterns of ventricular remodeling**
Cardiomyocytes change their morphology according to the nature of the inciting workload. Pressure-load increases the thickness of myocytes that leads to concentric hypertrophy, whereas volume-overload causes myocytes lengthening resulting into eccentric hypertrophy. Dilated cardiomyopathy occurs from various pathological stress-stimuli causing mixed burden of workload on the heart. Regular physical training or exercise causes the heart to undergo physiological adaptations, which is beneficial for the body.

According to Grossman's systolic-stress-correction hypothesis, pressure-overload causes myocytes to grow in width to increase wall thickness, thereby normalizing the increased wall stress as per Laplace relationship, and this thickening leads to concentric hypertrophy. In case of sustained volume load, Grossman proposed that increased diastolic stress directs myocyte stretching that increases LV internal diameter, causing eccentric hypertrophy[9] (reviewed in[10]) described in figure 2.

Assessment of the functional consequences of reactive cardiac growth is important to understand the role of "hypertrophy" in the integrated cardiovascular system and overall

health of the organism. Based on the left ventricular chamber ejection performance and the presumed stage of evolution in an inevitably deteriorating condition, hypertrophy can also be categorized as "compensated" or "decompensated".[11, 12] These terms are often used to describe the presence or absence of cardiac failure as a whole, but do not reflect the myocyte contractile function. As these terms indicate the assumed stage of disease progression, and there are few examples showing disconnect between the heart failure and its individual myocyte function,[13, 14] it is not really so useful in mechanistically classifying the hypertrophy as compensated or decompensated (reviewed in[8]).

Like ventricles, atria can also go in to hypertrophy situations in response to afterload. For example the mitral valve stenosis, that results into thickening of atrial walls. In this condition, due to resistance for the blood flow to move across the valve causes high pressure inside the left atrium to drive ventricular filling and that lead to atrial hypertrophy.

## 2.1.2 Cellular features of hypertrophy

An increase in size is the characteristic feature of hypertrophied cardiomyocytes compared to normal cells. Sarcomerogenesis, a process of adding sarcomeres to the myocyte, is increased in response to hypertrophic stimulus along with the increased expression of the natriueretic polypeptides such as atrial natriuertic peptide (ANP) and B-type natriueretic peptide (BNP). It is believed that sarcomeres are added in parallel when the stimulus arose from pressure-overloaded condition that causes cardiomyocytes to increase its cross-sectional area. On the other hand, volume-overload results in a lengthening of the myocytes where sarcomeres are added in series.[15] In both conditions cardiac dry weight is increased. It is also important to determine whether the observed increase in cardiac mass is due to actual enlargement of the myocyte i.e. true hypertrophy or because of the cardiac hyperplasia (increase in number of cardiomyocytes). Such assessment enables to understand the underlying mechanism behind the reactive myotrophy. To determine the cardiomyocyte size *in situ*, fluorescein-tagged wheat-germ agglutinin or anti-dystrophin, which labels the sarcolemma of cells, are used and by computerized analysis of cross-sectional area or long-axis, size is determined. To measure cardiomyocyte hyperplasia, the number of α-sarcomeric actin-stain positive cells per myocardial area is generally used. *In vivo* nuclear labeling with bromodeoxyuridine (BrdU), a

biochemical marker of active DNA synthesis is also useful to determine cardiomyocyte hyperplasia (reviewed in[8]).

### 2.1.3 Molecular markers of cardiac hypertrophy

Next to the cellular features described above, there are specific genes that get expressed during hypertrophic growth of the heart, also referred as "markers of cardiac hypertrophy". It concerns often as reexpression of cardiac fetal genes, including β-myosin heavy chain (β-MHC) and α-skeletal actin (α-SA) along with the already mentioned ANP and BNP. Increased levels of these markers usually indicate cardiac dysfunction or a stressed heart.[16, 17] In addition, other studies have shown that decreased expression of calcium cycling protein sarcoplasmic reticulum $Ca^{2+}$ ATPase (SERCA2a) is associated with the hypertrophied or failing heart.[18] However, studies have also demonstrated that these markers show independent or variable patterns of expression based on the hypertrophy model used,[19] and therefore cannot be used alone to extrapolate the cardiac situation. In such cases, characterization of these markers is useful, as they reflect the underlying transcriptional pathways activated in that particular system.[20]

### 2.1.4 Remodeling of the heart: physiological and pathological adaptations

Although we now know that cardiac hypertrophy is a reactive process that increases cardiac mass in response to increased load, it is usually considered as a poor prognostic sign and it is associated with nearly all types of cardiac failure.[5] An exception to this correlation is the athlete's heart where chronic exercise induces cardiac enlargement through a hypertrophic response and cardiac function is normal or even enhanced.[21, 22] Such modification is termed physiological hypertrophy and is reversible in nature. Physiological hypertrophy differs from pathological hypertrophy in terms of nature of the stimuli, cardiac morphology, expression of hypertrophic genes, reversibility and importantly, cardiac function. A chronic exercise program or regular physical training stimulates the physiological growth of the heart. Physiological hypertrophy includes embryonic, fetal and postnatal stages of cardiac development, and also the growth occurring during pregnancy.[23] Like its pathological

counterpart, physiological hypertrophy can be sub-classified as concentric or eccentric. Isotonic exercise such as running, swimming, and cycling produces eccentric hypertrophy, whereas isometric or static exercise such as weight lifting leads to concentric hypertrophy.[21] Animal studies in which pathological hypertrophy was compared with the physiological one showed distinct structural and molecular bases.[24, 25] For example during physiological hypertrophy, a fine network of collagen fibers surrounds the growing cardiomyocytes, creating a framework, whereas in pathological conditions cardiac fibroblasts and extracellular matrix (ECM) accumulate disproportionally in the heart, causing cardiac stiffness leading to systolic dysfunction in contrast to physiological hypertrophy. Hypertrophy markers such as ANP and β-MHC generally do not get re-expressed in models of hypertrophy induced by exercise training.[26] It is important to note that physiological hypertrophy does not decompensate into dilated cardiomyopathy or heart failure (reviewed in[27]).

## 2.1.5 Signaling pathways involved in cardiac hypertrophy

The initiating stimuli for cardiomyocytes to go into hypertrophy can be classified as stimuli from biomechanical and stress-sensitive mechanisms, or from neurohumoral mechanisms that are associated with the release of hormones, cytokines, chemokines and peptide growth factors. Based on the nature of the stimuli, different types of ligands or transmembrane receptors are activated, which in turn converge to downstream signaling cascades to initiate reactive hypertrophic growth.[28]

Despite having distinct characteristics, it was rather unclear until recently whether the physiological or pathological hypertrophy was induced by distinct biochemical pathways. Complexity occurs when these distinct signaling cascades overlaps in part with each other to yield hypertrophic growth. In general, hypertrophy induced through Gq-coupled receptors is considered as pathological whereas hypertrophy induced by tyrosine kinase receptor through PI3K/Akt/mTOR pathway is well characterized as physiological hypertrophy.

In brief, multiple agonists such as angiotensin II, endothelin-1, or noradrenalin are produced in response to the pathological stimulus. These ligands activate G-protein coupled receptors (GPCR), which leads to dissociation of Gαq, a common transducer for most of the pathological hypertrophy signals and causes activation of downstream signaling molecules.[29]

Downstream of Gαq, phospholipase Cβ (PLCβ) hydrolyzes the phosphatidylinositol biphosphate (PIP2) into diacylglycerol (DAG) and inositol triphosphate (IP3). IP3 causes the release of calcium ions from intracellular stores such as the endoplasmic reticulum, thus activating the calcineurin phosphatase, which in turn dephosphorylates NFAT (Nuclear factor of activated T cells). Dephosphorylation of NFAT causes its nuclear translocation and leads to pathological hypertrophy. DAG, with or without calcium, activates protein kinase C (PKC) family members that also induce hypertrophic gene expression (illustrated in figure 3).
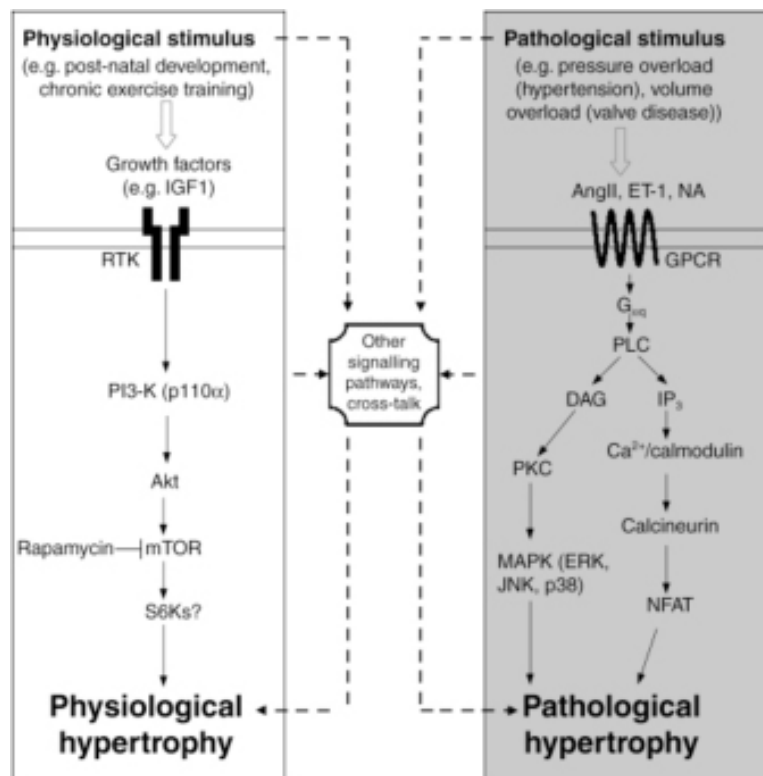


**Figure 3. A flow chart showing signaling pathways involved in induction of physiological and pathological hypertrophy [27]**

In the case of physiological cardiac growth such as during development, in exercise- or pregnancy-induced hypertrophy, insulin or insulin-like growth factor-1 (IGF-1) has been shown to play major role. Briefly, these and other peptide growth factors bind to their membrane tyrosine kinase receptors and cause receptor dimerization.[30] This leads to their autophosphorylation and activation of the p110α subunit of PI3K. Activated PI3K phosphorylates PIP2 to PIP3, and PIP3 in turn causes recruitment of the kinase Akt to the

15

plasma membrane and leads to its activation by phosphorylation. Activated Akt then stimulates the protein synthesis machinery through its downstream target mTOR and also by inhibiting glycogen synthase kinase (GSK) (reviewed in[27, 31]).

To date, as explained above, the GPCR-induced and Insulin/IGF/PI3K/Akt-induced pathways are the best-characterized signaling pathways of pathological and physiological hypertrophy, respectively. Along with these, there are other signaling cascades that when activated lead to cardiac hypertrophy (reviewed in[32]).

## 2.2 The mTOR kinase and its regulation

### 2.2.1 History and structure

The bacterial strain, *Streptomyces hygroscopicus* was first isolated in 1970 from a soil sample of Easter Island, a small Chilean island in the South Pacific Ocean. These bacteria secreted a potent antifungal macrolide that was named rapamycin after Rapa Nui (name of the island in native language). Rapamycin was initially developed as antifungal agent as it contains macrocyclic lactone, but later it was proven to have immunosuppressive and anti-proliferative properties. These observations encouraged further research into the mechanism of action of rapamycin and its targets.

The target of rapamycin (TOR) was originally identified by two mutations in budding yeast, *Saccharomyces cerevisiae* in 1991, termed *TOR1-1* and *TOR2-1*.[33] These mutations allowed yeast to escape cell cycle arrest caused by rapamycin treatment. Upon entering the cell, rapamycin binds to an intracellular cofactor FKBP12 (FK506-binding protein 12kDa) and forms a complex. This complex then binds to TOR protein and interferes with its function. Extensive studies in yeast have shown that TOR plays a central role in cell growth metabolism. Subsequent studies in mammals led to the identification and cloning of mammalian TOR (mTOR), also known as FRAP, RAFT, RAPT or SEP (reviewed in[34, 35]). All eukaryotic genomes possess a copy of the *TOR* gene with a high degree of sequence conservation among species, indicating an important role for TOR (reviewed in[36]).

mTOR is an atypical serine/threonine protein kinase belonging to the phosphatidylinositol kinase-related kinase (PIKK) family with a molecular weight of ~290 kDa. Structurally,

mTOR has 20 tandem HEAT repeats (a protein-protein interaction structure of two tandem anti-parallel α-helices found in huntingtin, elongation factor3, PR65/A and TOR) at the amino-terminal domain, followed by a FAT (FRAP, ATM, and TRRAP, all PIKK family) domain (shown in figure 4). FRB (FKBP12-rapamycin binding) domain is situated next to FAT domain, followed by the mTOR kinase domain. FATC (FAT C-terminus) domain is located at the extreme carboxy-terminal of the protein. Presence of HEAT repeats give mTOR the extended super-helical structure that helps for protein-protein interactions; the FRB domain serves as a docking site for rapamycin-FKBP12 complex whereas FAT and FATC domains modulate mTOR kinase activity via unknown mechanisms (reviewed in[37]).
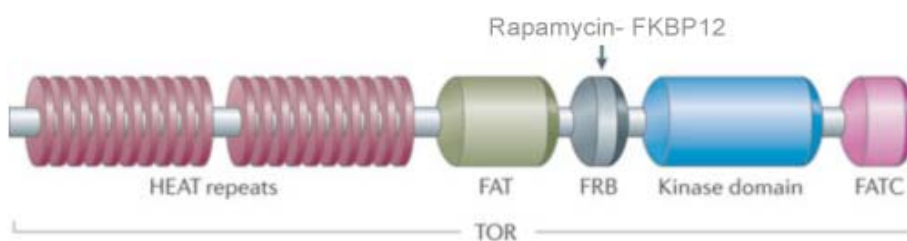


**Figure 4. A schematic representation of the mTOR domain structure**
mTOR is a large protein of around 290 kDA and consists of different domains in its structure as shown in this figure. Rapamycin-FKBP12 complex binds to FRB domain of the mTOR that causes inhibition of some of mTOR downstream functions (figure from[38]).

The binding of the rapamycin-FKBP12 complex to mTOR at the FRB domain blocks some of the physiological functions of mTOR. The exact mechanism behind this inhibition is poorly understood, as rapamycin's effect on mTOR intrinsic kinase activity is not yet clear. Some scientists believe that the binding of rapamycin-FKBP12 complex blocks mTOR from interacting with its substrates. Ser2481 is an autophosphorylation site of mTOR. Recent studies have shown that phosphorylation at this site happens mainly to mTOR mTORC2 (mTOR complexes described in next section) and is insensitive to acute rapamycin treatment.[39, 40] The majority of the functions occur through phosphorylation at Ser2448 of the mTOR mainly in mTORC1.[41, 42] Studies have shown that mTOR also get phosphorylated at Thr2446 presumably by cAMP-activated protein kinase (AMPK)[43] and at Ser1261, a site whose phosphorylation promotes mTOR autophosphorylation and activity.[44] To date, studies have suggested that mTOR phosphorylation appears to alter its kinase activity rather than its association with other components in the mTOR complexes.

For most eukaryotic cells, inhibition of mTOR by rapamycin results in growth arrest, as the cells arrest in the cell cycle and become unresponsive to nutrients and growth factors.

Sensitivity of such inhibition varies according to the type of cell, for example; lymphocytes and certain cancer cells are highly susceptible to rapamycin. As mentioned before, rapamycin does not block all the mTOR activities because mTOR exists in the cell in two different complex forms and only one of them is inhibited by rapamycin.

## 2.2.2 Components of the two mTOR complexes

As mTOR is a large protein with many domains for protein-protein interactions, genetic and biochemical studies have demonstrated that mTOR occurs in cells in two multiprotein structures, mTOR complex 1 (mTORC1) and mTORC2. Rapamycin gives these complexes a unique distinguishing feature, where mTORC1 is rapamycin-sensitive while mTORC2 is rapamycin insensitive. Along with mTOR, mTORC1 consists of PRAS40 (proline-rich AKT substrate 40 kDa), mLST8 (mammalian lethal with SEC13 protein 8, also known as GβL), Deptor (DEP domain-containing mTOR-interacting protein) and Raptor (regulatory-associated protein of mTOR) (reviewed in[36, 45]). Instead, mTORC2 consists of mTOR, mSIN1 (mammalian stress-activated map kinase-interacting protein 1), Rictor (rapamycin-insensitive companion of mTOR) along with Protor 1 and 2 (also known as PRR5, prolin-rich repeat protein-5), Deptor and mLST8. Raptor and rictor are the two accessory scaffolding proteins that give structural stability to the two complexes and play a role in substrate and regulator binding.[46, 47] Biochemical and structural analysis suggests that both mTORC1 and mTORC2 exists as dimeric complexes in cell.[48] The multimerization of the TOR complexes may play a role in regulating its kinase activity as multimeric TORC2 appears to be more active than monomeric TORC2.[49]

The best-characterized and functionally important components of mTORC1 and mTORC2 are shown in figure 5 and described below.

*Raptor*

The individual functions of the mTOR complex components are not well understood. Raptor is a large protein (around 150 kDa) and is a non-enzymatic subunit of mTORC1.[46, 50] It contains a highly conserved amino-terminal region followed by three HEAT repeats and seven WD40 (terminating in tryptophan-aspartic acid dipeptide) repeats at the carboxy-terminal end. The interaction between raptor and mTOR is dynamic and requires multiple regions from both proteins for binding. The raptor-mTOR complex can sustain 0.3% CHAPS

or 0.3% Tween-20 containing buffer but dissociates in buffer containing 1% NP-40 or 1% Triton X-100 (reviewed in[51]). In addition, treatments such as amino acid withdrawal increase the binding between raptor and mTOR, whereas rapamycin decreases it.[52]
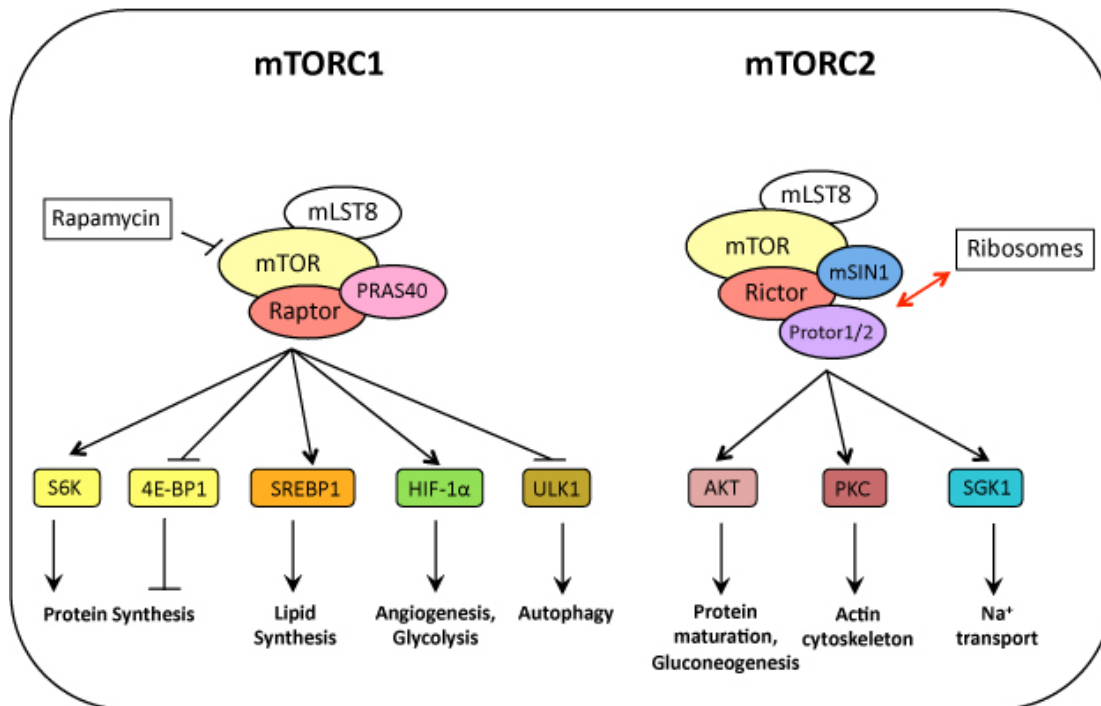


**Figure 5. Components, targets and functions of the two mTOR complexes**

### *mLST8*

mLST8 is a subunit that is part of both mTORC1 and mTORC2, however little has been reported regarding its interaction with mTOR.[53, 54] It is a 36kDa protein that has seven WD40 repeats and binds to the kinase domain of mTOR. Knockout mice for mLST8 die around E10.5. Initial knockdown studies have suggested a positive role for mLST8 in the regulation of kinase activity of mTOR in mTORC1 but later observations from mice and Drosophila (with dLST8) indicate that mLST8 is neither required for mTORC1 integrity nor for its function.[55] However, LST8 is required for full catalytic activity of TOR.[49] These different results require further studies to elucidate the exact function of mLST8 in mTORC1. In contrast to mTORC1, mLST8 is needed for mTORC2, as knockout of mLST8 disrupts mTORC2 assembly as well as loss of Akt phosphorylation at Ser473, a downstream target of mTORC2.

*Rictor*

Rictor (also known as mAVO3) is a large protein of ~200 kDa and the defining member of the rapamycin-insensitive mTORC2. It has domains that are conserved among species, but no obvious catalytic motif. Knockdown of rictor results in loss of both actin polymerization and chemotactic signaling,[47, 56] whereas rictor knockout mice die during mid-gestation period around E10.5.[55, 57] In addition, rictor also interacts with other proteins such as integrin-linked kinase (ILK),[58] Myo1c[59] and heat shock protein 70 (Hsp70).[60] The significance of these interactions is unclear but through such bindings rictor may act as an adaptor to bring mTORC2 to its targets.

*mSIN1*

mSIN1 (also known as MAPKAP1) is the integral member of the mTORC2, important for complex assembly and function.[61, 62] SIN1 is conserved in all eukaryotic species with a tissue expression pattern similar to that of mTOR and mLST8. It has a Ras-binding domain (RBD) and a C-terminal pleckstrin homology (PH) domain that is likely to interact with phospholipids. Phosphorylation of SIN1 by mTOR is required for mTORC2 integrity.[63] The interaction between mSIN1 and rictor is more stable and forms the foundation of mTORC2 as knockdown of either of two decreases other mTORC2 proteins levels. Recently, it has been shown that mSIN1 protein is required for SGK1 interaction and its subsequent phosphorylation by mTORC2.[64]

## 2.2.3 Components affecting mTOR activity

*TSC1 and TSC2 inhibit mTORC1*

Mutations in *TSC1* and *TSC2* lead to tuberous sclerosis complex syndrome, an inherited genetic disorder manifested with tumor occurrence in multiple organs (reviewed in[65, 66]). The genes were initially identified as tumor suppressor genes and their products TSC1 and TSC2 (also known as hamartin and tubrin) form a heterodimeric complex that has GTPase-activating protein (GAP) activity. TSC1 stabilizes the complex, while TSC2 contains the GAP homology domain. Studies in *Drosophila* identified the small GTPase Rheb (Ras-homolog enriched in brain) as a downstream target of TSC1 and TSC2 and upstream of TOR. Subsequent studies in mammalian cells confirmed that TSC1-TSC2 complex hydrolyzes GTP-bound active Rheb to its inactive GDP-bound form, which in turn decreases mTOR kinase activity. [67, 68] Coexpression of TSC1 and TSC2 reduces levels of GTP-bound Rheb,

whereas insulin stimulation increases the levels in a PI3K-dependant manner.[69] Phosphorylation of TSC2 decreases its GAP activity. TSC2 is phosphorylated at multiple residues by various kinases involved in different pathways including Akt, AMPK and ERK, which in turn impairs its function directly or indirectly. Thus ability to get phosphorylated by multiple kinases and accordingly altering the GAP activity to integrate and then transfer signals to downstream mTOR, made TSC1/2 as an important mTORC1 regulator (figure6, reviewed in[70]).
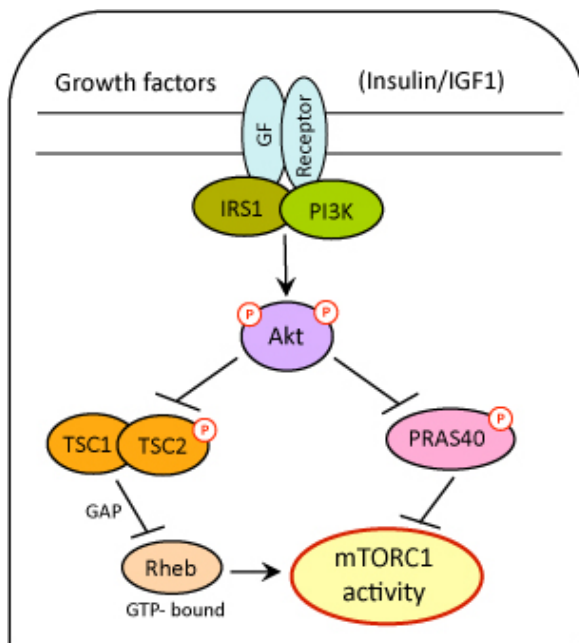


**Figure 6. Upstream regulators of mTORC1**

### GTP-bound Rheb activates mTORC1

As explained above, Rheb is a small GTPase, which acts as positive cell growth regulator. Rheb is close to Ras both structurally as well as the way it binds to its effector in a GTP-dependent manner, but its intrinsic GTPase activity is lower than that of Ras. The TSC1/2 complex acts as a GTPase for Rheb, converting GTP-bound active Rheb to GDP-bound inactive form to inhibit its function.[67, 71] Rheb regulates mTORC1 activity positively as over-expression of Rheb increases phosphorylation of the mTORC1 targets S6K1 and 4EBP1 and these effects can be blocked by rapamycin treatment or by dominant-negative mTOR. Rheb directly binds to mTOR and regulates its activity.[72] GTP-bound active Rheb binds to FKBP38 and releases it from mTORC1, where FKBP38 exerts inhibitory action on mTORC1 by binding in a manner similar to FKBP12.[73]

*PRAS40 inhibits mTORC1*

PRAS40 was initially identified as a binding partner of the protein 14-3-3 upon phosphorylation by Akt. Later it was also recognized as a component of mTORC1 by mass spectroscopy. PRAS40 binds to raptor through a TOR signaling (TOS) motif and inhibits mTOR kinase activity. The TOS motif is usually found in mTORC1 substrates such as S6K and 4E-BP1, indicating that PRAS40 is also the mTORC1 substrate. The binding of PRAS40 to mTORC1 increases under conditions of serum or nutrient deprivation or in metabolic stress, indicating that PRAS40 is an inhibitor of mTORC1 activity.[74] It is phosphorylated by mTORC1 at several sites including Ser183, Ser212 and Ser221, which weakens its association with raptor and releases mTORC1 from the exerted inhibitory effect. This may also cause the positive feed-forward mechanism for mTORC1 activation.[75, 76] Phosphorylation of PRAS40 at Thr246 by Akt or PIM1 creates a docking site for protein 14-3-3 for binding that leads to interference with its association with mTOR and causes increase in mTORC1 activity.[77]

*Other components*

Along with the above described, recently some molecules were recognized that have the ability to regulate mTORC1 activity. These include IκB kinase (IKK), phosphatidic acid and phospholipase D, Translationally controlled tumor protein (TCTP), p53, the Rag small GTPase and mVps34 (reviewed in[78]).

## 2.2.4 Upstream regulators of mTOR signaling

*Growth factors*

Growth factors activate mTOR signaling through the PI3K-Akt signaling pathway. Binding of insulin or IGF to their respective receptors lead to phosphorylation of insulin receptor substrate (IRS) and subsequent recruitment of PI3K to the membrane. Active PI3K converts PIP2 in the cell membrane to PIP3 that recruits PDK1 and Akt to the membrane. PDK1 then phosphorylates Akt, which in turn phosphorylates TSC2 leading to its inactivation. Thus, via inhibition of the TSC1/2 complex, which as described above activates GTP-bound Rheb, growth factors including insulin and IGF stimulate mTORC1 through PI3K-Akt pathway (reviewed in[78]). Growth factors can also phosphorylate and thereby inhibit TSC2 via ERK, via part of the Ras-Raf-MEK-ERK axis.[79] Furthermore, the canonical Wnt pathway prevents glycogen synthase kinase 3β- (GSK3β) induced phosphorylation of TSC2, thus acting as

upstream activator of mTORC1.[80] Growth factors also regulate mTORC1 independently of the TSC complex, as phosphorylated Akt inhibits PRAS40 and thus reverses its negative inhibition on mTORC1.[81]

### Nutrients

Nutrients, such as amino acids, activate mTORC1 signaling. Amino acids constitute proteins and are also required for the synthesis of DNA, glucose and ATP. Early studies showed that amino acid starvation, in particular of leucine, results in a loss of mTORC1 downstream signaling that can be restored by re-addition of amino acids.[35, 82] The identity and mode of action of such a primary amino acid sensor is not yet clearly understood, but recent studies have provided some important clues for the mTORC1 activation by amino acids. Players downstream to amino acid sensing, such as the Rag family of small GTPase, [83, 84] sterile 20 (STE20) family kinase mitogen-activated protein kinase kinase kinase kinase 3 (MAP4K3)[85, 86] and PI3K catalytic subunit type 3 (VPS34),[87, 88] have emerged as activators of mTORC1. The Rag GTPase, which exists as heterodimer complex, is in an inactive conformation in the absence of amino acids. Once present, amino acids cause a GTP switch in the heterodimer complex that results in active Rag GTPase, which allows active Rag GTPase to physically interact with raptor, leading to transport of mTORC1 to the surface of late endosomes and lysosomes.[84, 89] This relocalization may enable mTORC1 to interact with growth factor-activated Rheb.[67] The mechanism by which amino acids activate mTORC1 downstream of MAP4K3 is not well characterized. By inducing extracellular calcium influx, amino acids activate calmodulin, which binds to mVPS34. Active mVPS34 produces PIP3, which activates mTORC1. More recently, Duran et al showed that p62 is an integral part of mTORC1 as it interacts directly with raptor. Such interaction is amino acid dependent and required for mTORC1 activation. In addition, p62 binds with the Rags protein and favors the formation of active Rag heterodimer causing mTORC1 activation through small GTPase Rheb as described above.[90]

### Energy

Cellular energy status regulates mTOR function as demonstrated by the observation that mTORC1 activity decreases in response to glycolysis or mitochondrial function inhibitors.[91] mTOR-mediated processes of growth consume a large fraction of cellular energy, therefore energy sensing is a decisive process in case of hypoxic or starving cells. Cellular energy obtained from nutrients is stored in the form of ATP, and after consumption the drop in ATP

is indirectly sensed by mTOR and AMPK. Both AMP and ATP are allosteric regulators of AMPK; therefore an increase in the AMP/ATP ratio activates AMPK. Activated AMPK phosphorylates TSC2, thereby increases its GAP activity, causing decreased Rheb activity, thus leading to mTORC1 inhibition.[92] AMPK also phosphorylates raptor, thus promoting its binding with protein 14-3-3, leading to mTORC1 inhibition by allosteric mechanisms.[93]

*Stress*

Cells respond to a variety of the stress stimuli such as hypoxia, low energy or environmental factors by downregulating the mTOR-driven energy consuming processes. Along with an induction of AMPK, hypoxia also regulates mTORC1 by inducing expression of REDD1 (regulated in development and DNA damage response 1) that promotes assembly of the TSC1/2 complex, thus inhibiting mTORC1.[94, 95] In response to DNA damage, p53 directly activates transcription of *AMPKβ1, TSC2, IGFBP-3* and *PTEN* in insulin-sensitive tissues, each of which negatively regulates mTORC1 activity.[96] Another mechanism employed by p53 is the induction of sestrin1 and sestrin2, which activate AMPK directly.[78, 97]

*Upstream regulators of mTORC2 signaling*

Compared to mTORC1, which is activated by several factors as described above much less is known about the upstream regulators of mTORC2. Growth factors have been shown to activate mTORC2 signaling as demonstrated by Akt phosphorylation at Ser473.[98, 99] Recently, Gan et al showed that addition of PIP3 to a mTORC2 kinase assay enhances Akt phosphorylation *in vitro*.[100] mTORC2, by associating with translating ribosomes, phosphorylates Akt at Thr450 site and phosphorylation at this site is not inducible by growth factors.[101] The TSC1-TSC2 complex that downregulates mTORC1 is required for proper activation of mTORC2. TSC1-TSC2 complex directly associates with mTORC2 via rictor, and regulation of mTORC2 activity by this complex appears to be independent from its GTPase activity towards Rheb.[102, 103]

## 2.3 Effectors and downstream functions of the mTOR complexes

### 2.3.1 Effectors of mTORC1 signaling

mTOR signaling plays key roles in various growth related processes. The best-characterized targets of mTORC1 are ribosomal protein S6 kinase 1 (S6K1) and eukaryotic initiation factor

(eIF) 4E-binding protein 1 (4E-BP1). mTORC1 interacts with S6K1 and 4E-BP1 via association between raptor and a TOS motif present in S6K1 and 4E-BP1. The TOS motif is a conserved five amino acid residue found in the N-terminus of S6K1 and in the C-terminus of 4E-BP1 and as mentioned before, is essential for the phosphorylation by mTORC1.[104, 105] Phosphorylation of S6K1 by mTORC1 occurs at the Thr389 site within the hydrophobic motif, whereas 4E-BP1 gets phosphorylated by mTORC1 at four residues including Thr37, Thr46, Ser65 and Thr70.[106] Phosphorylation of these effectors leads to further activation of downstream molecules and enhances protein synthesis (reviewed in[36]).

## 2.3.2 Cellular functions of mTORC1

### *Protein synthesis*

Downstream of PI3K-Akt activation, mTORC1 plays major role in the phosphorylation of proteins that regulate or are involved in mRNA translation. As mentioned before, S6K1 and 4E-BP1 are the major direct targets of mTORC1 in this process. After activation by mTORC1, S6K phosphorylates several proteins that are associated with mRNA translation such as ribosomal protein S6, eukaryotic elongation factor 4b (eIF4B), S6K1 aly/REF-like target (SKAR), programmed cell death 4 (PDCD4) and eukaryotic elongation factor 2 kinase (eEF-2k).[107] Phosphorylation of 4E-BP on the other hand, prevents its binding with eIF-4E and thereby increases protein translation. mTORC1 increases translation of a subset of mRNA that contains 5' tract of oligopyrimidine (TOP). 5' TOP mRNA encodes components of the translation apparatus (reviewed in[108]). Recently, a novel example of translational control by mTOR has been shown that involves IRES- (internal ribosome entry segment) driven translation of specific mRNAs.[109]

### *Ribosome biogenesis*

Ribosome biogenesis is a high energy-demanding process, and mTOR tightly controls this process based upon nutrient and energy availability. The synthesis of ribosomal proteins and rRNA is positively regulated by mTORC1. Studies with rapamycin shown that mTOR inhibits transcription of RNA polymerase I (Pol I)-dependent rRNA genes, Pol II-dependent ribosomal protein genes, and Pol III-dependent tRNA genes, which altogether block ribosome biosynthesis. mTORC1 upregulates transcriptional activity of the rRNA polymerase RNA polymerase I (RNAPI) through S6K1[110] and regulates processing of 35s and 5s rRNA.[111]

Recent work by Michels et al suggests that mTORC1 might control Pol III through its direct substrate MAF1.[112]

### *Transcription*

mTORC1 controls a variety of cellular processes by controlling the rate of transcription of many genes. In mammalian cells, mTORC1 directly regulates SRBP1 (sterol regulatory element-binding protein), a transcription factor responsible for sterol and lipid biosynthesis.[113, 114] Cunningham et al showed that mTORC1 promotes transcriptional activity of PPARα coactivator PGC1α, which is a nuclear cofactor responsible for mitochondrial biogenesis and oxidative metabolism, by directly affecting its physical interaction with the ying-yang 1 (YY1) transcription factor.[115]

### *Metabolism*

mTORC1 regulates several metabolic pathways by controlling key steps at the transcriptional, translational and post-translational level in different tissues types (reviewed in[78]). Active mTORC1 promotes expression of hypoxia-inducible factor-1α (HIF-1α), mostly by regulating translation of its alpha subunit through 4E-BP1, which activates the transcription of many genes involved in cellular metabolism.[116] Recently, mTORC1 has also been shown to regulate glycolysis, sterol and lipid biosynthesis in addition to control key steps in the pentose phosphate pathway.[114]

### *Autophagy*

Autophagy is a catabolic process that recycles cellular organelles and proteins. It functions as a quality control, and also a mechanism by which cells replenishes their intracellular nutrients content under conditions of poor nutrient availability. Under nutrient-rich conditions mTORC1 maintains low levels of autophagy. It inhibits a conserved protein complex containing the protein kinases Atg1 and Atg2 that are required for induction of autophagy.[117] Recently, it has been shown that TORC1 directly phosphorylates Atg13 (ULK1) at multiple serine residues. Atg13 is an essential regulatory component of autophagy upstream of the Atg1 kinase complex and in its phosphorylated state directly inhibits the Atg1-driven autophagic process.[118]

## 2.3.3 Effectors of mTORC2 signaling

Studies have shown that mTORC2 recognizes and phosphorylates AGC kinases, which play key roles in multiple intracellular signaling pathways. The AGC kinases are Ser/Thr kinases from a large family of conserved proteins. The prototypical members of the AGC kinase family are cAMP-dependent protein kinase (PKA), protein kinase G (PKG), and protein kinase C (PKC). In addition, the family also includes Akt, S6K and serum and glucocorticoid-induced kinase (SGK). mTORC2 phosphorylates AGC kinases at their turn motif (TM) having specific Thr-Pro-Pro sequence and at hydrophobic motif (HM) when have specific Ser/Thr-Tyr/Phe sequence. Phosphorylation by mTORC2 allosterically activates AGC kinases in addition to catalytic activation of the kinases by PDK1 (reviewed in[119]). The substrates known for mTORC2 are described hereafter.

### Akt/PKB

Akt gets phosphorylated at two sites by mTORC2; firstly at Thr450 of the TM and secondly at Ser473 of the HM domain. TM phosphorylation of Akt is a one-shot irreversible step that occurs exclusively during the synthesis of nascent Akt, when the polypeptide is still attached to the ribosome. TM phosphorylation is essential for Akt stability and lack of it results in co-translational ubiquitination of nascent Akt.[101, 120] Thr450 phosphorylation of Akt at TM is solely done by mTORC2 and this is well conserved from yeast to human.[120] In contrast, phosphorylation at HM Ser473 is a post-translational modification that occurs at the membrane where mTORC2 is supposed to co-localize with Akt. Growth factors and hormones induce HM Ser473 phosphorylation that allosterically activates Akt, thereby increasing its activity towards many of its substrates such as forkhead box O1/3 (FoxO1/3). Studies have shown that HM phosphorylation by mTORC2 gives substrate specificity to Akt, as mTORC2-deficient cells showed defective FoxO1/3 phosphorylation but had normal GSK3 and TSC2 phosphorylation.[55, 61]

### PKC

PKCs are conserved signaling molecules with a variety of cellular functions, mainly responsible for distribution of signals.[121] Phosphorylation at the HM Ser657/660 of all conventional PKCs (cPKC) and of some novel PKC (nPKC), as well phosphorylation of PKCα/βII TM at Thr638/641, requires mTORC2. mTORC2 was shown to be engaged in PKC maturation and stability like Akt (reviewed in[119]). Inhibition of mTORC2 activity by

SIN1 deletion significantly decreases cPKC expression levels as TM phosphorylation is abolished. This is in contrast with Akt, which maintains its level with the help of Hsp90-induced TM phosphorylation of Akt.[122]

***SGK***

mTORC2 is required for Ser422 phosphorylation present in HM of SGK. SGK is a short-lived protein stimulated by growth factors and conditions of osmotic stress.[123] Unlike Akt and cPKC, SGK1 levels are not decreased in mTORC2-deficient cells, but rather increased in rictor null cells. Disruption of mTORC2 leads to decreased SGK1 phosphorylation, which in turn affects activation of its specific substrate NDRG1 (N-myc downregulated gene 1).[124] Protor-1 functions as the adaptor of mTORC2 activity to phosphorylate HM of SGK1.[125] Recently, mTORC2 has been shown to activate epithelial sodium channel (ENaC)-dependent sodium transport in kidney cells through phosphorylation of SGK1.[126]

## 2.3.4 Cellular functions of mTORC2

***Cytoskeleton organization***

Early studies by Loewith and colleagues have shown that TORC2 controls cell cycle-dependent polarization of the actin cytoskeleton in yeast via the activation of Rho1 GTPase switch.[56] mTORC2 activates PKCα by phosphorylating its HM site, which causes its interaction with small GTPase Rho and Rac and thereby it signals to actin cytoskeleton.[47, 56] Knockdown of mTOR, rictor, mLST8, but not raptor causes defective actin reorganization along with decreased Rac1 activation, upon serum restimulation in mammalian cells.[61] Recently, Rac1 was found to be a part of both mTOR complexes upon growth factor stimulation. Activated Rac1 could mediate actin rearrangement by translocating to plasma membrane, where it increases PIP3 synthesis and thereby could led to actin organization.[127]

***Protein synthesis and maturation***

Protein synthesis is a process mainly associated with mTORC1, but recent studies have suggested a role for mTORC2 in this basic cellular process. Intact mTORC2 localizes in polysome fractions and directly interacts with the 60S large ribosome subunit. In particular rictor that can form stable interactions with the ribosomal proteins L23a and L26 that are located at the exit tunnel of ribosomes.[101, 128] The nature of this interaction plays a role in

mTORC2-mediated co-translational maturation of the nascent Akt polypeptide.[101] Zinzalla and coworkers recently indentified a protein involved in ribosome biogenesis and rRNA maturation using yeast genetic screens, *NIP7*, which regulates mTORC2 activity. This suggests that association of mTORC2 with assembled ribosomes or ribosomal proteins activates mTORC2. Upon mTORC2 inhibition or disruption, total translation and polysomes were shown to be more attenuated compared to rapamycin treatment, which inhibits mTORC1, suggesting a role of mTORC2 in translation.[101, 129]

### *Chemotaxis, proliferation and survival*

In line with the early demonstration of its role in actin reorganization, mTORC2 was recently shown to be involved in cell migration and cancer metastasis.[130] Rictor interacts with PKCζ and regulates metastasis of breast cancer cells, where rictor acts as a mediator of chemotaxis.[131] In normal cell types such as neutrophils, chemotaxis is regulated by mTORC2 via activation of adenylyl cyclase 9 (AC9).[132] Recently, rictor/mTORC2 was reported to be essential for maintaining a balance between β-cell proliferation and cell size,[133] whereas in TSC-null cells, mTORC2 modulates its proliferation and survival through RhoA GTPase and Bcl2 proteins.[134]

### *Gluconeogenesis*

Gluconeogenesis is the process of biosynthesis of new glucose. A recent study by Wang and colleagues suggests a role of mTORC2 in regulating gluconeogenesis. Deletion of Sirt1, which positively controls rictor expression and thus mTORC2-mediated Akt S473 phosphorylation, causes increased gluconeogenesis in liver.[135] The Insulin/Akt/FoxO1 signaling pathway is a major regulator of glucose production and metabolism. Insulin-activated Akt phosphorylates FoxO1, which presents its translocation to the nucleus and leads to its degradation via the ubiquitin proteosome pathway. This causes a decrease in expression of genes involved in gluconeogenesis, such as glucose-6-phosphatase (G6Pase) and phosphoenolpyruvate carboxykinase.

### *Metabolism*

In *Caenorhabditis elegans,* rictor/TORC2 regulates fat metabolism, feeding, growth and life span[136] but little is known about the role of mTORC2 in metabolism in mammalian cells. Rictor-null fibroblasts were reported to display decreased metabolic activity.[57] Recently Colombi and coworkers using genome-wide shRNA screening revealed that mitochondrial

dependence increases upon mTORC2 addiction. They identified a group of genes, whose knockdown is selectively lethal in growth factor independent and mTORC2 addicted cells. Several of these genes required for mTOR addiction encode for mitochondrial functions.[137]

## 2.4 mTOR in the heart

Myocardial growth and metabolic regulation are crucial factors in various heart diseases. Therefore, extensive research has been focused on signaling molecules activated under conditions of increased workload or in pathological stress situations. In this regard, the IGF/PI3K/Akt/mTOR signaling axis is important and research on this signaling cascade has led to the identification of new potential therapeutic targets.

Mechanical stimulation or agonists that stimulate growth factor receptors, α- and β-adrenergic receptors or integrins activate mTORC1 and mTORC2 in numerous cell types.[138] Several studies demonstrated that mTORC1 is activated in pressure-overloaded myocardium, as evidenced by activation of its downstream targets S6K1 and 4E-BP1, phosphorylation of mTOR at Ser2448 and sensitivity to rapamycin inhibition. Moschella et al have shown that both PI3K-dependent and -independent mechanisms regulate mTORC1 activation in cardiomyocytes.[139] Class IA PI3K, activated by growth factors and insulin, class IB PI3K, activated by adrenergic stimulation,[140] or class III PI3K, activated during nutrient and amino acid availability,[141] can activate mTORC1 in cardiac muscle cells. Compared to mTORC1 much less is known about mTORC2 in the heart. p21-activated kinase (PAK) activates Akt at Ser473, a downstream target of mTORC2, in adult heart and in neonatal rat cardiomyocytes[142] but a direct role of mTORC2 has not yet been demonstrated. Studies suggested that nuclear localization of phosphorylated Akt plays a survival role in many cells types including cardiomyocytes.[143]

### 2.4.1 Activation of mTOR complexes during cardiac hypertrophy

As mentioned before, a read-out of mTORC1 activity is the phosphorylation of S6K1 at Thr389, whereas the phosphorylation of Akt at Ser473 generally indicates mTORC2 activity. *In vivo* models of pressure- or volume-overload and *in vitro* studies using hypertrophic stimuli in isolated neonatal or adult cardiomyocytes lead to the phosphorylation of S6K1 at Thr389.[144-148] Furthermore, such agonist-induced phosphorylation of S6K1 was blocked by

rapamycin pretreatment, indicating the requirement of active of mTORC1 during hypertrophic growth of cardiomyocytes.[139, 149] Stimulation of myocytes by insulin and to a lesser extent by RGD- (arginine-glycine-aspartic acid containing) peptides or mechanical stimulation of myocardium by pressure-overload induces phosphorylation of Akt at both Thr308 and Ser473, suggesting a possible role for mTORC2 in hypertrophic cardiomyocytes.[150] As discussed earlier, lack of a direct mTORC2-specific blocker limits our knowledge about the role of mTORC2 in heart. More direct approaches with gene silencing or knockout models are required to investigate its specific functions.

## 2.4.2 Role of mTORC1 in hypertrophic growth of the heart

As a mediator of protein synthesis mTORC1 activity has been demonstrated to be of central importance in cardiac hypertrophy. Studies using rapamycin, the mTORC1 inhibitor, elucidated part of the role of mTOR in cardiac hypertrophy. Rapamycin reverted or partially prevented hypertrophy induced by constitutive activation of Akt,[144] pressure overload,[147, 151-154] thyroid hormone,[155] uremia,[156] hypertension, [153] and myocardial infarction.[157] Although these studies demonstrated a role of mTOR and in particular of mTORC1-mediated protein synthesis in cardiac hypertrophy, other studies have questioned the extent and impact of mTOR function in the adaptive responses of the heart. For example, deletion of the ribosomal S6 kinases, direct downstream effectors of mTORC1, did not attenuate pathological, physiological or insulin-like growth factor-1 receptor-induced cardiac hypertrophy.[147] Additionally, a study by Shen et al reported that hypertrophic growth of the heart in response to physiological or pathological stimuli was not affected in mice expressing a kinase-dead mTOR.[158] In another study, Kemi and coworkers demonstrated that the activation status of the myocardial Akt-mTOR signal transduction pathway could distinguish between physiological and pathological hypertrophy. Exercise training activates the Akt-mTOR pathway while long-term mechanical stimulation by pressure-overload partially inactivated it.[159] Reduced mTOR activity is responsible for cardiac dysfunction induced by the anticancer drug doxorubicin.[160]

Although mTORC1 is considered the primary target of rapamycin, in some cell types long-term treatment with rapamycin also inhibits mTORC2, probably through blocking the assembling of new mTORC2 complex.[99] Furthermore, recent reports have demonstrated rapamycin-resistant functions of mTORC1 in some cells.[106] Studies using rapamycin in vivo, therefore, did not adequately dissect the relative roles of mTORC1 and mTORC2 in

cardiomyocytes. Using cardiac-specific mTOR knockout mouse model, Zhang and coworkers recently showed that mTORC1 regulates cardiac function and myocyte survival through 4E-BP1 inhibition. [161]

### 2.4.3 Role of mTORC2 in protection of the hypertrophying heart

Activated Akt is a key regulator of cell survival and, as mentioned earlier, mTORC2 is responsible for phosphorylation of Akt at Ser473. Activated Akt is sufficient to block cell death induced by a variety of apoptotic stimuli.[162] Transgenic mice over-expressing Akt exhibit increased cardiomyocyte size and contractility,[163-165] whereas in Akt1-deficient mice swim exercise or IGF1 treatment do not induce cardiac hypertrophy, suggesting the importance of Akt activation in the physiological growth of the heart.[166, 167] However, Akt1-deficient mice subjected to pressure overload showed exaggerated pathological hypertrophy and fibrosis,[166, 168] suggesting a role of mTORC2 signaling only in physiological hypertrophy. It was also suggested that acute activation of nuclear Akt is beneficial for the heart.[28] Other AGC kinase family member downstream of mTORC2 like SGK1 is shown to regulate cardiomyocyte survival and hypertrophic response of the heart. In cardiomyocytes, constitutively active SGK1 inhibits apoptosis induced by serum-deprivation or hypoxia, whereas kinase-dead SGK1 increases it.[169] SGK1 is dynamically regulated during acute biomechanical stress and inhibits apoptosis while enhancing hypertrophic response. The PKC isoenzymes are also involved in cardioprotection during the ischemia-reperfusion (reviewed in[170]). In cardiac tissue, a low dose of resveratrol, a polyphenolic phytoalexin found in plants and fruits, induces rictor expression, which then bind to mTOR and leads to activation of Akt Ser473. Treatment with resveratrol induces a cardioprotective effect via induction of autophagy. This effect is lost after silencing of rictor, which in turn decreases resveratrol-induced autophagy.[171] Taken together, we can conclude that mTORC2, either directly or indirectly, plays a vital role in the cardioprotection of the stressed heart.

## 2.5 Role of mTOR in other organs

As a full body knockout of any of the component of mTORC1 or mTORC2 is embryonic lethal,[52, 55, 57, 61, 62, 172] studies using rapamycin or tissue-specific knockout of the mTORC components were used to characterize their role in a specific organ or tissue system. Using such approaches, many of the mTOR downstream functions in different organs have been elucidated recently.

Mice with skeletal muscle specific *raptor* knockout showed downregulation of proteins involved in mitochondrial biogenesis and increased glycogen storage along with muscle dystrophy.[173] In case of muscle specific *rictor* knockout, no phenotype or little with glucose intolerance was observed.[173, 174] Adipose-specific *raptor* knockout mice are resistant to diet-induced obesity show improved glucose tolerance and insulin sensitivity, and are lean in nature.[175] In contrast, adipose-specific *rictor* knockout mice demonstrated increased body size due to enlargement of the non-adipose organs such as heart, kidney, spleen and bone. These mice are hyper-insulinemic with a bigger pancreas, but glucose tolerant.[176] A study by Kumar et al with fat cell-specific *rictor* deletion shows impairment of glucose and lipid metabolism.[177] Next to its regulatory role in organ and whole body metabolism, mTOR has been shown to play major role in neurological and inflammatory diseases (reviewed in[178]). mTORC2 also plays tissue specific roles in the pancreas, brain and immune system (reviewed in[119]).

## 2.6 Aims of the thesis

The main aim of this thesis work is to evaluate the different roles of mTORC1 and mTORC2 in the mouse heart. Previously, with the help of rapamycin, some of the functions of mTORC1 were analyzed, whereas very little was known about the role of mTORC2 in the mouse heart due to the lack of specific inhibitors. A full body knockout of any of the components of mTORC1 or mTORC2 is embryonic lethal. Therefore, we employed an inducible tissue-specific deletion approach to reduce mTORC1 or mTORC2 activity in the mouse heart.

The first part of the dissertation focuses on the role of mTORC1 during the adaptation of the heart to physiological or pathological increases in workload as well as during the maintenance of normal cardiac homeostasis. To achieve mTORC1-specific inactivation, we conditionally ablated raptor, an mTORC1-specific and -essential component, from cardiomyocytes in the mouse heart.

The second part of the dissertation focuses on the characterization of mice with cardiac-specific mTORC2 inactivation. The role of mTORC2 was evaluated during postnatal growth as well as in pathological hypertrophic growth induced by pressure-overload. To achieve this, rictor, an essential and specific component to mTORC2 was selectively deleted from the mouse heart.

# **Results**

# 3. Results

## 3.1 Characterization of the function of mTORC1 in the mouse heart

The results of this study have been published,

Shende et al., Circulation 2011; 123; 1073- 1082

# Cardiac raptor ablation impairs adaptive hypertrophy, alters metabolic gene expression and causes heart failure in mice.

*Pankaj Shende, MSc[1]; Isabelle Plaisance, PhD[1]; Christian Morandi, MSc[1]; Corinne Pellieux, PhD[2]; Corinne Berthonneche, PhD[3]; Francesco Zorzato, MD[1]; Jaya Krishnan, PhD[4]; René Lerch, MD[2]; Michael N. Hall, PhD[5]; Markus A. Rüegg, PhD[5]; Thierry Pedrazzini, PhD[3]; and Marijke Brink, PhD[1]*

*[1]Department of Biomedicine, University of Basel and University Hospital Basel; [2]Medical Research Foundation and Cardiology Division, University of Geneva and University Hospital Geneva; [3]Department of Medicine and Cardiovascular Assessment Facility, University of Lausanne Medical School; [4]ETH Zurich; [5]Biozentrum, University of Basel; Switzerland*

Correspondence:

Marijke Brink

CardioBiology, Department of Biomedicine

University of Basel and University Hospital Basel

Hebelstrasse 20, CH-4051 Basel

Tel: +41 61 265 33 61, Fax: +41 61 265 23 50

E-mail: marijke.brink@unibas.ch

# Summary

***Background*** – Cardiac hypertrophy involves growth responses to a variety of stimuli triggered by increased workload. It is an independent risk factor for heart failure and sudden death. Mammalian target of rapamycin (mTOR) plays a key role in cellular growth responses by integrating growth factor and energy status signals. It is found in two structurally and functionally distinct multiprotein complexes called mTOR complex (mTORC)1 and mTORC2. The role of each of these branches of mTOR-signaling in the adult heart is currently unknown.

***Methods and Results*** – We generated mice with deficient myocardial mTORC1 activity by targeted ablation of raptor, which encodes an essential component of mTORC1, during adulthood. At three weeks after the deletion, atrial and brain natriuretic peptide and β-myosin heavy chain were strongly induced; multiple genes involved in the regulation of energy metabolism were altered, while cardiac function was normal. Function deteriorated rapidly afterwards resulting in dilated cardiomyopathy and high mortality within six weeks. Aortic banding-induced pathological overload resulted in severe dilated cardiomyopathy already at one week without a prior phase of adaptive hypertrophy. The mechanism involved a lack of adaptive cardiomyocyte growth via blunted protein synthesis capacity, as supported by reduced phosphorylation of ribosomal S6K1 and 4E-BP1. In addition, reduced mitochondrial content, a shift in metabolic substrate use and increased apoptosis and autophagy were observed.

***Conclusions*** – Our results demonstrate an essential function for mTORC1 in the heart under physiological as well as pathological conditions, and are relevant for the understanding of disease states in which the insulin/insulin-like growth factor signaling axis is affected such as diabetes, heart failure, or after cancer therapy.

**Key Words:** heart failure; hypertrophy; myocardial metabolism; signal transduction

# Introduction

Although cardiac hypertrophy is a growth response that initially normalizes wall tension, it is associated with an unfavorable outcome: affected patients are threatened with sudden death or progression to heart failure.[32] Much research is therefore aimed at understanding myocardial growth regulation, and in this setting the IGF/PI3-kinase/Akt signaling cascade has been studied extensively.[179, 180] Experiments with cultured cardiomyocytes have suggested that downstream of Akt, mammalian target of rapamycin (mTOR) mediates responses to pathological stimuli.[145, 181] mTOR is an evolutionary conserved Ser/Thr kinase known to control cell growth.[182] Nutrient, energy and growth factor shortage will impair mTOR activity, resulting in diverse effects including the slow-down of macromolecule synthesis, enhanced autophagy and activation of nutrient- or stress-responsive transcription factors. mTOR is found in two structurally and functionally distinct multiprotein complexes termed mTOR complex (mTORC)1 and mTORC2. The two best characterized substrates of mTORC1 are S6 kinase (S6K) and eukaryotic initiation factor (eIF)4E-binding protein (4E-BP), through which mTORC1 regulates cap-dependent protein translation.[183] In addition, numerous novel effects downstream of mTORC1, not all related to translational activation, have recently been identified (reviewed in[36, 78, 184]). For instance, mTORC1 regulates autophagy and membrane trafficking for the delivery of nutrient transporters to the cell surface. mTORC2 controls actin organization and most likely also other processes that remain to be elucidated. The role of these distinct branches of mTOR signaling in cardiac tissue has not been investigated.

Support for a role of mTOR in pathological hypertrophy was provided in studies with rapamycin, which regressed or partially prevented hypertrophy induced by constitutive activation of Akt[144] and acute or sustained pressure overload.[147, 152-154, 163] However, other studies have challenged the importance of mTOR-mediated protein synthesis and growth. For example, deletion of the ribosomal S6 kinases, direct downstream effectors of mTOR, did not attenuate pathological, physiological or IGF-receptor-induced cardiac hypertrophy.[147] Moreover, physiological or pathological hypertrophic growth was not affected in mice expressing a kinase-dead mTOR.[158] It should also be noted that although mTORC1 is considered the primary target of rapamycin, long-term rapamycin treatment also inhibits mTORC2 in certain

cell types[99] and on the other hand, rapamycin does not inhibit all mTORC1 functions.[185] Studies using rapamycin systemically, therefore, have not adequately addressed the relative importance of mTORC1 and mTORC2 in cardiomyocytes.

In the present study, we used inducible cre-loxP recombination to delete raptor, which encodes an essential and specific subunit of mTORC1, selectively from cardiomyocytes. We demonstrate that raptor is required for normal physiological function of the heart as well as for the cardiac adaptation to increased workload. The attenuated mTORC1 activity critically affected cardiac protein and energy metabolism, mitochondrial content, apoptosis and autophagy, and rapidly led to cardiac failure.

## Methods

### Animal Models

Mice analyzed in this study were backcrossed to C57BL/6J for 6-8 generations and crossed to obtain mice positive for α-MHC-MerCreMer and carrying two floxed raptor alleles (α-MHC-MerCreMer/raptorfl/fl) or mice positive for α-MHC-MerCreMer carrying the wild-type raptor alleles. Littermates were assigned to the control and knockout groups, with each experimental group consisting of mice derived from at least four litters. None of the groups contained multiple mice from the same litter. Intraperitoneal injections of tamoxifen citrate (20 mg/kg, Sigma, St. Louis, MO) in 60% PBS/40% ethanol were used to induce excision of raptor. Exposures to pressure overload or exercise started two weeks after the last injection. For voluntary exercise, mice were individually housed in cages equipped with a running wheel. Transverse aortic constriction (TAC) was performed and cardiac function determined using the Vevo 770 Ultrasonograph (VisualSonics) as detailed in the supplement, with the investigator blinded to genetic background or treatment group. All animal experiments were carried out according to guidelines for the care and use of laboratory animals and with approval of the Swiss authorities.

### Statistical Analysis

Data are presented as mean±SEM. Differences in means between two groups were evaluated with unpaired 2-tailed Student t tests and those among multiple groups with

1-way analysis of variance (ANOVA) followed by Bonferroni post hoc tests. When cardiac function was measured at multiple timepoints, we used repeated-measures ANOVA. Mortality data was analyzed by the Logrank test. All statistics was performed with GraphPad Prism 4.0 software. P values of <0.05 were considered statistically significant.

### Supplemental Methodology

Routine procedures of surgery, echocardiography, isolated heart measurements, Western blotting, real-time PCR, histology, transmission electron microscopy are detailed in the Supplement.

## Results

### Analysis of Cardiac Raptor Knockout Mice at Two Weeks After Gene Excision

To study the function of mTORC1 in adult mouse heart, we generated mice homozygous for loxP-flanked raptor exon 6[173, 175] and positive for tamoxifen-inducible Cre recombinase driven by the cardiomyocyte-specific α-myosin heavy chain promoter (α-MHC-MerCreMer/raptorfl/fl).[186] Tamoxifen injections at the age of 10-11 weeks for five days induced Cre-mediated recombination, and Western analysis of protein lysates confirmed that raptor protein was reduced by 69% in cardiac (P=0.004), but not in skeletal muscle (Figure 1A). Thus, tamoxifen at 20 mg/kg body weight[186] was sufficient to induce tissue-specific raptor deletion. Hereafter, we refer to the tamoxifen-treated α-MHC-MerCreMer/raptorfl/fl mice as "raptor-cKO". Figure 1B shows that at two weeks after gene excision, raptor deficiency was accompanied by lower phosphorylated 4E-BP1 (61%, P=0.028) and ribosomal protein S6 (67%, P<0.0001) compared to tamoxifen-treated α-MHC-MerCreMer/raptor+/+ controls. Non-specific metabolic effects, previously reported to occur transiently in α-MHC-MerCreMer transgenic mice peaking at three days after high-dose tamoxifen (80 mg/kg)[187] were excluded, as no differences in expression of metabolic and stress-induced genes existed between three tamoxifen-treated groups: Cre-negative/raptorfl/fl, α-MHC-MerCreMer/raptor+/+ and α-MHC-MerCreMer/raptorfl/fl (raptor-cKO) mice (Figure 1C). Consistently, ex vivo working heart experiments at two weeks after tamoxifen revealed no differences in palmitate

(P=0.87) or glucose (P=0.71) oxidation (Figure 1D) and in developed pressure (P=0.96) or cardiac output (P=0.84) (Figure 1E). Thus, cardiac raptor deletion resulted in reduced levels of phosphorylated 4E-BP1 and S6, but no molecular, metabolic or functional changes were detected at this early timepoint.

### Cardiac Raptor Ablation Leads to Acute Dilated Cardiomyopathy in Response to Pressure Overload

As mTORC1 is known to accelerate protein synthesis via 4E-BP1 and p70-S6K, and protein synthesis is an intrinsic feature of growth responses, we tested whether raptor deficiency diminishes cardiac hypertrophy under conditions of pressure overload and if so, how this affects cardiac function. Raptor-cKO mice and controls were assigned to two subgroups for subsequent transverse aortic constriction (TAC) or sham surgery at two weeks after tamoxifen. Echocardiography prior to surgery showed no difference in cardiac function and geometry between the groups (Supplemental Table I). One week after surgery, the wild-type mice had a significantly thicker left ventricular free wall and septum compared to baseline and compared to values measured in the sham-operated group (Table I). End-systolic and –diastolic left ventricular internal diameters (LVID) were unchanged, and cardiac function was preserved in this wild-type group as ejection fractions (EF) and fractional shortening (FS) were not affected by TAC (Table I).

In contrast, aortic constriction significantly reduced EF and FS in raptor-cKO mice (Table I). This was accompanied by reduced ventricular wall (LVPW) and septal thickness (IVS) as well as an increase in LVID. Moreover, raptor-cKO mice displayed body weight loss, and post mortem analysis showed reduced epidydimal fat pad and gastrocnemius weights (Table I), a cachectic phenotype reminiscent of advanced congestive heart failure. Together, these data showed that raptor-cKO mice rapidly developed dilated cardiomyopathy and severe cardiac dysfunction in response to pressure overload.

### Raptor Knockout Mice Do Not Increase Heart Weight and Cardiomyocyte Cross-Sectional Area After Aortic Constriction, but ANP, BNP and $\beta$-MHC Are Induced

To evaluate the development of hypertrophy, we determined ventricular weight to tibia length ratios (VW/TL) one week after TAC (Figure 2A). No differences existed

between the sham-operated wild-type and raptor-cKO groups. In TAC-operated wild-type mice, VW/TL showed an increase in heart mass of 47% over sham-operated controls. In contrast, raptor-cKO mice demonstrated no hypertrophic growth. A modest increase in size observed in raptor-cKO mice was due to dilatation of the heart rather than an increase in weight (Figure 2B). To assess whether this impaired adaptive response was related to an inability to induce an increase in cardiomyocyte size, we stained cardiac sections with wheat germ agglutinin (Figure 2C). TAC increased cardiomyocyte cross-sectional area (CSA) in wild-type mice by 50%. In contrast, the CSA of cardiomyocytes in raptor-cKO mice after TAC was not different from that in sham-operated mice.

Quantitative increases in cardiac mass after pressure overload are usually accompanied by the re-expression of a fetal gene program. Already under basal conditions, raptor deficiency reduced $\alpha$-MHC to 52%, whereas it robustly increased $\beta$-MHC, ANP, and BNP mRNA levels by 12.3-, 25.9- and 12.2-fold compared to wild-type, respectively. For $\beta$-MHC and ANP these changes were similar to those observed after TAC in wild-type mice (Figure 3A). In raptor-cKO mice subjected to TAC, $\beta$-MHC and BNP mRNA increased even further. In contrast, $\alpha$-skeletal actin was not changed after raptor deletion in sham mice. After TAC, its expression increased in wild-type as expected, but this increase was attenuated in the raptor-cKO mice (Figure 3A), suggesting that its induction depends on mTORC1. Along with mRNA levels, protein amounts of ANP and $\beta$-MHC were increased in hearts of raptor-cKO (Figure 3B and C). The observed induction of compensatory genes under baseline conditions indicates that raptor deficiency is a stress stimulus for the heart.

### *Raptor Deficiency Alters Mediators of Protein Synthesis and Degradation*

To address the mechanisms behind the observed defects, we analyzed protein extracts by Western blotting. In wild-type mice, TAC significantly increased the cardiac amounts of Akt and mTOR, increases that were absent after raptor deletion (Figure 4A and B). Total protein of 4E-BP1, direct downstream target of mTOR, was also increased after TAC, and the presence of the two higher molecular weight bands $\beta$ and $\gamma$ indicated that it was to a large extent phosphorylated (Figure 4A and C). In the raptor-cKO mice a shift toward the lower molecular weight $\alpha$-band indicated reduced 4E-BP1 phosphorylation, which was confirmed for the TAC-operated mice after

quantification of the β-band (Figure 4C) or with an antibody to the Thr70 site of 4E-BP1 (Figure 4A). Moreover, while total p70-S6K1 protein was equal for all groups, phosphorylation of its effector S6 was decreased in raptor-cKO hearts compared to pressure-overloaded hearts of wild-types (Figure 4A and C). Interestingly, despite the fact that raptor deficiency was accompanied by reduced total Akt protein, Akt phosphorylation at Thr308 and Ser473 was markedly increased compared to wild-type mice (Figure 4D). Finally, glycogen synthase kinase 3β (GSK3β), a target of Akt, showed strongest phosphorylation at Ser9 in the raptor-cKO mice subjected to sham-surgery (Figure 4A and D). Importantly, hyperphosphorylation of Akt at Ser473, one of the known downstream targets of mTORC2, indicated selective inhibition of the mTORC1 pathway solely.

Figure 4E shows that muscle atrophy F-box (MAFbx) and muscle-specific RING finger protein (MuRF)1 mRNA levels were modestly decreased under baseline conditions, whereas MuRF3 mRNA was significantly higher after TAC in raptor-cKO compared to wild-type. Thus, reduced mTORC1 activity affected protein synthesis as well as degradation pathways.

### Raptor Deficiency Leads to Cardiac Dysfunction and Mortality under Physiological Conditions

As we observed a re-induction of the fetal gene program without concurrent changes in function under conditions of normal cardiac load at three weeks of gene ablation, we followed up on the consequences of raptor deletion at later timepoints under physiological conditions, i.e. in sedentary mice or mice exercising on a voluntary basis in a running wheel. Ejection fractions were normal in near to all mice up to three weeks after raptor deletion, but decreased to lower values at 38 days (Figure 5, P<0.01). Raptor-cKO mice started to die during the fifth week after tamoxifen. At that timepoint, a trend towards increased mortality was observed in exercising (64%, n=14) compared to sedentary (36%, n=11) mice (P=0.097). Surviving sedentary raptor-cKO mice had a mean EF of 17.3±1.9%, LVPW of 0.60±0.03 and 0.71±0.02 mm, and LVID of 5.0±0.1 and 4.6±0.1 mm during diastole and systole, respectively. After exercise, similar values were obtained. Thus, the EF was 18.9±7.5%, the LVPWd/s 0.63±0.01/0.69±0.02 mm, and the LVIDd/s 4.8±0.1/4.4±0.2 mm. These

values indicate a significant loss of function culminating with sudden death. None of the wild-type mice died during this period.

### *Raptor Deficiency Causes a Switch from Fatty Acid to Glucose Oxidation*

The heart is known to predominantly oxidize fatty acids, but switches to carbohydrate metabolism in response to neurohormonal, nutritional, hypoxic, or other stress stimuli.[188, 189] Next to its role in protein synthesis, recent studies have shown that mTOR modulates energy metabolism.[173, 175, 190] We therefore tested in ex vivo working heart experiments whether cardiac raptor ablation changes metabolic substrate use. At two weeks after tamoxifen substrate use was normal, but at later timepoints, palmitate oxidation was decreased to 51% and glucose oxidation increased by 24% above wild-type levels (Figure 6A). In subsequent experiments we tested whether at three weeks after tamoxifen, a timepoint at which cardiac function was still normal, raptor ablation changed gene expression of factors that regulate substrate use. In the heart, fatty acid oxidation is regulated by ERRα and PPARα, binding partners of PGC1α.[191] A decrease of ERRα to 75% in the raptor-cKO mice did not reach significance, but PPARα and PGC1α were significantly reduced to 40.5% and 52.3% of wild-types, respectively (Figure 6B). These decreases were associated with reduced transcript levels of the fatty acid regulatory genes known to be dependent of PPARα, namely carnitine palmitoyltransferase-Iβ (CPT-Iβ), known for controlling fatty acid transfer into mitochondria, and malonyl-CoA decarboxylase-1 (MCD-1) (Figure 6C). Malonyl-CoA is a strong inhibitor of CPT-Iβ, and reduced decarboxylation by MCD-1 in raptor-cKO mice may therefore, by causing accumulation of malonyl-CoA, contribute to reduce fatty acid oxidation.[192] However, in our study gene expression of the enzyme responsible for synthesis of malonyl-CoA, acetyl-CoA carboxylase (ACC2), was decreased concomitantly (Figure 6C), which may attenuate the increase of malonyl-CoA in the myocardium. Finally, gene expression of succinyl-CoA-3-oxoacid CoA transferase (SCOT), a regulator of ketone body metabolism, was reduced (Figure 6C).

Changes in fatty acid oxidation were associated with changes in glucose transporters. Figure 6D shows that raptor deficiency by itself reduced GLUT4 mRNA levels to 23% of those in wild-type sham mice, an effect far more drastic than that observed after TAC. In contrast, transcripts of GLUT1 were 2.2-fold higher in raptor-

cKO than in wild-types and those of GAPDH, an enzyme of glycolysis, were also increased, consistent with enhanced carbohydrate metabolism. Taken together, our results suggest that mTORC1 is involved in the regulation of metabolic substrate use in the heart.

### *Raptor Knockout Mice Show Abnormal Mitochondria, Increased Apoptosis and Increased Autophagy*

Besides modulating fatty acid oxidation, PGC1α is known to regulate mitochondrial biogenesis. After TAC, raptor deletion resulted in significantly decreased mitochondrial DNA normalized for genomic NADH (P<0.05, Figure 7A). Moreover, ultrastructural analysis revealed swollen mitochondria with irregular cristae as a feature of raptor-cKO mice (Figure 7B). To identify further mechanisms that potentially contributed to the observed phenotype, we assessed apoptosis by immunohistochemistry (Figure 7C). Cleaved caspase-3 appeared increased after raptor deletion, an effect that we confirmed quantitatively by immunoblotting (Figure 7D) and which indicated that apoptotic pathways were activated. mTOR is known to regulate autophagy, a protective mechanism that cells activate in case of nutrient deficiency or other stress. Figure 7E shows that LC3BII was increased after raptor deletion along with ULK1, supporting that autophagy was enhanced. We conclude that changes in mitochondria, apoptosis and autophagy are part of the cascade of events that precede the development of heart failure after mTORC1 inactivation.

## Discussion

In this study we analyzed the function of mTORC1 in the adult mouse heart by conditionally deleting raptor from cardiomyocytes. Raptor-cKO mice had normal cardiac architecture, function and metabolism at two weeks after gene ablation. Function was maintained for up to three weeks, but at this time-point significant changes in metabolic gene expression along with a strong induction of ANP, BNP and β-MHC, indicative of a stress response, were measured. Cardiac function began to deteriorate afterwards and developed all features typical of severe dilated cardiomyopathy at four weeks after raptor ablation. Pressure overload applied to

raptor-cKO mice resulted immediately in severe cardiac dilation with strongly reduced EFs; a prior phase of adaptive cardiomyocyte hypertrophy was missing. With these experiments we established that mTORC1 is a critical mediator of adaptive ventricular growth in conditions of pressure overload, but importantly, that it also is an essential component for cardiac homeostasis under physiological conditions. Our study provides evidence for a causal relationship between depressed mTORC1 activity and cardiac dysfunction.

Metabolic stress may have been one of the early triggers preceding the dysfunction that developed after three weeks and culminated in heart failure in our raptor-cKO mice. This notion is supported by recent studies in which mTORC1 was shown to control mitochondrial gene expression and oxygen consumption via transcriptional mechanisms that involve direct interactions between mTOR and raptor as binding partners of YY1, and PGC1α.[115, 193] Consistently, PGC1α expression was reduced and mitochondrial content and structure were negatively affected in the raptor-cKO mice, in line with our previous report on skeletal muscle.[173] Interestingly, expression of PPARα and ERRα, PGC1α-binding partners that regulate transcription of fatty acid oxidation genes in the heart, was also decreased. The effects were confirmed because CPT-Iβ and MCD-1 were reduced concomitantly. Furthermore, there was a shift in mRNA expression from GLUT4 to GLUT1, and our working heart experiments indeed showed a switch from fatty acid towards glucose oxidation, typically observed after myocardial infarct and in heart failure.[194, 195] Along with these metabolic changes, we found an isoform change towards β-MHC, reminiscent of the switch from fast- to slow-twitch muscle described after raptor ablation in skeletal muscle.[173] As β-MHC generates force in an energetically more economic manner than the α-isoform, it may represent a compensatory energy-preserving effort after raptor ablation. Taken together, our data demonstrate that raptor deletion changes mitochondria and metabolic gene expression at a timepoint that cardiac function and geometry are normal, and that this is followed by increased carbohydrate metabolism and loss of cardiac function. Further studies are required to elucidate how exactly deletion of raptor induces this shift in the metabolic gene program.

Our study also provides support for a role of mTORC1 in regulating cardiac apoptosis and autophagy, because cleaved caspase-3 and LC3B II were increased after raptor ablation. This is in line with what is known for mTORC1 in other cell-

types, in which for example the regulation of autophagy involves direct interactions between raptor and ULK1.[196] Our results also provide additional support for the conclusion of a recent study by Zhang, which were based on the combined inactivation of mTORC1 and mTORC2 after mTOR ablation.[161]

The hearts of sham-operated raptor-cKO mice did not decrease in weight, suggesting either that 4E-BP1 and S6-mediated reductions in protein translation were not sufficient to yield an atrophic response during this time period, or that alternate pathways of protein synthesis were activated, or that degradation via mTORC1-independent pathways was diminished. In support of attenuated degradation, we observed reduced MAFbx and MuRF1 mRNA levels as a possible consequence of the hyperphosphorylated Akt in raptor-cKO hearts. Akt hyperphosphorylation has previously been explained by lacking negative feedback through S6K1, a feedback loop that normally causes IRS-1 degradation thereby controlling Akt phosphorylation.[173, 175, 197] Our present observation of hyperphosphorylated Akt supports the existence of a similar feedback loop in the heart.

The consequences of blunted protein synthesis were more pronounced after TAC and likely became an important reason for precipitated functional deterioration. Accelerated protein synthesis is required for the adaptive hypertrophic response that preserves cardiac function. Consistently, we found an increase in total and phosphorylated levels of multiple mediators of protein synthesis in wild-type and their blockade in the raptor-cKO mice explains why ventricular weight and cardiomyocyte CSA did not increase. The resulting high wall stress likely triggered neurohormonal and inflammatory responses. Moreover, the induction of β-MHC already observed under baseline conditions became significantly more pronounced after TAC and probably contributed to cardiac dysfunction as reported previously.[198] Finally, MuRF3 was induced in TAC-operated raptor-cKO mice, which, consistent with its role in degrading β-MHC,[199] provides another mechanism for the rapid wall thinning and heart failure.

Consistent with our findings after mTORC1 inactivation, rapamycin treatment resulted in reduced hypertrophic responses to hemodynamic stress.[144, 147, 153] Like in our study, β-MHC was reported to be increased after rapamycin, suggesting a stress response of the cardiomyocytes.[147, 154] In contrast, studies with rapamycin reported either preserved function or protection from overload-induced dysfunction.[144, 147] This

discrepancy might be explained by the dosing and timing of the rapamycin treatment. Notably, rapamycin fully inactivated S6K1 but nevertheless, suppression of the growth response to overload was incomplete. This suggests that rapamycin-resistant effects of mTORC1, recently reported for other systems,[200] may have contributed to incomplete inhibition of hypertrophy and maintenance of cardiac function. In addition, a major difference with our model is that rapamycin affects all compartments of the heart, including fibroblasts, microvasculature, and inflammatory cells. While our study demonstrates the essential function of mTORC1 in cardiomyocytes in vivo, extensive further studies are required to dissect its relative importance in other cell types of the heart. In conclusion, our study demonstrates that mTORC1 activity in cardiomyocytes is critical for the preservation of cardiac function in response to pressure overload. Importantly, we show that mTORC1 is also essential under normal workload conditions. Thus, cardiac raptor deficiency caused severe heart failure with high mortality within six weeks after gene ablation in mice. Our study underlines that monitoring of cardiac function in clinical studies with mTOR inhibitors is important.

**Disclosures**

None

**Figure 1**
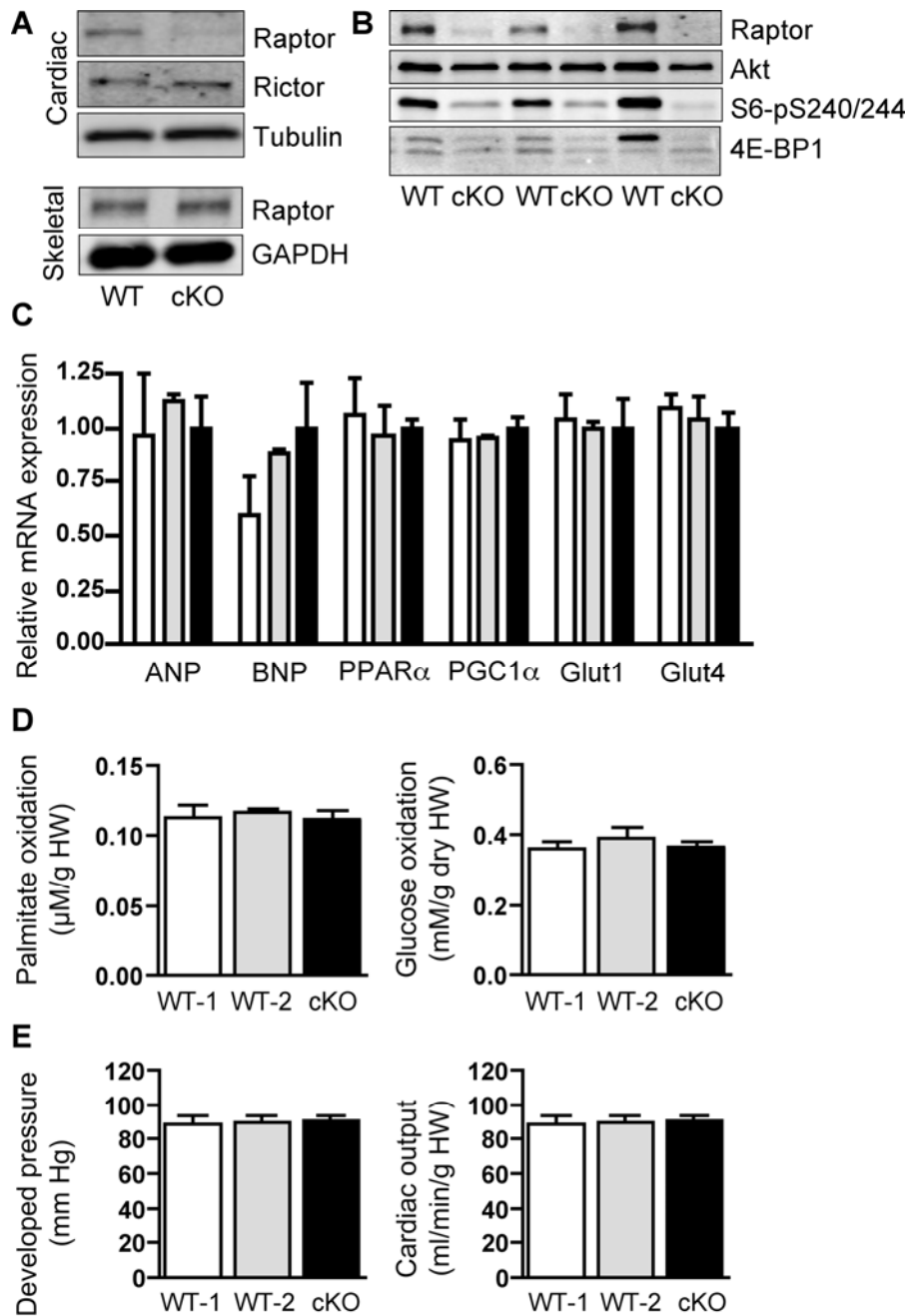


*Figure 1. Functional, molecular and metabolic analysis of raptor-cKO and control mice reveals no differences at two weeks after tamoxifen. Adult male MHC-MerCreMer/raptor$^{fl/fl}$ and control mice were injected with tamoxifen or vehicle for five days and sacrificed two weeks later for analysis by Western blotting (A and B), real-time PCR (C) or ex vivo isolated heart experiments (D and E). For A and B, cardiac (20 µg) or skeletal (10 µg) muscle proteins were separated by SDS-PAGE and probed with antibodies as indicated. WT-1=vehicle/MHC-MerCreMer/raptor$^{fl/fl}$; WT-2=tamoxifen/MHC-MerCreMer/raptor$^{+/+}$; cKO=tamoxifen/MHC-MerCreMer/raptor$^{fl/fl}$; n=3-5 per group. For C, 1-way ANOVA analysis resulted in P-values of 0.90, 0.42, 0.86, 0.81, 0.98 and 0.72 for ANP, BNP, PPARα, PGC1α, Glut1 and Glut4, respectively.*

**Figure 2**
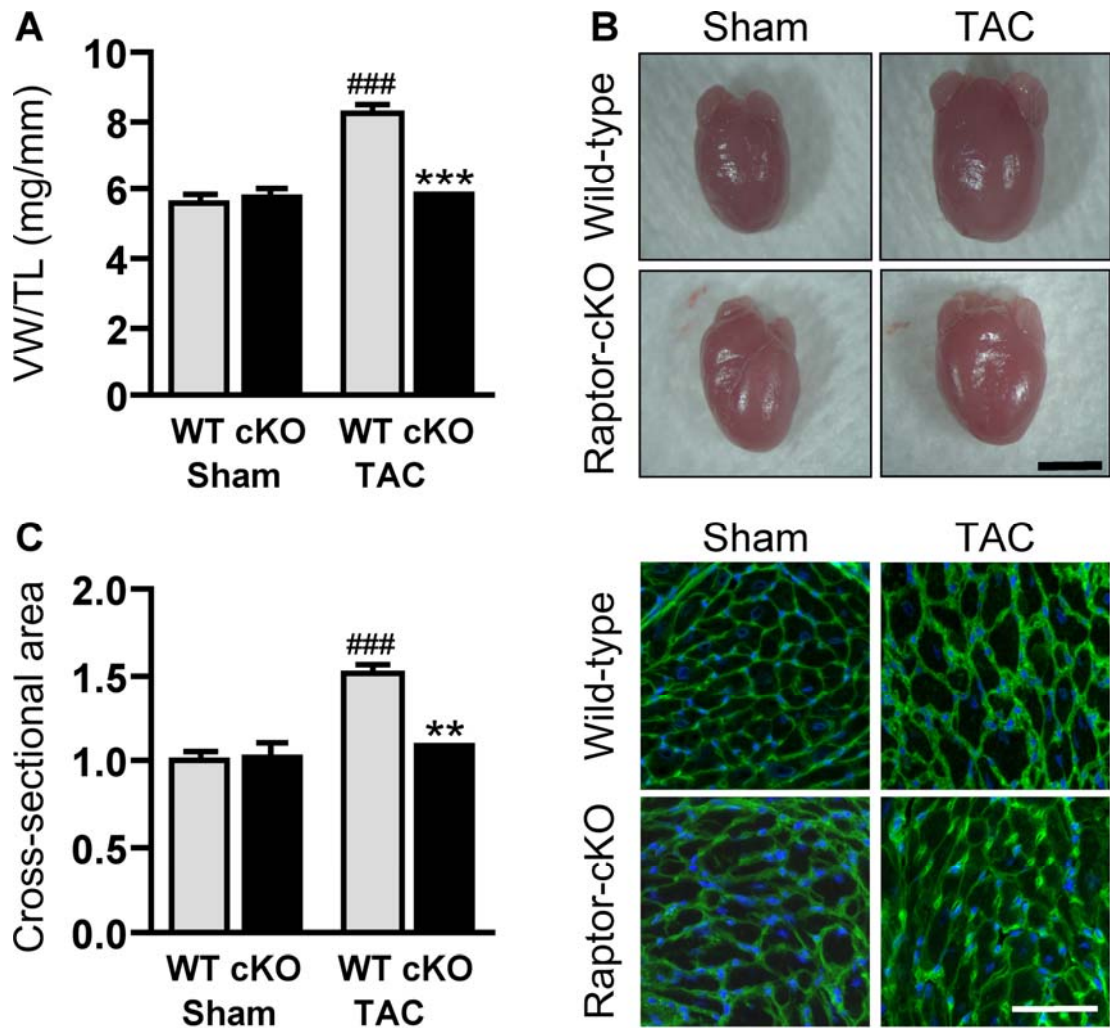


*Figure 2. Raptor deletion prevents TAC-induced hypertrophy. A, ventricular weight to tibia length ratios of wild-type (vehicle/MHC-MerCreMer/raptor$^{fl/fl}$) and raptor-cKO mice (vehicle/MHC-MerCreMer/raptor$^{fl/fl}$) one week after surgery (n=6-8 per group). B, Representative images of the hearts. C, Wheat germ agglutinin staining and quantification of cardiomyocyte cross-sectional area (n=3-4 per group). \*\*\*P<0.001, \*\*P<0.01 for raptor-cKO vs wild-type, $^{###}$P<0.001 for TAC vs sham. Scale bars indicate 5 mm in B and 25 μm in C.*
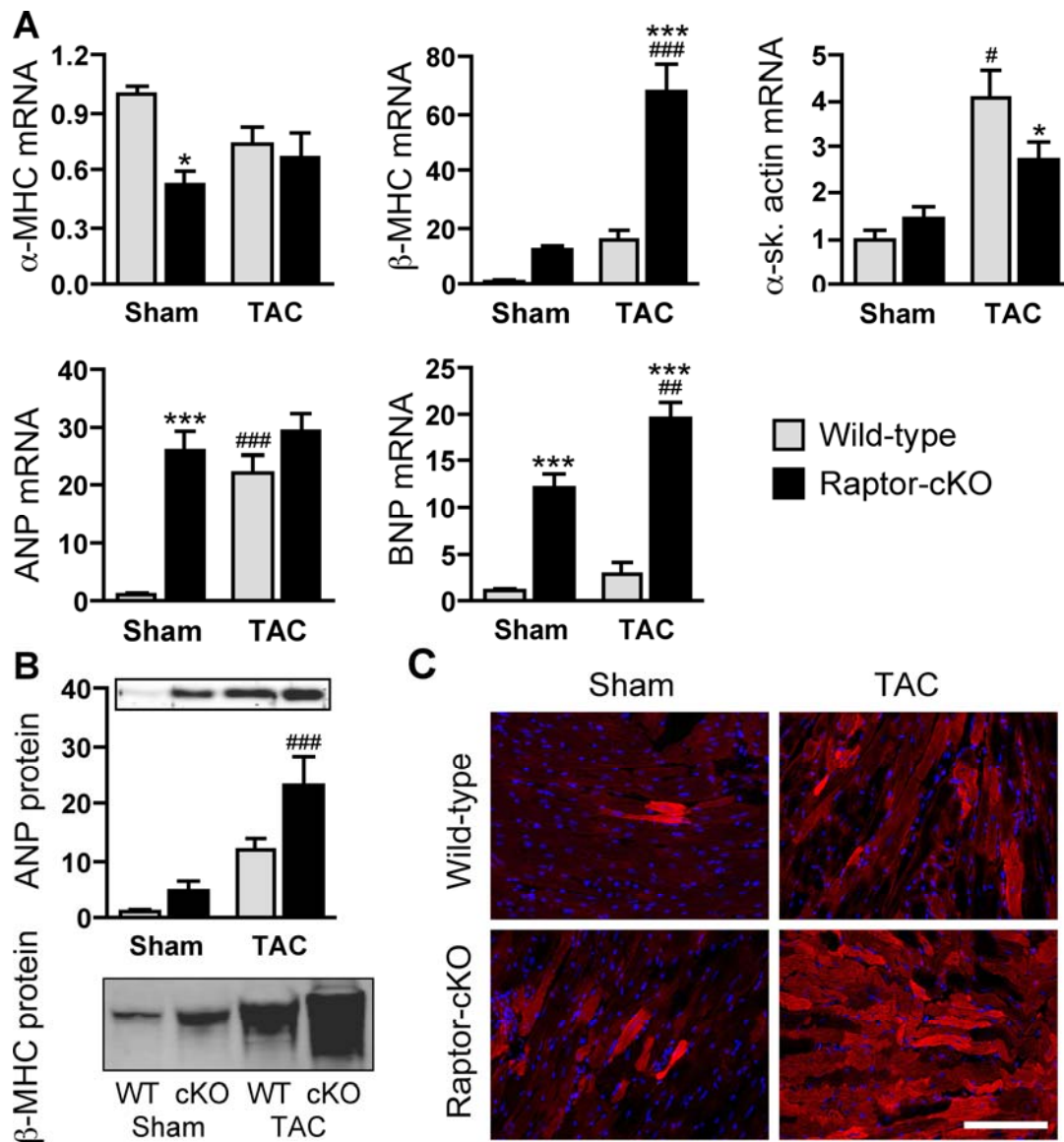
**Figure 3**



*Figure 3. Raptor deficiency induces fetal gene expression in the heart. A, Quantitative PCR analysis to assess relative mRNA levels of the indicated genes one week after sham or TAC surgery (n=4-6 per group; groups as for Fig. 2). B, Analysis of ANP and β-MHC by immunoblotting shows that mRNA induction is correlated with increased protein expression.*
*###P<0.001 and ##P<0.01 for TAC vs sham; ***P<0.001 and *P<0.05 for raptor-cKO vs wild-type. C, Immunofluorescence microscopy confirms increased β-MHC protein in cardiomyocytes. Nuclei were visualized with DAPI. The scale bar represents 25 μm.*
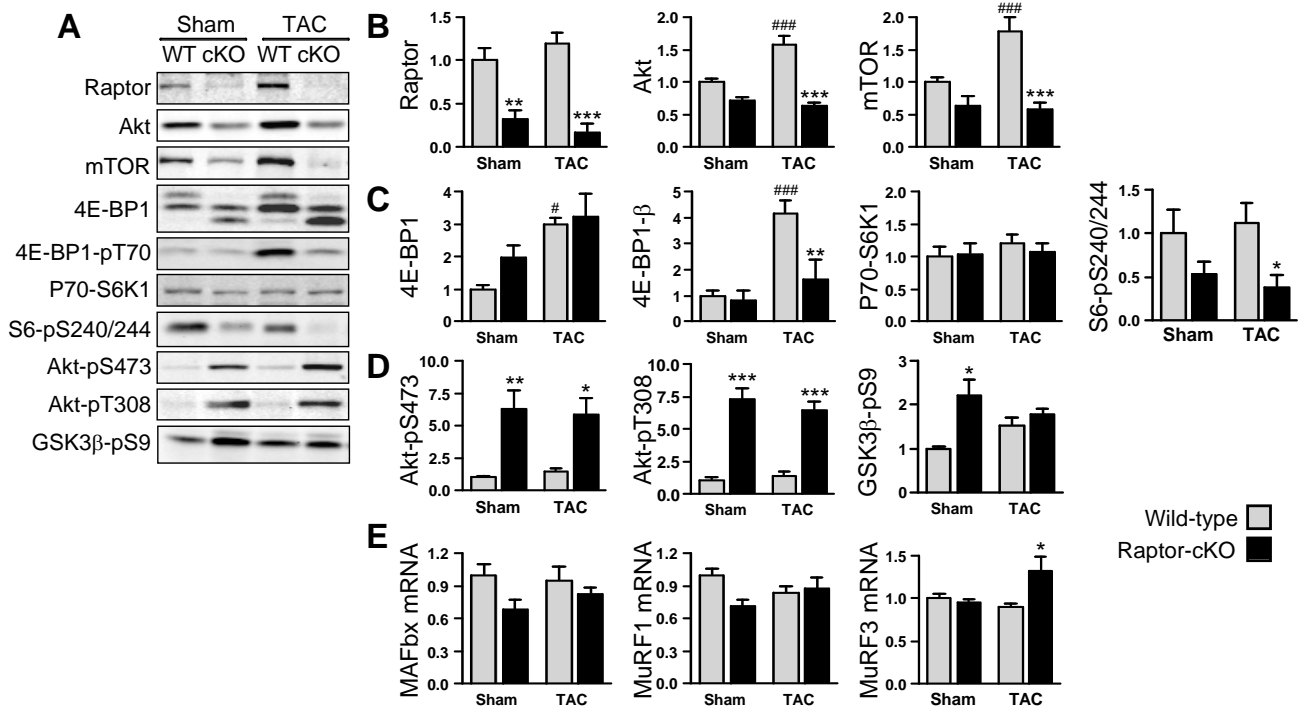
**Figure 4**



***Figure 4.** Effect of raptor deletion on molecules that regulate protein synthesis (A-D) and on gene expression of E3 enzymes involved in proteasomal degradation (E) at one week after surgery with groups as in Figure 2-3. A, Representative immunoblots of cardiac protein extracts (20 μg). Equal loading was verified with Ponceau C, and membranes probed with specific antibodies to indicated proteins. For B-D, labeled bands were quantitated using LI-COR Odyssey imaging software (n=6 per group). For E, total RNA was used to determine relative mRNA levels by quantitative PCR with primers as listed in the online supplement (n=4 per group). [###]P<0.001 and [#]P<0.05 for TAC vs sham; ***P<0.001, **P<0.01 and *P<0.05 for raptor-cKO vs wild-type.*

**Figure 5**
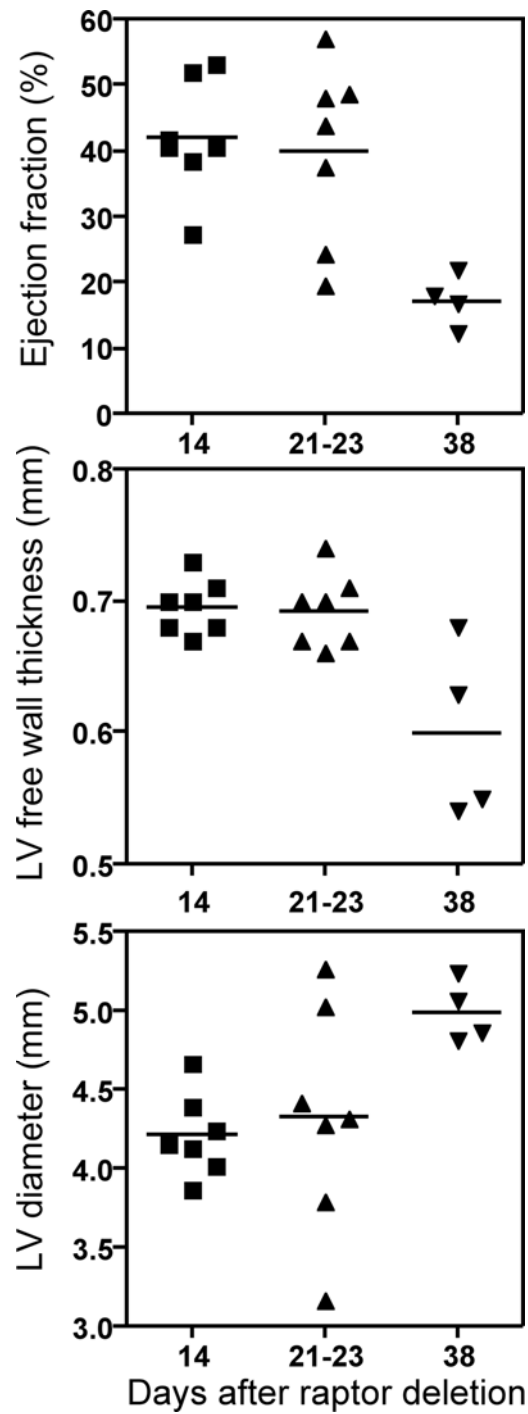


*Figure 5*. *Time course of changes in cardiac function and geometry in sedentary raptor-cKO mice. Echocardiography was performed at 14, 21-23 and 38 days after stopping tamoxifen. Shown are the ejection fractions as well as LV free wall thickness and diameter during diastole.*

**Figure 6**
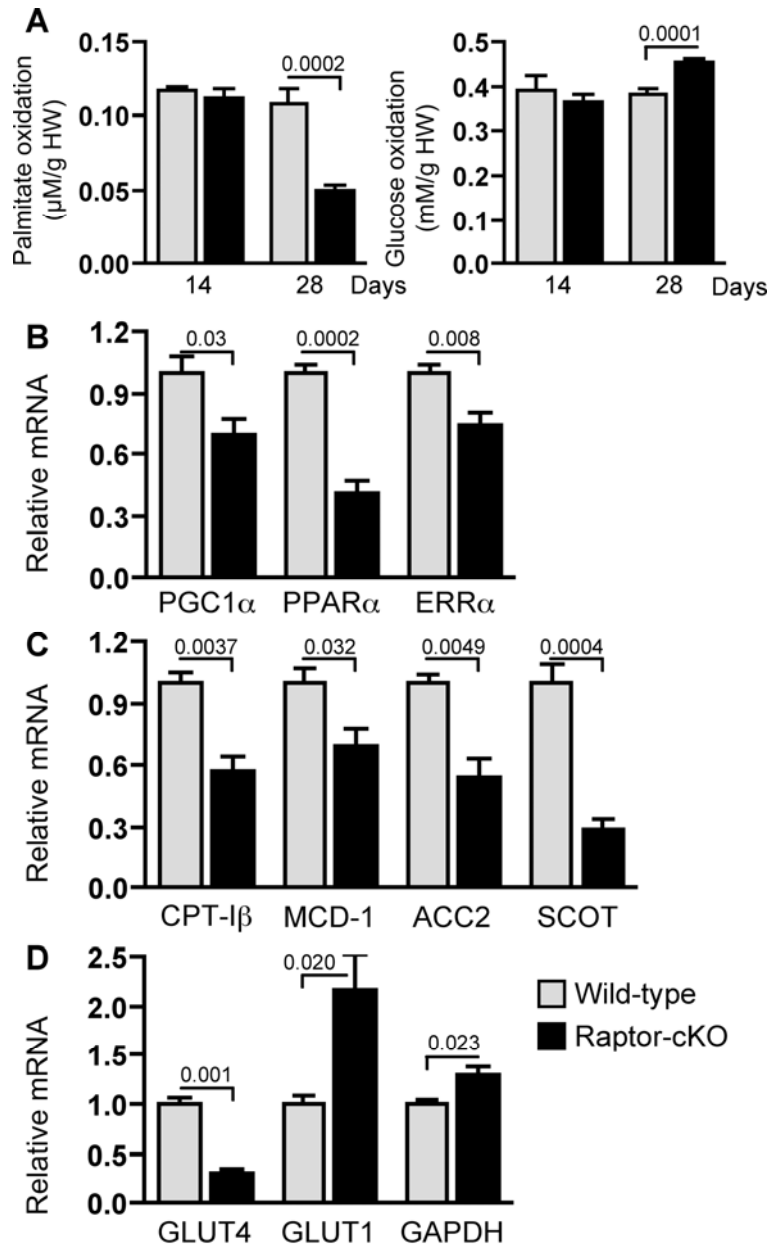


*Figure 6. Raptor deletion changes cardiac substrate oxidation (A) and metabolic gene expression (B-D). A, Ex vivo palmitate and glucose oxidation rates were measured in isolated working hearts of raptor-cKO and controls (tamoxifen/MHC-MerCreMer/raptor^{+/+}, n=4-7 per group) at two and four weeks after tamoxifen. B-D, Cardiac RNA extracts from mice sacrificed three weeks after raptor deletion were analyzed by real-time PCR with primers specific to regulators of fatty acid metabolism (B-C) and carbohydrate metabolism (D) (n=4 per group).*

**Figure 7**
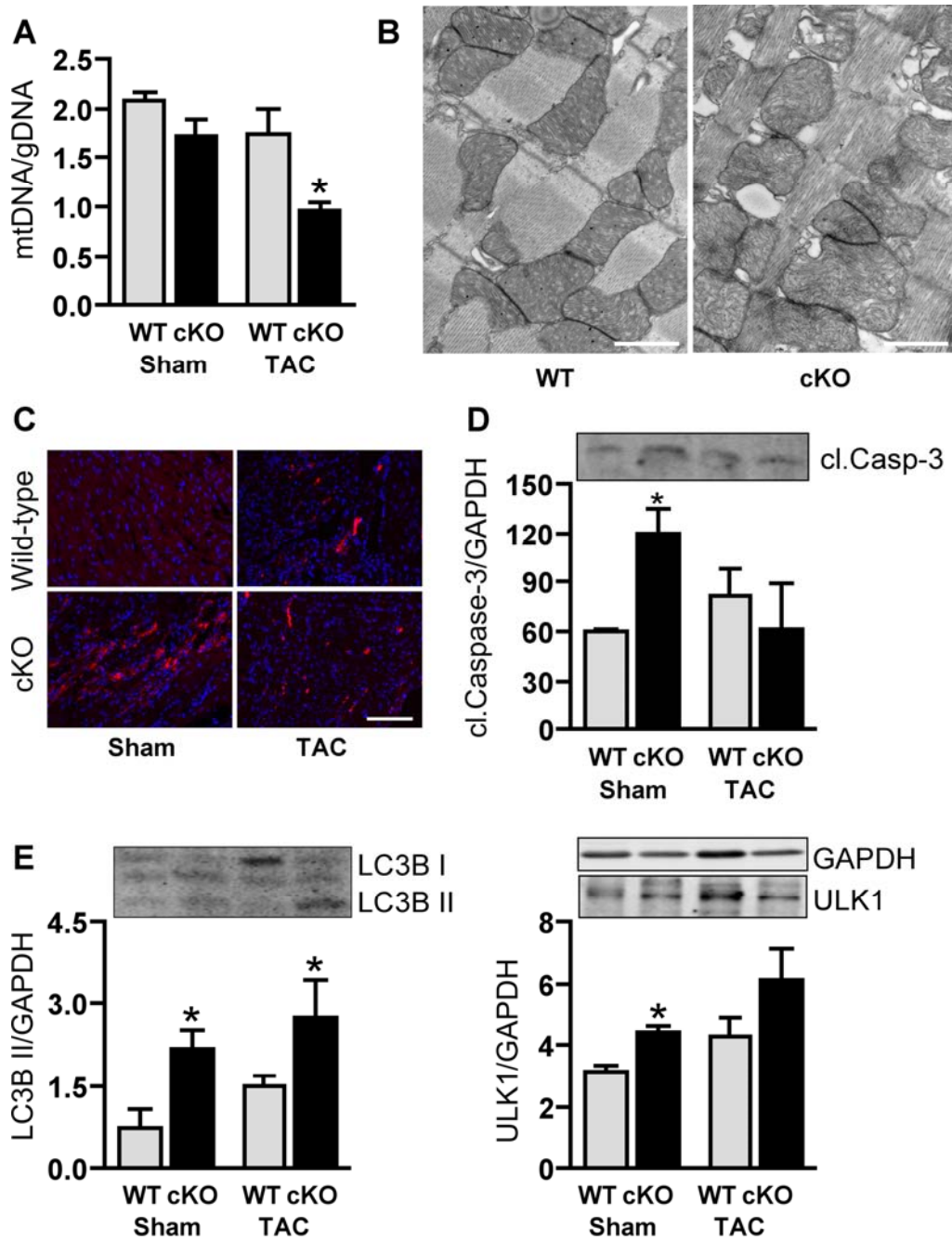


*Figure 7*. *Raptor deletion changes mitochondrial content (A) and structure (B), and increases caspase-3 cleavage (C-D) and autophagy (E). A, Mitochondrial DNA (D-loop non-coding region) was measured in total DNA by quantitative PCR and normalized for genomic Ndufv1. B, Representative transmission electron micrographs of raptor-cKO and wild-type (tamoxifen/MHC-MerCreMer/raptor$^{+/+}$) at three weeks after tamoxifen (bar: 1 μm). For C, cryosections were incubated with an antibody selective for the cleaved fragment of caspase-3. D, Quantification of cleaved caspase-3 by immunoblotting. E, Quantification of the autophagy markers LC3B II and ULK1 (n=3-4 per group, groups as in Fig. 2-4). \*P<0.05 for raptor-cKO vs wild-type.*

# Supplemental material

### *Generation of Inducible, Cardiac-Specific Raptor Knockout Mice*

Mice homozygous for loxP-flanked raptor exon 6[173, 175] were crossed with mice expressing Cre recombinase under the control of the cardiomyocyte-specific α-myosin heavy chain (MHC) promoter in a tamoxifen-inducible manner.[186] Resulting heterozygous floxed raptor mice positive for the α-MHC-MerCreMer transgene (α-MHC-MerCreMer/raptorfl/+) were further mated with homozygous floxed raptor (raptorfl/fl) mice to obtain mice positive for α-MHC-MerCreMer and carrying two floxed raptor alleles (α-MHC-MerCreMer/raptorfl/fl). Mice analyzed in this study were backcrossed to C57BL/6J for 6-8 generations. PCR genotyping of floxed raptor mice was performed using the forward primer: 5'-ATG GTA GCA GGC ACA CTC TTC ATG-3' and reverse primer: 5'-GCT AAA CAT TCA GTC CCT AAT C-3', resulting in an amplicon of 228 bp for floxed raptor and of 141 bp in case of wild-type allele. Genotyping of mice for the presence of Cre recombinase was performed using the forward primer 5'-GTT CGC AAG AAC CTG ATG GCA A-3' and the reverse primer 5'-CTA GAG CCT GTT TTG CAC GTT C-3' yielding a product of 340 bp for the recombined allele and no product for the wild-type.

### *Experimental models*

For voluntary exercise, mice were individually housed in cages equipped with a running wheel. A sensor was attached to the wheel and connected to a computer for continuous monitoring of running activity. Transverse aortic constriction was performed and cardiac function determined using the Vevo 770 Ultrasonograph (VisualSonics) according to published procedures.[173, 201, 202] Both models were started at two weeks after the last tamoxifen injection.

### *Wheat Germ Agglutinin Staining and Immunohistochemistry*

Hearts were arrested with ice cold 0.9% NaCl and frozen in OCT (Medite, Nunningen, Switzerland) using isopentane cooled in liquid nitrogen. Cryosections were fixed for 20 min at RT with 4% paraformaldehyde and washed with PBS-glycine (100 mmol/l) for 10 min. Sections were permeabilised with 0.1% Triton X-100 for 20 min and incubated with FITC-labeled wheat germ agglutinin (4 µg/ml) for

90 min at RT. Cross sectional areas of at least hundred cardiomyocytes in three independent sections of 3-4 mice per group were measured. For immunohistochemistry, sections were incubated with antibodies to β-MHC (Abcam) and cleaved caspase-3 (Becton, Dickinson and Company), followed by Cy3- (Jackson Immunoresearch) or Alexa555- (Molecular Probes) labeled secondary antibodies. Nuclei were stained with DAPI (Sigma, 1 µg/ml).

### Protein Extraction and Western Blot Analysis

Tissue for protein analysis was flash-frozen in liquid nitrogen and stored at –80°C. Total protein was extracted using a Polytron homogenizer and RIPA buffer (50 mmol/l Tris-HCl, pH=7.4, 150 mmol/l NaCl, 1% NP40, 0.25% Na deoxycholate, 5 mmol/l EDTA, 10 µmol/l leupeptin, 1 mg/ml benzamidine, 100 U/ml bacitracin, 0.1 TIU/mL aprotinin, 1 mg/ml TAME, 1 mg/ml BAEE, 10 mmol/l Na-pyrophosphate, 10 mmol/l glycerophosphate 0.5 % phosphatase inhibitor cocktail 1 and 2 (Sigma), 2 mmol/l Pefabloc plus and "Mini-Complete" protease inhibitor cocktail (Roche Diagnostics)). Equal amounts of protein were separated on SDS-PAGE and after transfer to PVDF membrane, incubated overnight with primary antibody. The unbound primary antibody was removed by 3-4 consecutive washings, the membrane incubated with IRDye labeled secondary antibody for 1 h, and the signal detected and quantitated using Odyssey imaging software (LI-COR Biosciences, Lincoln, Nevada, USA).

Polyclonal rabbit antibodies against phospho-Akt (Ser473), phospho-Akt (Thr308), Akt total, GSK3β (Ser9), phospho-4E-BP1 (Thr70), 4E-BP1 total, phospho-S6 kinase (Ser240/244), p70 S6 kinase, mTOR and monoclonal antibody against raptor were all from Cell Signaling Technology (Danvers, MA). The GAPDH mouse monoclonal antibody and ANP rabbit polyclonal antibody were from Santa Cruz Biotechnology (Santa Cruz, CA).

### RNA Preparation and Quantitative RT-PCR

Total RNA was extracted from frozen hearts using Tri Reagent (Sigma) and treated with DNAse I (Ambion, Austin, TX). Concentration, purity and quality of the RNA were assessed by spectrophotometry and agarose gel eletrophoresis. cDNA was prepared from these total RNA extracts using the high capacity DNA reverse

transcription kit (Applied Biosystems). The product was diluted 1:100 and 5 µl were amplified on a 7500 fast real-time PCR system (Applied Biosystems), with 1x ITaQ SYBR Green Supermix Kit (Bio-Rad, Reinach, Switzerland) and 300 nmol/l for forward and reverse primers in a total volume of 20 µl. The mRNA level was based on the critical threshold (Ct) value. The primers used for the real time PCR were designed with the software Primers Express (Applied Biosystems, Foster City, CA) and synthesized by Microsynth (Balgach, Switzerland). Primer sequences for quantitative real-time PCR are provided in the following table:

Table: Primers used in RT-PCR

| Gene | Forward primer | Reverse primer |
|------|----------------|----------------|
| *GAPDH* | 5'-CGG CCG CAT CTT CTT GTG-3' | 5'-CAC CGA CCT TCA CCA TTT TGT-3' |
| *β-actin* | 5'-CAG CTT CTT TGC AGC TCC TT-3' | 5'-GCA GCG ATA TCG TCA TCC A-3' |
| *ANP* | 5'-TGG GAC CCC TCC GAT AGA TC-3' | 5'-TCG TGA TAG ATG AAG GCA GGA A-3' |
| *α-MHC* | 5'-CTA CGC GGC CTG GAT GAT-3' | 5'-GCC ACT TGT AGG GGT TGA C-3' |
| *β-MHC* | 5'-TTG AGA ATC CAA GGC TCA GC-3' | 5'-CTT CTC AGA CTT CCG CAG GA-3' |
| *α-sk.actin* | 5'-CAG CTC TGG CTC CCA GCA CC-3' | 5'-AAT GGC TGG CTT TAA TGC TTC A-3' |
| *GLUT1* | 5'-GGG CAT GTG CTT CCA GTA TGT-3' | 5'-ACG AGG AGC ACC GTG AAG AT-3' |
| *GLUT4* | 5'-AGA GAG AGC GTC CAA TGT CCT T-3' | 5'-CCG ACT CGA AGA TGC TGG TTG A-3' |
| *PGC1α* | 5'-AAC GAT GAC CCT CCT CAC AC-3' | 5'-TCT GGG GTC AGA GGA AGA GA-3' |
| *MAFbx* | 5'-CTC TGT ACC ATG CCG TTC CT-3' | 5'-GGC TGC TGA ACA GAT TCT CC-3' |
| *MuRF1* | 5'-ACG AGA AGA GAG GCG AGC TG-3' | 5'-CTT GGC ACT TGA GAG GAA GG-3' |
| *MuRF3* | 5'-CCA TTT ACA AAC GCC AGA AGAGT-3' | 5'-GCC CGC CAC CAG CAT-3' |
| *MCD1* | 5'-ACC CCT GGT GGT TCT GCA T-3' | 5'-TCG AGG GCA CTC CTT CA-3' |
| *CPT1β* | 5'-CCG CAG GAG GAA GGG TAG AG-3' | 5'-GTC TCA TCG TCA GGG TTG TAG CT-3' |
| *ACC2* | 5'-GAA TCT CAC GCG CCT ACT ATG A-3' | 5'-GAA ATC TCT GTG CAG GTC CAG TT-3' |
| *PPARα* | 5'-CAA GGC CTC AGG GTA CCA CT-3' | 5'-TTG CAG CTC CGA TCA CAC TT-3' |
| *SCOT* | 5'-AAG CCA TCA CGG GAG ATT TT-3' | 5'-CCA CGG TAG TTC CTG CAG C-3' |

***Glucose and Palmitate Oxidation and Cardiac Function During Ex Vivo Heart Perfusion***

Cardiac function and substrate oxidation were measured in isolated perfused hearts essentially as described.[203] Briefly, the hearts were perfused with a modified Krebs–Henseleit bicarbonate buffer supplemented with 0.5 mmol/l palmitate, 5 mmol/l glucose and 100 µU/ml insulin. The preload pressure was 7.5 mm Hg, while hearts were ejecting against an afterload of 50 mm Hg. The amount of 3H2O released from

[9,10-3H] palmitate was measured to determine fatty acid oxidation and the amount of 14CO2 released from [U-14C] glucose to determine glucose oxidation. Metabolic rates were normalized for cardiac mass. Functional data were obtained since a 2-Fr micromanometer-conductance catheter (Millar Instruments, Houston, TX) was inserted in the left ventricle through the apex. Developed pressure, cardiac output, cardiac power and myocardial oxygen consumption (MVO2) were analyzed as described.[204, 205]

### *Transmission Electron Microscopy (TEM)*

Mouse heart was perfused with 2.5% glutaraldehyde in 0.1 mol/l sodium phosphate (pH7.4), for 10-15 min. After isolation of heart, cardiac muscles were post-fixed overnight at 40C in 2.5% glutaraldehyde in 0.1 mol/l sodium phosphate. The next day, heart was cut into small pieces of around 2 mm3. After treatment with 1% OsO4 in 0.1 mol/l cacodylate buffer (pH 7.2), muscle pieces were rinsed in 1% Na2SO4 in 0.1 mol/l cacodylate buffer and embedded in Epon. Sections (60-nm thick) were cut on a microtome (Ultracut E; Leica) and post-stained with uranyl acetate and lead citrate. The specimens were examined with an electron microscope (Philips EM400) at an accelerating voltage of 80 kV.

### *Measurement of Mitochondrial Content*

DNA was purified from frozen heart tissue using a routine phenol/chloroform protocol after proteinase K digestion. The amount of mtDNA and genomic DNA was measured by quantitative PCR using the following primers. Mitochondrial DNA, D-loop non-coding region: forward GGTTCTTACTTCAGGGCCATCA, reverse GATTAGACCCGTTACCATCGAGAT; Genomic DNA, NADH dehydrogenase flavoprotein 1 (Ndufv1): forward CTTCCCCACTGGCCTCAAG, reverse: CCAAAACCCAGTGATCCAGC.

**Supplemental Table**

Table SI: Physiological and echocardiography parameters of wild-type and raptor-cKO mice prior to surgery.

| Echocardiography | Wild-type | | Raptor cardiac knockout | |
|---|---|---|---|---|
| | Pre-sham ($n = 7$) | Pre-TAC ($n = 11$) | Pre-sham ($n = 7$) | Pre-TAC ($n = 14$) |
| Heart rate (beats/min) | 433±11 | 461±15 | 453±11 | 461±13 |
| Septum thickness (mm) | | | | |
|    diastole | 0.70±0.02 | 0.73±0.01 | 0.72±0.01 | 0.71±0.01 |
|    systole | 0.88±0.02 | 0.92±0.02 | 0.89±0.02 | 0.89±0.02 |
| Left ventricular free wall thickness (mm) | | | | |
|    diastole | 0.70±0.01 | 0.73±0.01 | 0.70±0.01 | 0.70±0.01 |
|    systole | 0.88±0.02 | 0.92±0.03 | 0.88±0.02 | 0.89±0.01 |
| Left ventricular diameter (mm) | | | | |
|    diastole | 4.06±0.06 | 4.08±0.05 | 4.21±0.10 | 4.28±0.06 |
|    systole | 3.13±0.07 | 3.15±0.08 | 3.35±0.13 | 3.30±0.07 |
| Ejection fraction (%) | 46.3±1.4 | 46.1±2.6 | 41.9±3.3 | 46.4±1.8 |
| Fraction of shortening (%) | 22.8±0.8 | 22.9±1.6 | 20.5±1.9 | 23.0±0.9 |
| Body weight (g) | 25.9±0.6 | 28.0±0.5 | 26.7±0.6 | 27.8±0.6 |

## 3.2 Characterization of the function of mTORC2 in the mouse heart

The results of this study have been prepared as a preliminary manuscript.

# Rictor deficiency impairs the cardiac adaption to pressure overload

*Pankaj Shende, MSc[1]; Lifen Xu, PhD[1]; Christian Morandi, MSc[1]; Laura Pentassuglia, PhD[1]; Corinne Berthonneche, PhD[2]; Thierry Pedrazzini, PhD[2]; Beat Kaufmann, MD[1]; Michael N. Hall, PhD[3]; Markus A. Rüegg, PhD[3]; and Marijke Brink, PhD[1]*

[1]*Department of Biomedicine and Cardiology, University of Basel and University Hospital Basel;* [2]*Department of Medicine and Cardiovascular Assessment Facility, University of Lausanne Medical School;* [3]*Biozentrum, University of Basel; Switzerland*

Correspondence:

Marijke Brink

CardioBiology, Department of Biomedicine

University of Basel and University Hospital Basel

Hebelstrasse 20, CH-4051 Basel

Tel: +41 61 265 33 61, Fax: +41 61 265 23 50

E-mail: marijke.brink@unibas.ch

# Summary

***Background -*** mTOR, a central regulator of growth and metabolism, has distinct targets with tissue-specific functions depending on whether it is part of the multiprotein complex mTORC1 or mTORC2. Previously, we have shown that cardiac mTORC1 is required for adaptive hypertrophic growth and maintenance of function in response to pressure overload. In the present study, we aimed to elucidate the role of mTORC2 in cardiac pathophysiology.

***Methods and Results -*** We reduced cardiac mTORC2 activity by deleting the mTORC2-specific component rictor from mouse cardiomyocytes using tamoxifen-induced cre-recombinase driven by the α-MHC promoter. The deletion resulted in significantly reduced total and phosphorylated Akt (Ser473) and PKCα (Thr638). Deletion at an age of 4 weeks and follow-up with ultrasound imaging until adulthood revealed no changes in postnatal cardiac growth, geometry and function. When induced during adulthood, rictor ablation did not change cardiac function or geometry under basal conditions up to an age of 54 weeks. However, one week of aortic constriction-induced pressure overload caused eccentric hypertrophy and decreased ventricular function in the rictor-deficient mice. Thus, compared to wild-type, the rictor knockout mice developed less profound increases in wall thickness along with increases in chamber diameter, whereas cardiac mass was similarly increased after aortic constriction for both groups. The rictor knockout hearts displayed increased fibrosis, apoptosis and β-MHC transcript levels. Myocytes isolated from adult rictor-cKO hearts and neonatal rat cardiomyocytes in which rictor was knocked-down had increased cleaved caspase-3 levels. Furthermore, treatment with the mTOR kinase inhibitor PP242, but not with the mTORC1 inhibitor rapamycin, led to increased apoptosis in cardiomyocyte cultures.

***Conclusion -*** Our study demonstrates that under baseline conditions, rictor deficiency does not affect postnatal cardiac growth or function. However, rictor/mTORC2 is playing a protective role during the cardiac hypertrophic adaptation to pressure overload. The protective effects are explained, at least in part, by the anti-apoptotic actions of mTORC2.

**Key Words-** heart failure; hypertrophy; remodeling; signal transduction

# Introduction

Mechanistic target of rapamycin (mTOR), an evolutionary conserved serine/threonine kinase belonging to the phosphoinositide 3-kinase (PI3K)-related kinase family of proteins, is a central regulator of cell growth and metabolism. mTOR regulates homeostasis and growth by responding to various stimuli including nutrient and energy status, growth factors, oxygen levels and stress. Correspondingly, the activation state of mTOR switches energy-demanding processes on or off.[36, 45, 178, 206] In mammalian cells, mTOR occurs in two distinct multiprotein complexes, termed mTOR complex 1 (mTORC1) and mTORC2, each of which regulates different branches of mTOR signaling. Sensitivity to rapamycin distinguishes the two complexes from each other, where mTORC1 is to a large extent inhibited by rapamycin while mTORC2 is not. Along with mTOR, mTORC1 contains raptor, PRAS40, mLST8, and deptor, whereas mTORC2 consists of rictor, mSIN1, protor-1 and -2, deptor and mLST8. mTORC1, through its best-characterized substrates S6K and 4E-BP1, regulates cap-dependent RNA translation.[107] Moreover, it controls cellular processes such as ribosome biogenesis, transcription, metabolism and autophagy and correspondingly, it is implicated in cancer and aging as well as metabolic, neurological and inflammatory diseases (reviewed in[45, 78, 178, 206]).

Much less is known about the function of mTORC2 owing to the unavailability of selective inhibitors, like rapamycin for mTORC1. By activating members of the AGC kinase family such as PKC, Akt and SGK1, mTORC2 regulates cytoskeletal actin organization, cell survival and other processes.[47, 56, 119] mTORC2 phosphorylates Akt at Ser473 and thereby influences some but not all targets of Akt.[128] It has been reported that mTORC2 is involved in the maturation process of Akt that involves direct association of mTORC2 with ribosomal proteins.[101, 128] A full-body deletion of any component of mTORC2 is embryonic lethal and therefore tissue-specific knockout approaches were necessary to reveal functions of mTORC2 *in vivo*. Knockout of the mTORC2 component rictor in skeletal muscle showed either no phenotype,[173] or impaired insulin-stimulated glucose transport and enhanced glycogen synthase activity.[174] Adipose specific *rictor* deleted mice showed increased body size due to the enlargement of the non-adipose organs; the mice had enlarged pancreas and were hyperinsulinemic but glucose tolerant.[174, 176] Furthermore, β-cell-specific rictor

knockout showed a decrease in β-cell mass and proliferation[133] and a recent study with liver-specific rictor knockout mice provided evidence for a role of mTORC2 in the regulation of hepatic glucose and lipid metabolism.[207] These studies provided important insights into the function of mTORC2 in different tissues and underlined its role in metabolism and in the pathology of various disease states. The role of mTORC2 in the heart has not been analyzed yet.

The heart is an organ with strong metabolic demands and has developed highly complex signaling networks to regulate metabolism and hypertrophic growth, thereby securing or optimizing pumping function under a wide variety of physiological and pathological conditions. Cardiac hypertrophy is an adaptive remodeling process that occurs in response to hemodynamic stress including chronic hypertension, myocardial infarction or valvular dysfunction. It becomes maladaptive and may lead to heart failure when metabolic and structural requirements for contractile function are not met. The remodeling process involves a reactive increase in myocardial mass that requires increased protein synthesis, in which the PI3K/Akt/mTOR pathway plays a central role. Using cardiac-specific *raptor* deletion, we have recently demonstrated that mTORC1 is required for adaptive cardiac hypertrophy and maintenance of cardiac function.[208] Cardiac remodeling also involves important metabolic adaptations. Given the metabolic and anti-apoptotic functions of mTORC2 reported for other tissues, the present study investigated whether mTORC2 is involved in the cardiac adaptations to hemodynamic stress. To this end, we used an inducible cre-loxP system to delete *rictor* specifically from cardiomyocytes. Postnatal growth and function of the heart were not affected by rictor deficiency. During adulthood, deletion of *rictor* also did not have any effect on cardiac function and geometry up to an age of 54 weeks. However, in response to a pathological increase in cardiac work induced by aortic constriction, cardiac function was significantly decreased and associated with eccentric hypertrophy, along with apoptosis and fibrosis in the rictor knockout mice. Altogether our data support that rictor/mTORC2 plays a protective role in pathological hypertrophy, but is not required for postnatal cardiac growth.

# Materials and Methods

### *Generation of Inducible Cardiac-Specific Rictor Knockout Mice*

Mice homozygous for loxP-flanked rictor exon 6[173, 175] were crossed with mice expressing tamoxifen-inducible Cre recombinase under control of the cardiomyocyte-specific α-myosin heavy chain (MHC) promoter.[186] Resulting heterozygous floxed rictor mice positive for the α-MHC-MerCreMer transgene (α-MHC-MerCreMer/rictor^{fl/+}) were further mated with floxed rictor (rictor^{fl/+}) mice to obtain mice positive for α-MHC-MerCreMer and carrying two floxed rictor alleles (α-MHC-MerCreMer/rictor^{fl/fl}). Mice positive for α-MHC-MerCreMer carrying the wild-type rictor alleles were used as controls. PCR genotyping of floxed rictor mice was performed using the forward primer 5'-TTA TTA ACT GTG TGT GGG TTG-3' and reverse primer 5'-CGT CTT AGT GTT GCT GTC TAG-3', which results in an amplicon of 295 bp for the floxed rictor allele and 197 bp for the wild-type allele. Genotyping of mice positive for the Cre transgene was performed using the forward primer 5'-GTT CGC AAG AAC CTG ATG GCA A-3' and reverse primer 5'-CTA GAG CCT GTT TTG CAC GTT C-3' that gives a product of 340 bp for the recombined allele and no product for the wild-type.

### *Experimental Animal Models*

Injections of tamoxifen citrate (20 mg/kg, Sigma, St. Louis, MO) in 60% PBS and 40% ethanol were given I.P. for 5 consecutive days to mice (10-11 weeks or 4 weeks old) homozygous for the floxed rictor or wild-type rictor gene. In some experiments, a second control group was included (indicated in the figure legends) consisting of Cre-positive mice, homozygous for the floxed rictor gene, and injected with vehicle instead of tamoxifen. Transverse aortic constriction (TAC) was performed at the age of 12-13 weeks, two weeks after the last tamoxifen injection according to published procedures.[201, 202] Echocardiography was carried out using a Vevo 770 or Vevo 2100 high-frequency ultrasound system (VisualSonics). For the ultrasound examinations, the mice were anesthetized with inhaled isoflurane (2%) in room air. The body temperature of the mice was kept constant at 37°C. M-mode recordings of the left ventricle were acquired in a left parasternal short axis and long axis plane. Images were transferred to an offline computer for assessment by an investigator blinded to

genetic background or surgery group. Diastolic and systolic anteroseptal wall thickness (AWD, AWS), left ventricular end diastolic diameter (LVEDD), left ventricular end systolic diameter (LVESD), and left ventricular diastolic and systolic posterior wall thickness (PWD, PWS) were measured on M-mode tracings. Fractional shortening was calculated as ([LVEDD-LVESD]/LVEDD x 100). Ejection fraction was calculated as ([LVEDD$^3$-LVESD$^3$]/LVEDD$^3$ x 100). Left ventricular mass was calculated as {1.04 x ([AWD+LVEDD+PWD]$^3$-LVESD$^3$) x 0.8}.[209] All animal experiments were carried out according to guidelines for the care and use of laboratory animals and with approval of the Swiss authorities.

### *Neonatal Rat Cardiomyocyte Culture and Transfection*

Rat neonatal cardiomyocytes were isolated and transfected as published.[210] Freshly isolated cardiomyocytes were transfected with scrambled, rictor or raptor siRNA (4 µg/2x10$^6$ cells, Dharmacon) using the AMAXA cardiomyocyte kit according to the manufacturer's instructions. After overnight incubation in serum-free DMEM, cells were incubated for 1 h with rapamycin (Calbiochem, 20 ng/mL), PP242 (Sigma, 2 µM), or IGF-I and extracted in lysis buffer as described below.

### *Adult Mouse Cardiomyocyte Isolation*

Adult mouse cardiomyocytes were isolated from wild-type and rictor-cKO mice at 12 weeks of age as published[211] with minor modifications. Briefly, after IP injection with 200U of heparin, hearts were rapidly dissected under isofluorane anaesthesia and transferred to ice-cold Ca$^{2+}$-free Tyrode's solution (137 mM NaCl, 5.4 mM KCl, 0.5 mM MgCl$_2$, 10 mM HEPES, 10 Glucose, pH=7.4). Retrograde perfusion was performed in a Langendorff system with Ca$^{2+}$-free Tyrode's solution at 37°C for 5 min, followed by 1 mg/ml Collagenase IV (Worthington) and 0.05 mg/ml protease (Sigma) for 22 min. After digestion, the myocytes were mechanically released from the left ventricle, allowed to pellet for 15 min, and resuspended in Tyrode's buffer at rt with increasing concentrations of Ca$^{2+}$ (0.06 mM, 0.24 mM, 0.6 mM and 1.2 mM). Cells were allowed to attach to laminin-coated dishes in 20% FBS containing DMEM medium for 1 h, washed, kept in serum-free medium for 1 h or overnight, followed by extraction of total proteins as described below.

*Protein Extraction and Western Blot Analysis*

Tissue for molecular analysis was flash-frozen in liquid nitrogen and stored at –80°C. Total protein was extracted using a Polytron homogenizer and RIPA buffer (50 mmol/l Tris-HCl, pH=7.4, 150 mmol/l NaCl, 1% NP40, 0.25% Na deoxycholate, 5 mmol/l EDTA, 0.5 % phosphatase inhibitor cocktail 1 and 2 (Sigma), SDS 0.1% and "Mini-Complete" protease inhibitor cocktail (Roche Diagnostics). Cultured cardiomyocytes were extracted with the same extraction buffer after 2 washes in ice-cold PBS. Equal amounts of protein were separated on SDS-PAGE and after transfer to PVDF membrane, incubated overnight with primary antibody. All antibodies were from Cell Signaling Technology (Danvers, MA), except the antibodies to GAPDH and ANP, which were from Santa Cruz Biotechnology (CA) and to β-MHC, which was from Sigma (St. Louis, MO). After 3-4 consecutive washings, the membrane was incubated with IRDye-labeled secondary antibody for 1 h and the signal detected and quantified using Odyssey imaging software (LI-COR Biosciences, Lincoln, Nevada, USA).

*RNA Preparation and Quantitative RT-PCR*

Total RNA was extracted from frozen hearts using Tri Reagent (Sigma) and treated with DNAse I (Ambion, Austin, TX). Concentration, purity and quality of the RNA were assessed by spectrophotometry and agarose gel eletrophoresis. cDNA was prepared from these total RNA extracts using the high capacity DNA reverse transcription kit (Applied Biosystems). The product was diluted 1:100 and 5 µl were amplified on a 7500 fast real-time PCR system (Applied Biosystems), with 1x ITaQ SYBR Green Supermix Kit (Bio-Rad, Reinach, Switzerland) and 300 nmol/l for forward and reverse primers in total volume of 20 µl. The mRNA level was based on the critical threshold (Ct) value. The primers used for the real time PCR (Supplementary Methods) were designed with the software Primers Express (Applied Biosystems, Foster City, CA) and synthesized by Microsynth (Balgach, Switzerland).

*Analysis of Fibrosis and Apoptosis on Paraffin Sections*

The excised cardiac tissue was fixed overnight in 4% paraformaldehyde, dehydrated and embedded in paraffin. Sections of 4 µm thickness were de-paraffinized, rehydrated and stained with hematoxylin and eosin (H&E) or picrosirius red as

published.[212] The amount of cardiac fibrosis was expressed as percentage of a given total tissue area that was Sirius red positive. An average of 17 microscopic fields was analyzed of at least 3 sections per animal. TUNEL assay was performed using an in situ apoptosis detection kit (Roche Diagnostics) and the nuclei were stained with DAPI (Sigma, 1 µg/ml).

### *Wheat Germ Agglutinin and Immunohistochemistry of Cryosections*

Hearts were rapidly frozen in OCT (Medite, Nunningen, Switzerland) using isopentane cooled in liquid nitrogen. Cryosections were fixed for 20 min at RT with 4% paraformaldehyde and washed with PBS-glycine (100 mmol/l) for 10 min. Sections were permeabilised with 0.1% Triton X-100 for 20 min and incubated with FITC-labeled wheat germ agglutinin (Sigma, 4 µg/ml) for 90 min at RT. Cross sectional areas of at least hundred cardiomyocytes in three independent sections of 3-4 mice per group were measured. For immunohistochemistry, sections were incubated with antibodies to β-MHC (Abcam), cleaved caspase-3 (Becton, Dickinson and Company), or myomesin (Developmental Studies Hybridoma Bank) followed by Cy3- (Jackson Immunoresearch) or Alexa555- (Molecular Probes) labeled secondary antibodies. Nuclei were stained with DAPI (Sigma, 1 µg/ml).

### *Statistical Analysis*

Data are presented as mean±SEM. Differences in means between two groups were evaluated with unpaired 2-tailed Student t tests and those among multiple groups with 1-way or 2-way analysis of variance (ANOVA) followed by Bonferroni post hoc tests. When measurements of the same mice were performed at multiple timepoints, we used repeated-measures ANOVA. All statistics was performed with GraphPad Prism 4.0 software. P values of $<0.05$ were considered statistically significant.

# Results

## *Conditional Deletion of Rictor Does Not Affect Cardiac Weight, Function or Geometry in Adult or Growing Mice*

To characterize the role of mTORC2 in the heart during adulthood, we bred mice homozygous for floxed rictor and transgenic for inducible cre recombinase driven by the α-myosin heavy chain promoter (rictor$^{fl/fl}$ α-MHC-MerCreMer$^{Tg/0}$), and injected them at the age of 10 weeks with tamoxifen for five consecutive days. Western analysis of cardiac lysates at 3 weeks after induction of the deletion showed that rictor protein was reduced to 38% of the wild-type levels. Echocardiography was performed at 4, 6, 10, 16 and 25 weeks after tamoxifen to assess cardiac function and geometry at the age of 14, 16, 20, 26 and 35 weeks (Figure 1A and Supplementary Table I). At all time-points, the ejection fraction and fractional shortening values of the rictor knockout (rictor-cKO) mice were similar to those measured in the wild-type mice. Systolic and diastolic septum and LV free wall thickness were also indistinguishable over the 25 weeks that the mice were followed. Consistently, *post mortem* analysis at the age of 35 weeks revealed no differences in ventricular weight to tibia length ratios between the wild-type and rictor-cKO mice (Figure 1B). In an independent experiment with a different batch of mice, we confirmed that also at the age of 54 weeks, rictor-cKO mice were indistinguishable from wild-type mice with respect to cardiac function and geometry (Table I).

As mTOR and Akt have been implicated in growth-related mechanisms, we next deleted the rictor gene in cardiomyocytes of growing mice by injecting tamoxifen at an age of 4 weeks. Figure 2 shows an increase in LV mass over time with no differences between the two control groups of wild-type mice and the rictor-cKO mice. Ventricular weight to body weight ratio were also identical for the groups over time. Moreover, ejection fractions (Figure 2) and all other echocardiographic parameters (Supplementary Table II) were normal at all time-points measured up to an age of 16 weeks.

### *Rictor Deletion Reduces Phosphorylated and Total Akt and PKCα*

In contrast to a complete lack of effects of rictor ablation on cardiac function, geometry and mass over this period, expression of several signaling proteins was substantially changed (Figure 3, Supplementary Table III). As expected, rictor protein was significantly lower in rictor-cKO than in wild-type hearts at 25 weeks after tamoxifen. The amounts of phosphorylated Akt (Ser473) and PKCα (Thr638) were markedly reduced (Figure 3A), indicating that mTORC2 activity was reduced in cardiomyocytes of the rictor-cKO mice. It is of note however that total levels of Akt and PKCα protein were also reduced. After normalization for these reductions, the Ser473/total Akt ratio was significantly decreased and the Thr308/total Akt ratio was not affected, which confirmed that mTORC2 kinase activity was reduced in our model at 25 weeks after the tamoxifen-induced rictor deletion. In contrast, for PKCα the phosphorylated/total ratio was higher in rictor-cKO than in wild-type (Supplementary Table III), suggesting compensatory PKCα phosphorylation in response to the decrease in total PKCα protein. Previously it has been demonstrated that mTORC2, by co-translational phosphorylation of the turn motif of members of the AGC kinase family such as Akt (Thr450), prevents their degradation.[101, 122] Our observation of reduced Akt and PKCα total protein may be explained by this mechanism, and confirms that rictor ablation led to inactivation of mTORC2.

To test if long-term rictor deficiency alters mTORC1 or its downstream effectors, we analyzed raptor, mTOR, 4E-BP1, P70-S6K1 and S6 (Figure 3B and Supplementary Table IV). Total or phosphorylated levels of these proteins were not different between the wild-type and knockout groups. Furthermore, Erk1/2 and GSK3β phosphorylation were not affected by rictor ablation.

Taken together, the above data show that despite marked decreases in total and phosphorylated Akt (Ser473, Thr308) and PKCα (Thr638), the rictor-cKO mice maintained normal cardiac function under baseline conditions.

### *Rictor Deficiency Accelerates the Development of Cardiac Dysfunction after Aortic Constriction*

We next investigated whether mTORC2 plays a role under pathological conditions, because its downstream target Akt is an important survival kinase,{Sussman, 2011 #1323} and PKCα is known to be involved in cardiomyocyte contractility.{Liu, 2011

#1362} Rictor-cKO and wild-type mice were assigned randomly to sham or transverse aortic constriction (TAC) groups for surgery at two weeks after the last tamoxifen injection. Echocardiography before surgery showed no differences between the wild-type and knockout groups (Supplementary Table IV). One week after aortic constriction, the wild-type mice displayed concentric left ventricular remodeling with increased LV and anteroseptal wall thickness during diastole and with unchanged end-systolic and decreased LV end diastolic diameters (LVEDD) compared to the pre-surgery measurements (P<0.001, < 0.001, and <0.05 for LV wall, septum, and LVEDD, respectively) and compared to sham-operated wild-type mice (Table II, Figure 4A and B). The wild-type mice maintained normal cardiac function after aortic constriction, as their ejection fraction and fractional shortening values were similar to those measured before surgery (not shown) and in time-matched sham-operated wild-type mice (Table II, Figure 4A).

On the other hand, the rictor-cKO mice showed eccentric left ventricular remodeling and a decline in cardiac function after TAC. Thus, one week of aortic constriction resulted in significantly lower ejection fraction and fractional shortening values in the rictor-cKO mice compared to their pre-surgery baseline values (P<0.01 and P<0.05, respectively), and compared to time-matched sham-operated rictor-cKO or TAC-operated wild-type mice (Table II, Figure 4A). In contrast to the wild-type mice, the rictor-cKO mice had increased LV internal diameters during diastole and systole (Figure 4A). Finally, although the rictor-cKO mice displayed an increase in anteroseptal and LV free wall thickness compared to pre-surgery baseline and to sham-operated rictor-cKO, this increase was significantly less pronounced than that measured in wild-type mice after TAC (Table II, Figure 4B).

*Post mortem* analysis revealed that the ventricular weight to tibia length ratio at one week after TAC was not different between wild-type and rictor-cKO. Thus, both groups developed similar increases in cardiac mass compared to the corresponding sham-operated group (Figure 4B). Consistent with this hypertrophic response, ANP expression was induced similarly (Figure 4C and D), and BNP mRNA levels were also not different between the wild-type and rictor-cKO mice after TAC (data not shown). Interestingly however, β-MHC mRNA transcript levels were 2.2-fold higher in the rictor-cKO mice than in wild-type controls under banded conditions (Figure 4C). This was associated with a smaller 1.45-fold increase in protein, a

difference that did not reach statistical significance (Figure 4D). In sham-operated rictor-cKO mice, β-MHC mRNA levels were 2.8-fold higher than in controls (Student's T-test: $P<0.001$), an increase that was again not fully mirrored at the protein level (1.34-fold increase in protein). In addition to these markers of hypertrophy, we measured mRNA levels of genes that regulate energy metabolism. As expected TAC induced GLUT1 and decreased both GLUT4 and PGC1α ($P<0.001$ for all genes), but rictor deficiency did not change this response to pressure overload.

Taken together, we conclude that wild-type mice develop concentric hypertrophy with preserved cardiac function, whereas the rictor-cKO mice show a phenotype of eccentric hypertrophy with decreased function at one week of aortic constriction. The eccentric hypertrophy is associated with increased β-MHC expression, whereas other hypertrophic or metabolic genes are not affected by rictor deficiency.

*Analysis of mTOR Signaling in Cardiac Rictor Knockout Mice After Aortic Constriction*

The above findings demonstrate that the activity of mTORC2 is important during the cardiac adaptation to pressure overload. To investigate the mechanisms that underlie this protective role, we analyzed cardiac protein extracts (Figure 5). In sham-operated cKO mice, rictor protein was significantly reduced, but in spite of the deletion, TAC significantly increased rictor expression (2-fold for cKO, 1.6-fold for wild-type). These increases provide additional support for a role of mTORC2 during the response to overload. In the rictor-deficient mice, the ratio of phosphorylated (Ser473) to total Akt was decreased significantly compared to wild-type for both sham- and TAC-operated mice (Figure 5B). Phosphorylation at Thr308 showed high variability with no clear difference between the experimental groups. The amount of total PKCα, another downstream target of mTORC2, was significantly reduced (Figure 5A); nevertheless the phosphorylated/total PKCα ratios were also lower after rictor deletion (Figure 5B). As Akt (Ser473) and PKCα both are direct targets of mTORC2, these data confirm that mTORC2 activity was reduced. Examination of mTORC1 targets on the other hand revealed that phosphorylated 4E-BP1 was not different between the wild-type and rictor-cKO mice, consistent with the fact that we found unchanged Akt-Thr308 phosphorylation upstream of mTORC1 and normal levels of

raptor after rictor deletion (Figure 5C). It is of note that levels of raptor and 4E-BP1 were increased after TAC in rictor-cKO, with no difference between the rictor-cKO and wild-type, suggesting that protein synthesis via this pathway was activated normally after TAC. Interestingly, phosphorylation of S6, a substrate of S6K1, which in-turn is a target of mTORC2, was reduced in rictor-cKO mice (Figure 5D).

### Fibrosis and Apoptosis Are Increased in Cardiac Rictor Knockout

The rictor-cKO mice exhibited normal increases in cardiac mass in response to TAC, but at the same time their ventricular wall and septum thickness was significantly less increased than in wild-type controls, in line with a pattern of eccentric hypertrophy. Analysis of the cross sectional area of cardiomyocytes using wheat-germ agglutinin did not reveal any difference between wild-type and rictor-cKO mice after TAC (Figure 6A). On the other hand, picro-sirius red staining showed a 2.8-fold increase in fibrosis after TAC in the rictor-cKO mice (Figure 6B).

To identify further mechanisms that potentially contributed to the observed phenotype, we assessed apoptosis using the TUNEL assay and cleaved caspase-3 labeling (Figure 7A and B). The hearts of rictor-cKO mice contained more TUNEL positive cells than those of wild-type mice. Quantification of cleaved caspase-3 labeling confirmed increased apoptosis: after TAC, rictor-cKO mice (N=6) had 2.2-fold more positive cells per section area than wild-type mice (N=5). Double-labeling experiments with antibodies to myomesin revealed that the cleaved caspase-3 positive cells were negative for this cardiomyocyte marker, indicating that apoptosis took place in the non-myocyte compartment of the heart. Apoptosis may have remained undetected in cardiomyocytes because it was a rare event at the time point that we analyzed the tissues. To further assess the involvement of mTORC2 in regulating apoptosis in cardiomyocytes, we therefore performed experiments with primary cultures prepared from neonatal rat and adult rictor-cKO mouse hearts. Figure 7C shows that the mTOR kinase inhibitor PP242 increased the cleaved caspase-3 fragment, whereas rapamycin did not increase it. As rapamycin only inhibits mTORC1 whereas PP242 inhibits both mTORC1 and mTORC2, these results suggest that mTORC2 is involved in the protection of cardiomyocytes against apoptosis. However, rapamycin-resistant effects of mTORC1 have been described, and we therefore performed additional experiments in which mTORC2 activity was decreased

by knockdown of rictor in neonatal rat cardiomyocytes using silencing technologies. Figure 7D shows that rictor protein was reduced after transfection of siRNA and that at the same time cleaved caspase-3 fragment was increased. Together, these data support that mTORC2 regulates apoptosis in neonatal cardiomyocytes. Finally, Figure 7E shows that in cardiomyocytes isolated from the hearts of adult rictor-cKO cleaved caspase-3 was increased, confirming that rictor deficiency causes enhanced apoptosis not only in neonatal but also in adult mouse cardiomyocytes.

Taken together, our histological analysis shows fibrosis with increased apoptosis in the non-myocyte compartment of the heart, whereas our experiments with cultured cells support that mTORC2 prevents apoptosis in neonatal and adult rodent cardiomyocytes. These observations may explain, at least in part, the development of cardiac dysfunction in the rictor-cKO mice after pressure overload.

## Discussion

In the present study we demonstrated that cardiac deletion of *rictor* during postnatal growth or adulthood had no effects on cardiac geometry and function under baseline conditions up to 54 weeks of age. However, hemodynamic stress induced by aortic constriction caused a decrease in cardiac function in rictor-cKO mice, whereas in wild-type mice function was preserved. Thus, in wild-type mice, one week of TAC caused an adaptive increase in posterior and anteroseptal wall thickness and a decrease in LVEDD while ejection fraction and fractional shortening were maintained, indicating that the mice were in the compensatory phase of cardiac hypertrophy. In the rictor-cKO mice, ventricular weight was increased as much as in the wild-type mice, but ejection fraction and fractional shortening were reduced. Although an increase in LV wall thickness was developed by the rictor-cKO mice, this increase was less pronounced than in wild-type mice and moreover, the LVEDD was increased. These results demonstrate that cardiac rictor-deficient mice developed a phenotype reminiscent of decompensated eccentric hypertrophy at one week of aortic constriction and point to a role for mTORC2 during the adaptive response of the heart to pressure overload. This role is furthermore supported by our observation that rictor protein is significantly increased after TAC.

We showed that cardiac rictor ablation strongly diminished Akt phosphorylation at Ser473, confirming that the deletion decreased mTORC2 activity. In cancer and other cells, mTORC2-mediated Akt phosphorylation was reported to regulate apoptosis.[213] Although Akt is known to modulate apoptosis in the heart (reviewed in[214]), it has not been investigated whether mTORC2 is implicated in regulating apoptosis in this organ. The reduced LV wall thickness, increased LVEDD and the associated decrease in cardiac function that we observed in the rictor-cKO mice may in part be a consequence of cardiomyocyte apoptosis. We found that numbers of apoptotic cells were indeed increased in the rictor deficient hearts. Interestingly, the apoptotic cells were part of the non-cardiomyocyte compartment as demonstrated after double labeling with myomesin antibodies, whereas apoptosis in cardiomyocytes was below detection levels at 7 days of TAC. Three independent cell culture experiments provided support that mTORC2 regulates apoptosis also in the cardiomyocytes.

Firstly, in primary rat neonatal cardiomyocytes, the mTOR kinase inhibitor PP242 rapidly increased cleaved caspase-3 whereas rapamycin had no effects. As rapamycin-resistant effects of mTORC1 have been described, we provided further support for this conclusion after silencing of rictor with siRNA, which increased cleaved caspase-3. Finally, cardiomyocytes isolated from adult rictor-cKO mouse hearts had higher levels of cleaved caspase-3 than those prepared in parallel from wild-type hearts. Altogether, our data indicate that prevention against apoptosis represents one of the mechanisms by which mTORC2 protects the heart during pressure overload.

Next to a decrease in contractile tissue due to apoptosis, fibrosis may have contributed to the observed decrease in cardiac function, as it is known to enhance myocardial stiffness and impede systolic ejection function.[215] While fibroblasts and extracellular matrix are necessary for structural support of the heart under physiological conditions, increased fibrosis as observed in the rictor-cKO mice indicates a repair process triggered by cardiomyocyte stress or cardiomyocyte loss. Alternatively, the fibrotic response could be due to changed communication between the cardiomyocytes and their neighboring cells as a direct consequence of the deletion. Rictor deletion in fat tissue increases the size of other organs including the heart via systemic signaling[176] and similarly, reduced mTORC2 activity in cardiomyocytes may in a paracrine manner affect the fibrotic response in the heart. Whether or not the observed fibrosis is due to paracrine effects that depend on mTORC2 or secondary to the stress response to reduced cardiomyocyte viability or performance needs further evaluation.

We have recently shown that mTORC1 is essential for the cardiac adaptation to pressure overload with protein synthesis being one of the prior mechanisms implicated.[208] mTORC2-mediated phosphorylation of Akt at Ser473 allosterically activates Akt. Akt in turn is one of the activators of protein translation via TSC1/TSC2, Rheb and mTORC1, but Jacinto and Guertin suggested that mTORC2-induced Akt HM site phosphorylation confers substrate specificity to Akt, which would narrow down its role to FoxO-regulated functions such as apoptosis and protein degradation, whereas functions regulated by GSK3 and TSC2 would remain unchanged.[55, 61] Consistently we show here that 4E-BP1 phosphorylation was increased in the rictor-cKO as much as in wild-type mice, which indicates that mRNA translation via this pathway was not affected by rictor ablation. To our surprise

however, rictor ablation for 3 weeks resulted in significantly reduced S6 phosphorylation (Figure 5). Our data suggest that in the heart, mTORC2 regulates p70 S6K upstream of S6. Ribosomal S6Ks regulate the 5'TOP mRNAs, which include ribosomal proteins and elongation factors involved in translation, but it remains unclear what the phosphorylation of substrates of the S6Ks contribute to mRNA translation.[216] It has previously been shown with S6K1 and S6K2 knockout mice that ribosomal S6 kinases are not essential for TAC-induced pathological hypertrophy.[147] Moreover, recent work demonstrates that the acute effects of mTOR inhibition on mRNA translation are predominantly mediated by the 4E-BPs; this concerns in particular TOP and TOP-like mRNA translation but to some extent also the translational suppression of all mRNAs.[217] Consistent with these studies, as well as with our observation that other pathways that may activate protein synthesis independently such as MAPK/Erk1/Erk2 and GSK3β were unchanged, we found that cardiomyocyte cross-sectional areas were not decreased after rictor ablation. Altogether, we conclude that overall protein synthesis intrinsic to the hypertrophic response of the heart to TAC was not influenced by rictor ablation.

The cardiac hypertrophic response normally involves specific changes in gene expression towards fetal genes. ANP levels were equally induced after TAC in wild-type and cKO mice in accordance with the similar magnitudes of their hypertrophic growth responses. In contrast, we found that β-MHC mRNA levels were more strongly increased after rictor ablation, indicating an enhanced cardiomyocyte stress response and consistent with the accelerated development of cardiac dysfunction in the rictor-cKO mice. In fact, of all hypertrophic markers measured, β-MHC was the only gene that was induced by rictor deficiency under baseline conditions of normal cardiac load. These results could mean that mTORC2 has a direct effect on β-MHC gene expression. Alternatively, the observed β-MHC induction may be secondary to other deleterious consequences of mTORC2 inactivation, and represent a compensatory mechanism that contributed to the normal cardiac function observed under baseline conditions.

The direct functional consequence of rictor deficiency may be, in addition to apoptosis, related to one of the other targets of mTORC2. The currently known targets include, next to Akt, the AGC kinase family members serum/glucocorticoid-regulated

kinase 1 (SGK1)[124] and several protein kinase C isozymes.[122,218] We demonstrated that rictor ablation strongly reduced Thr638 phosphorylation in the turn motif of PKCα. This effect was accompanied by reduced total PKCα protein, consistent with a previous report in which it was demonstrated that this phosphorylation site is substrates of mTORC2 important for the maturation and stability of PKCα.[122] The PKC family of kinases contains downstream effectors of the Gq/PLCβ signaling pathway that induces hypertrophy in response to biomechanical stress such as aortic constriction (reviewed in[219]). PKCα reduces cardiomyocyte contractility.[220, 221] Deletion of the gene or its inhibition with drugs, inhibitory peptides, or dominant negative mutant PKCα has yielded considerable protective effects in heart failure models. Moreover, PKCα knockout mice displayed improved cardiac contractility (reviewed in[219]). Based on these earlier studies, we conclude that the reduced PKCα is most likely not the reason for reduced ejection fractions and contractility measured in rictor-deficient hearts. In fact, reduced phosphorylated and total PKCα may have contributed to the maintenance of cardiac performance that we observed in the sham-operated rictor-cKO mice.

In conclusion, our study shows that rictor deficiency leads to decompensated eccentric cardiac hypertrophy associated with enhanced fibrosis and apoptosis after transverse aortic constriction and points to a protective role for mTORC2 during the adaptation of the heart to hemodynamic stress. Our cell culture experiments support that mTORC2 has anti-apoptotic activities and that the mTOR kinase inhibitor PP242 increases apoptosis in cardiomyocytes. Several compounds inhibiting both mTOR complexes are in clinical trials for the treatment of cancer,[38] and special attention should be paid in these studies to patients with concurrent heart disease. Moreover, our data on mTORC2 in the heart may open up new avenues for the treatment of cardiac disease.
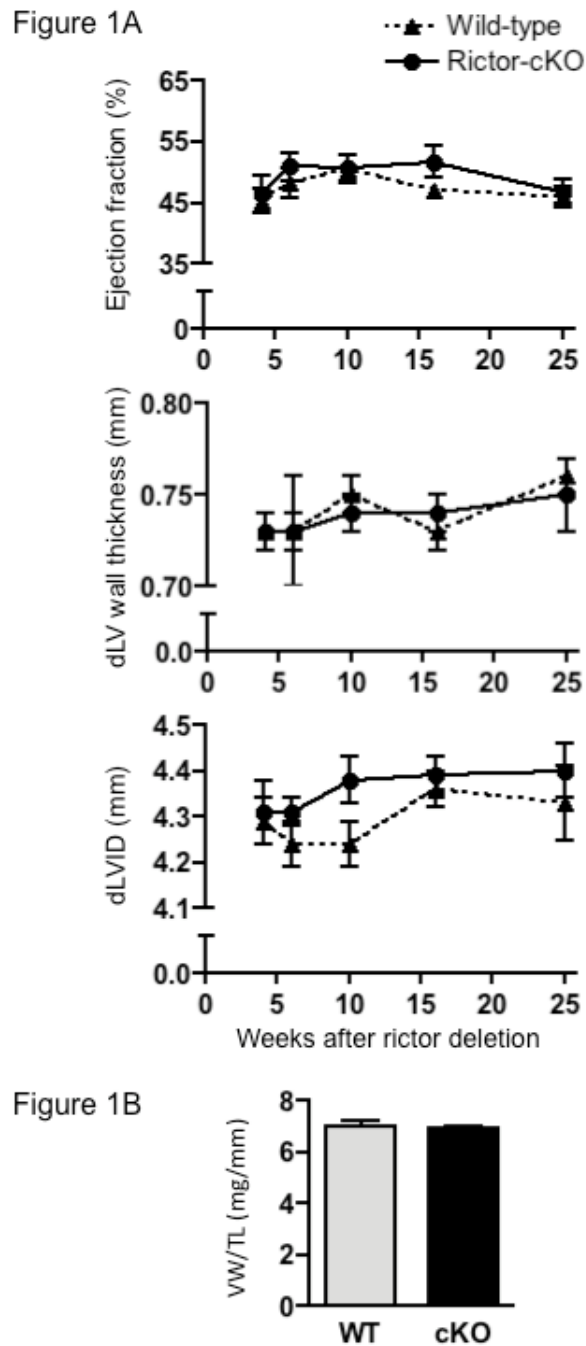
Figure 1A



Figure 1B

**Figure 1.** *Rictor deletion in the heart of adult male mice has no effects under baseline conditions. A, shown are graphs of the repeated measurements of ejection fraction and LV wall thickness after rictor deletion at the age of 10 weeks. B, Post mortem analysis of cardiac weight- 24 weeks of rictor deficiency does not change cardiac weight.*

## Figure 2
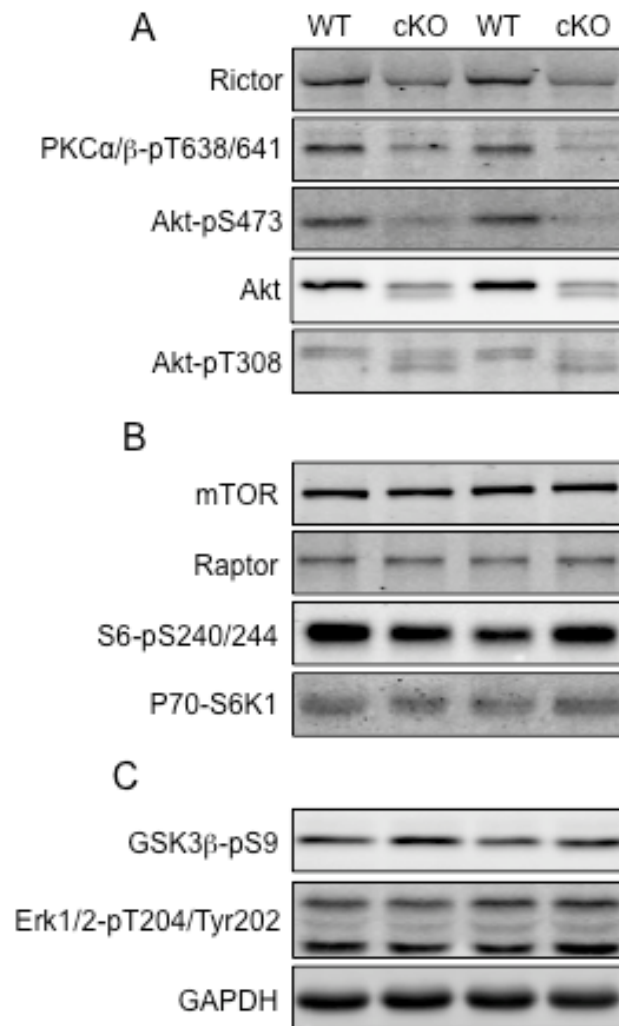


*Figure 2*. *Analysis of cardiac protein extracts of wild-type (WT) and rictor cardiac knockout (cKO) mice by Western blotting. A, shows that phosphorylation of downstream targets of mTORC2 is inhibited. B, shows that mTORC1 targets are not affected. C, shows that potential compensatory pathways are not affected. GAPDH was used as loading control.*

Figure 3
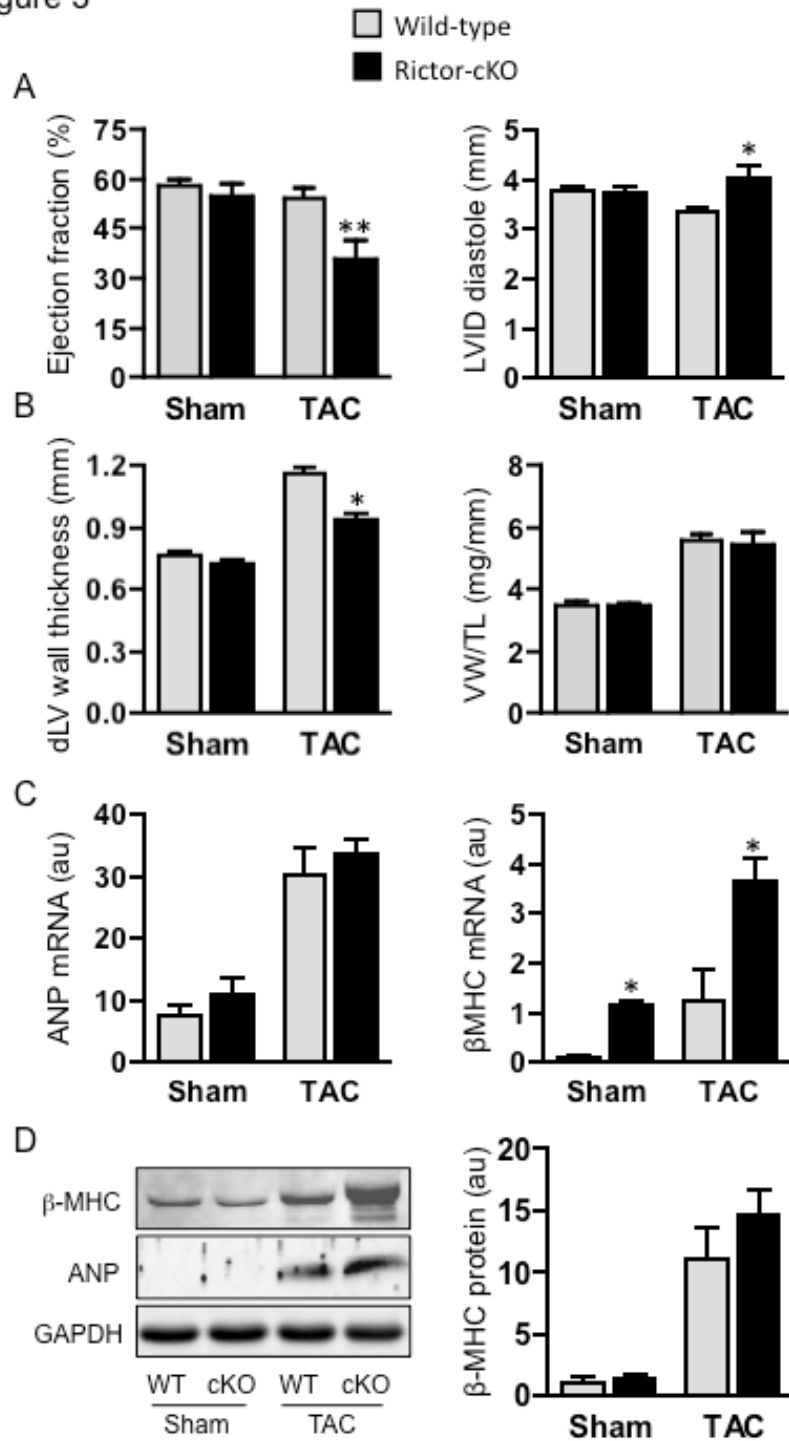


*Figure 3. Effect of rictor deletion on cardiac function, geometry and hypertrophic markers. Aortic constriction surgery was performed at the age of 10 weeks and cardiac parameters were measured by ultrasound one week later. A, LVID: Left ventricular internal diameter. B, LVWT: LV wall thickness; VW/TL: ventricular weight/tibial length ratio. C, qPCR analysis of ANP and β-MHC and D, protein levels of ANP and β-MHC.*
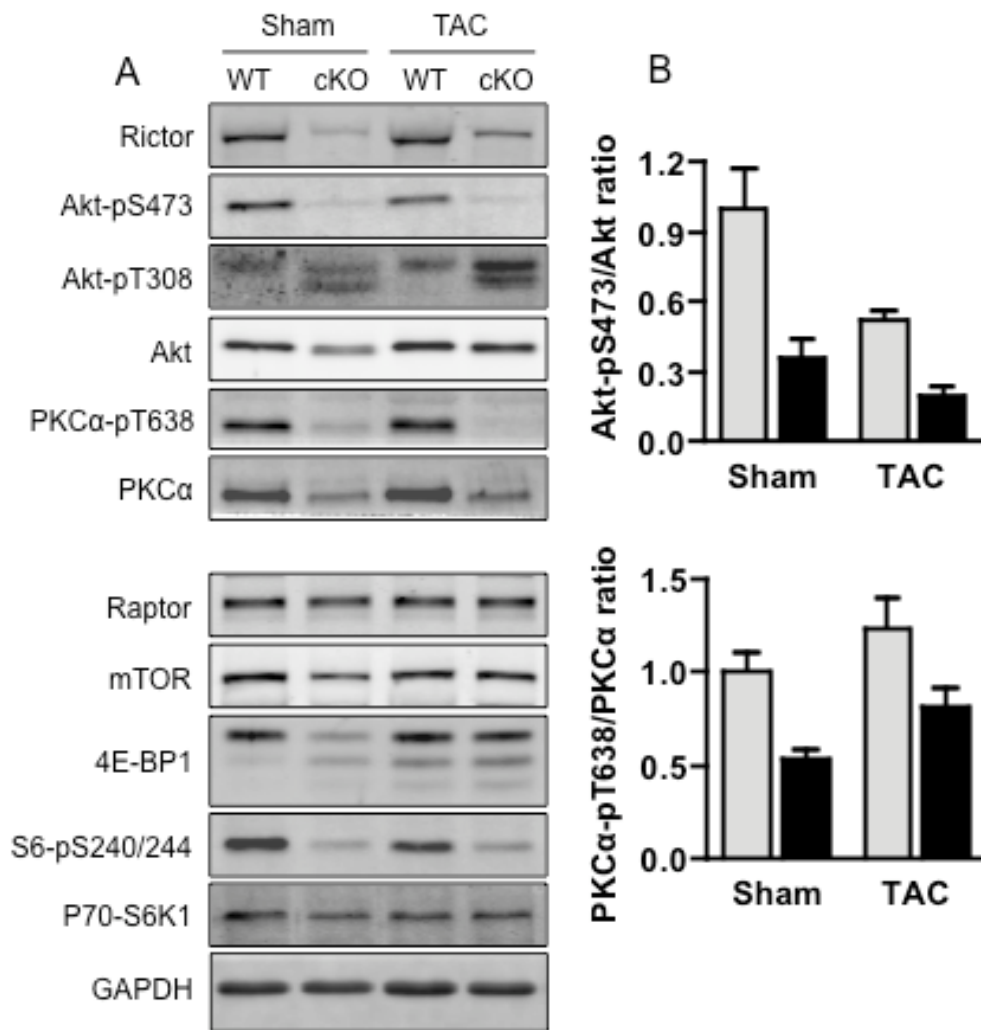
Figure 4



*Figure 4*. *Effect of rictor deletion on mTORC1 and mTORC2 signaling 1 week after aortic constriction (TAC) or control surgery (Sham). A, Western blot analysis of the proteins involved in mTOR signaling. B, Quantification of the ratios of phosphorylated to total Akt and PKCα.*

Figure 5
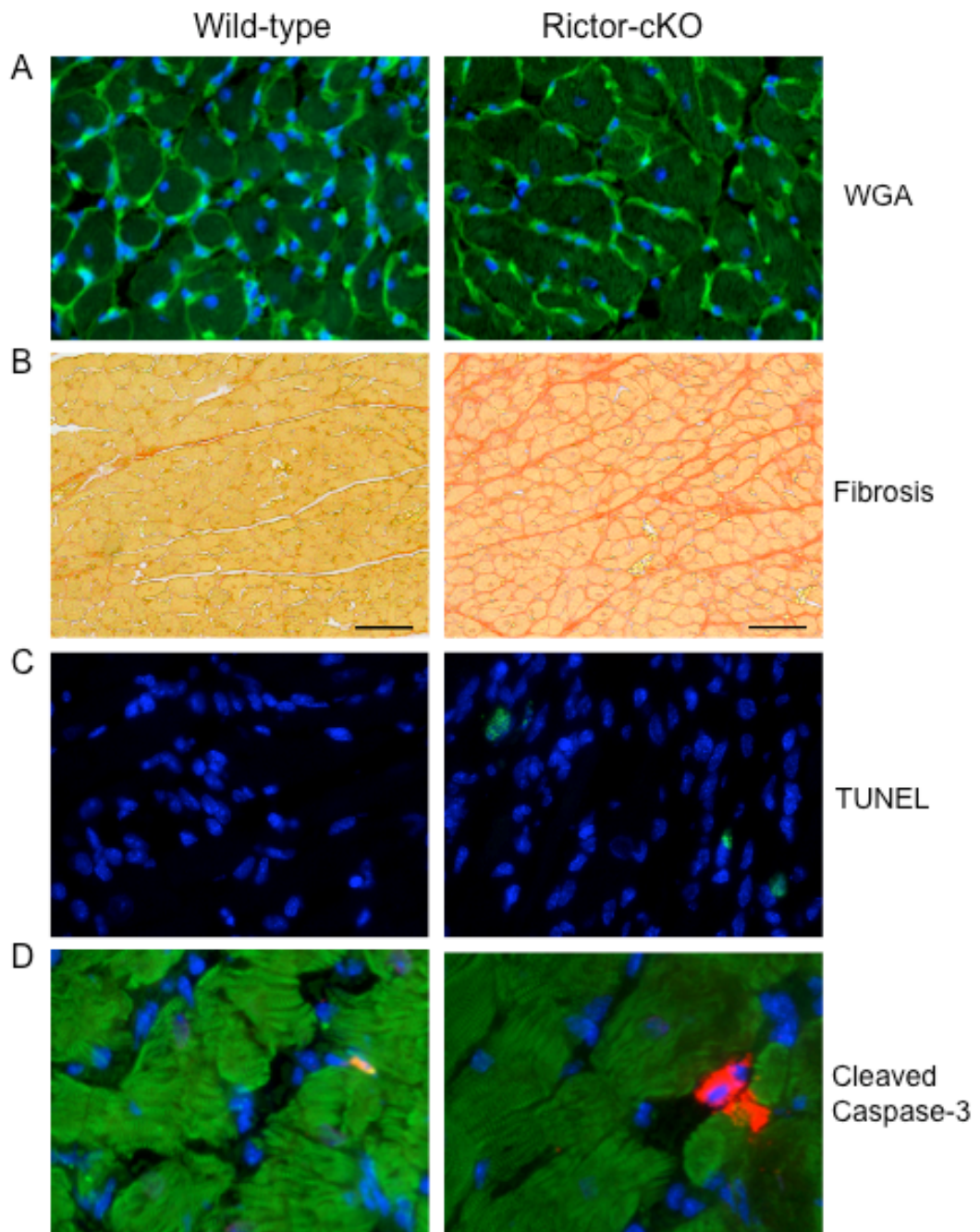


*Figure 5. Microscopic images of cardiac tissue sections after 1 week of aortic constriction. A, Analysis of cardiac cross-sectional area by wheat-germ agglutinin (WGA) on cryosections. B, Analysis of fibrosis by picro-sirius red staining on paraffin sections. C, Analysis of apoptosis by TUNEL assay and D, by immunostaining using an antibody against cleaved caspase-3 fragment.*

Figure 6
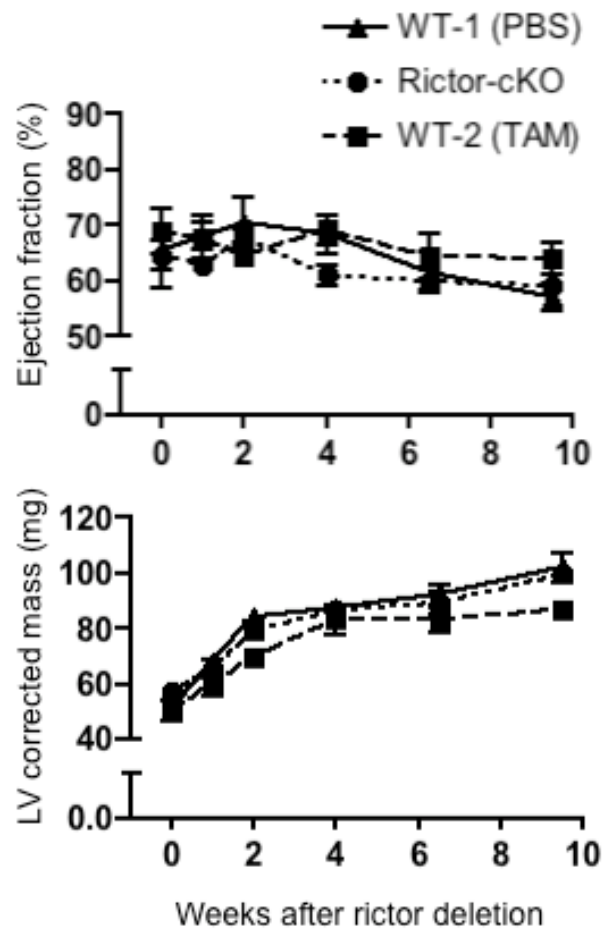


***Figure 6****. Effect of rictor deletion during postnatal cardiac growth. Rictor deletion was induced at the age of 4 weeks and echocardiography was performed at the indicated timepoints after rictor deletion up to the age 14 weeks. Shown are the graphs for repeated measurements of ejection fractions and LV corrected mass during the growth phase.*

**Table I**. Physiological and echocardiographic parameters of wild-type and rictor knockout mice after 1 week of sham and TAC surgery

| Echocardiography | Wild-type | | Rictor-cKO | |
|---|---|---|---|---|
| | Sham (N=8) | TAC (N=5) | Sham (N=5) | TAC (N=6) |
| Heart rate (beats/min) | 528±24.2 | 497±15.1 | 473±16.3 | 518±14.6 |
| Septum thickness (mm) | | | | |
|     diastole | 0.76±0.01 | 1.05±0.01*** | 0.73±0.02 | 0.90±0.03**$^{\$\$}$ |
|     systole | 1.02±0.02 | 1.40±0.03*** | 0.97±0.04 | 1.13±0.05*$^{\$\$}$ |
| Left ventricular wall thickness (mm) | | | | |
|     diastole | 0.76±0.02 | 1.16±0.03*** | 0.72±0.02 | 0.94±0.03***$^{\$\$\$}$ |
|     systole | 1.02±0.02 | 1.37±0.02*** | 0.97±0.04 | 1.10±0.04*$^{\$\$\$}$ |
| Left ventricular internal diameter (mm) | | | | |
|     diastole | 3.78±0.09 | 3.37±0.09** | 3.73±0.13 | 4.03±0.24$^{\$}$ |
|     systole | 2.64±0.09 | 2.45±0.13 | 2.70±0.18 | 3.36±0.30$^{\$}$ |
| Ejection fraction (%) | 58.04±1.71 | 54.24±3.14 | 54.58±3.71 | 35.95±5.31*$^{\$}$ |
| Fraction of shortening (%) | 30.12±1.11 | 27.41±1.93 | 27.93±2.36 | 17.22±2.74*$^{\$}$ |
| Post-mortem analysis | | | | |
| Body weight (g) | 28.7±0.4 | 25.8±0.8 | 26.8±0.8 | 26.7±0.6 |
| Ventricular weight (VW, mg) | 107.3±5.3 | 140.6±2.8*** | 103.9±3.1 | 136.9±4.7*** |
| VW / tibial length (mg/mm) | 5.89±0.30 | 7.68±0.19** | 5.69±0.18 | 7.56±0.24*** |

*P<0.05, **P<0.01, ***P<0.001 TAC- vs corresponding Sham-operated group

$^{\$}$P<0.05, $^{\$\$}$P<0.01, $^{\$\$\$}$P<0.001 Knockout vs corresponding Wild-type group

**Supplementary Table I**: Physiological and echocardiographic parameters of wild-type and rictor knockout mice at 24 weeks after induction of the deletion

|  | Wild-type | Rictor-cKO |
|---|---|---|
| Echocardiography | (N=10) | (N=8) |
| Heart rate (beats/min) | 461±13 | 505±18 |
| Septum thickness (mm) |  |  |
| diastole | 0.79±0.01 | 0.78±0.01 |
| systole | 1.00±0.03 | 0.98±0.03 |
| Left ventricular wall thickness (mm) |  |  |
| diastole | 0.76±0.01 | 0.75±0.02 |
| systole | 0.99±0.03 | 0.97±0.03 |
| Left ventricular internal diameter (mm) |  |  |
| diastole | 4.33±0.08 | 4.40±0.06 |
| systole | 3.35±0.09 | 3.37±0.09 |
| Ejection fraction (%) | 45.9±1.7 | 46.8±1.9 |
| Fraction of shortening (%) | 22.7±1.0 | 23.3±1.1 |
| Post-mortem analysis |  |  |
| Body weight (g) | 36.1±1.1 | 37.4±1.5 |
| Ventricular weight (VW, mg) | 130.1±3.3 | 129.9±1.7 |
| VW / tibial length (mg/mm) | 7.0±0.18 | 6.9±0.08 |

**Supplementary Table II.** Physiological and echocardiographic parameters of wild-type and rictor knockout mice at baseline prior to surgery.

| Echocardiography | Wild-type | | Rictor-cKO | |
|---|---|---|---|---|
| | Pre-sham (N=9) | Pre-TAC (N=8) | Pre-sham (N=5) | Pre-TAC (N=8) |
| Body weight (g) | 27.5±0.6 | 26.4±0.4 | 26.9±1.0 | 27.5±0.5 |
| Heart rate (beats/min) | 486±17 | 485±18.5 | 474±12.6 | 533±15.8 |
| Septum thickness (mm) | | | | |
| diastole | 0.77±0.01 | 0.73±0.01 | 0.75±0.01 | 0.74±0.01 |
| systole | 0.98±0.02 | 0.95±0.04 | 0.99±0.02 | 0.99±0.03 |
| Left ventricular wall thickness (mm) | | | | |
| diastole | 0.75±0.01 | 0.70±0.01 | 0.73±0.02 | 0.74±0.01 |
| systole | 0.98±0.03 | 0.94±0.03 | 0.99±0.02 | 0.99±0.02 |
| Left ventricular internal diameter (mm) | | | | |
| diastole | 3.91±0.12 | 3.80±0.10 | 3.79±0.15 | 3.93±0.11 |
| systole | 2.87±0.14 | 2.78±0.15 | 2.62±0.19 | 2.89±0.15 |
| Ejection fraction (%) | 52.89±2.6 | 52.97±3.6 | 59.26±3.5 | 52.56±3.0 |
| Fraction of shortening (%) | 26.94±1.6 | 27.14±2.4 | 31.11±2.4 | 26.76±1.8 |

# Conclusions and remarks

# 4. Final conclusions and remarks

Based on studies with rapamycin, mTOR kinase has been implicated in protein synthesis and growth. However, this role was challenged by some studies on the heart.[147, 160] Rapamycin has been shown to inhibit mTORC2 in certain cell types[99] and additionally, rapamycin resistant functions of mTOR have been described recently.[106] Altogether this underlines the importance of analyzing cardiac functions of mTOR, even more so as several rapalogs are in clinical trials for the treatment of various types of cancers or cardiovascular diseases. Furthermore, active-site mTOR inhibitors have recently been developed that inhibit both mTORC1 and mTORC2. The aim of this dissertation project was therefore to elucidate the roles of mTORC1 and mTORC2 in the heart.

As global deletion of any component of the mTOR complexes is embryonic lethal,[52, 55, 57, 61, 62, 172] we used inducible cre-loxP methodology to selectively inactivate mTORC1 or mTORC2 in the mouse heart. Mice lacking the mTORC1- or mTORC2-specific components raptor and rictor in cardiomyocytes were subjected to various physiological or pathological conditions to analyze the growth response and function of the heart.

In the first part of the thesis, the role of mTORC1 in the adult mouse heart was characterized. The raptor-cKO mice showed deterioration of cardiac function, leading to heart failure. Four weeks after raptor deletion raptor-cKO mice showed typical signs of dilated cardiomyopathy in normal cage conditions that culminated to cardiac sudden death during the fifth week. Voluntary exercise in a running wheel did not make things any better. Under pathological conditions of pressure-overload, raptor deleted mice did not develop any adaptive hypertrophy but went directly into dilated cardiomyopathy. With this observation we established mTORC1 as a critical mediator of hypertrophic growth under the conditions of stress. This is in line with previous studies that demonstrated a role of mTOR in cardiac hypertrophy using rapamycin.[147, 151-154] However, rapamycin treatment resulted in maintained cardiac function in the initial period of the hypertrophic response to aortic constriction, in contrast to the raptor deficient hearts, in which function started to deteriorate already during the first

week. How and why rapamycin treatment showed this difference in comparison to our mTORC1 inactivation model requires further study, where systemic effects of rapamycin, if any, along with dosing should be evaluated.

The other major observation with the raptor knockout mice was the altered pattern of mitochondrial gene expression and distorted mitochondria. This is consistent with the results from the skeletal muscle raptor knockout mice, indicating the similar role for mTORC1 in these different muscle tissues.[173] Metabolic stress can be the early trigger for cardiac dysfunction caused by depressed mTORC1 activity. Along with changes in metabolic gene expression including PPARα, PGC1α, GLUT4 and GLUT1, we observed a shift from fatty acid to glucose oxidation in our *ex-vivo* working heart experiments. These experiments therefore suggest a role for mTORC1 as a regulator of the metabolic switch that adapts the prime energy source according to cardiac stress conditions. Our study also provides support for a role of mTORC1 in regulating apoptosis and autophagy in the heart. How exactly mTORC1 controls these processes in cardiac tissue needs further study. In conclusion, our study with the raptor deletion provides a causal relationship between depressed mTORC1 activity and cardiac dysfunction. It establishes mTORC1 as an essential component of cardiac homeostasis.

The second part of the thesis focused on the *in vivo* functions of mTORC2 in the heart. Unavailability of an mTORC2-selective inhibitor, like rapamycin for mTORC1, has limited the knowledge about mTORC2 downstream functions. Employing the inducible and tissue-specific gene deletion approach, our study demonstrates for the first time a role of mTORC2 in the adult mouse heart, as cardiac rictor ablation resulted in significantly decreased cardiac function in response to pathological pressure-overload. It is interesting to note that rictor-cKO mice showed signs of eccentric hypertrophy already after 1 week of aortic constriction, whereas the increased afterload induced by this surgical procedure generally first leads to concentric hypertrophy. Similar increases in cardiac mass after aortic constriction in both rictor-cKO and wild-type mice indicated that bulk protein synthesis was not affected. As mTORC2-mediated TM phosphorylation of Akt Ser473 is important for its stability and thus for Akt activity, it could have affected the mTORC1-mediated

protein synthesis. Unchanged levels of 4E-BP1 phosphorylation suggested normal cap-dependent translation occurring via mTORC1, though we did not measure cardiac protein synthesis directly. Further studies are required to analyze the effect of rictor deletion on cardiac protein content as it is influenced by protein synthesis as well as degradation. The eccentric phenotype seen in our rictor-cKO mice may be due to the consequence of various defects induced by the deletion. The mice showed increased apoptosis and fibrosis in response to aortic constriction, which likely contributed to the observed decrease in cardiac function. Paracrine effects of rictor deletion from cardiomyocytes might have affected neighboring non-myocytes cells to increase apoptosis and fibrosis but further studies are required to confirm paracrine effects of rictor deletion.

In further experiments, we demonstrated that in normal physiological situations, reduced mTORC2 activity in adult mice did not affect cardiac function or geometry up to 34 weeks of age, suggesting that mTORC2 is not required for normal cardiac homeostasis. Additional experiments with the rictor-cKO mice during their postnatal growth phase supported the above notion, because rictor deletion did not change cardiac growth or geometry. Interestingly, despite the loss of two important targets of mTORC2, Akt and PKCα, these mice maintained their normal cardiac function. This might be explained by compensatory mechanisms taking over the functions downstream of mTORC2. Alternatively, these signaling molecules may have an important function only in case of stress. To answer these questions, further *in vitro* studies using gene silencing are needed.

In summary, using genetic knockout models, I have characterized the functions of mTORC1 and mTORC2 in the mouse heart. Both signaling branches of mTOR are crucial for the heart, where mTORC1 is essential during physiological and pathological growth situations, while mTORC2 is required to maintain cardiac function under conditions of pathologically increased workload. Therefore during the use mTOR-active site inhibitors in clinical trials, which block both complexes of mTOR, monitoring of the cardiac performance is very important.

# Appendix

# 5. Appendix

During my PhD research period, I was involved in a related project together with my colleague Isabelle Plaisance. The project aimed to elucidate the role of mTORC1 role IGF- or TNFα-induced cardiac hypertrophy. Along with the scientific discussions and planning related to the project, I was mainly doing the neonatal rat primary culture. The culture involves the isolation of primary cardiomyocytes from neonatal rat hearts (1-2 days old). The project is ongoing and since I was giving primarily the technical support with experiments, here I am appending only an abstract of the study.

**Abstract**

**Blocking of mTORC1 prevents IGF- but not TNF-induced hypertrophy in rat neonatal cardiomyocytes**

*Isabelle Plaisance, Pankaj Shende, Katrin Bühler, Christian Morandi and Marijke Brink*
*CardioBiology, Institute of Physiology, Department of Biomedicine, University of Basel and University Hospital Basel, Switzerland*

**Background:** mTOR, a key regulator of cellular growth, associates in cells with distinct partner proteins in two complexes, mTORC1 and mTORC2. Several in vivo studies with rapamycin have implicated mTORC1 in cardiac hypertrophy. Tumor necrosis factor-α (TNF) and insulin-like growth factor-I (IGF) are very important factors involved in cardiac remodeling. However, very little is known about the role of mTORC1 in TNF- or IGF-induced cardiac hypertrophy. In the present study we analyzed the effects of TNF on cardiomyocyte protein content in comparison to IGF, and assessed the role of mTORC1 in the responses to both factors.

**Methods:** Neonatal rat ventricular cardiomyocytes were isolated from 1-3 days old Wistar rats. Cells depleted of serum were treated with TNF (5 ng/ml) or IGF (10 ng/ml). Total protein and DNA content were analyzed in Lowry and Hoechst assays , and the protein/DNA ratio was used as a measure for cellular protein content. Protein

kinase activity was assessed with phospho-antibodies on Western blots. Expression of mTOR or raptor was blocked by using siRNA technology and electroporation.

**Results:** Treatment of cardiomyocytes with TNF or IGF for 24 h resulted in significant increases in cellular protein content of 65±5% and 76±7%, respectively (p<0.001 for both). TNF and IGF caused marked phosphorylation of Akt, mTOR and its targets p70-S6K and 4E-BP1. The mTOR inhibitor rapamycin (Rap 2 ng/ml) fully blocked TNF or IGF-induced p70-S6K phosphorylation. Rap also inhibited IGF-induced phosphorylation of 4E-BP1. Interestingly, TNF kept its ability to significantly phosphorylate 4E-BP1 in the presence of Rap. Correspondingly, protein content remained significantly higher in the TNF-treated cardiomyocytes while protein synthesis was completely abolished by Rap in the IGF-treated cells. To further investigate the role of mTORC1, cardiomyocytes were transfected with specific siRNAs, which resulted in strong decreases in mTOR or raptor protein expression compared with control cells transfected with non-targeting siRNA. mTOR- or raptor-silenced cells showed a complete inhibition of TNF- or IGF-induced phosphorylation of p70S6K. Both siRNAs fully abolished the stimulation of 4E-BP1 phosphorylation by IGF while TNF was still strongly increasing it. The IGF-induced hypertrophic response was abrogated in mTOR- or raptor-silenced-cells whereas TNF retained its ability to stimulate increases of protein content. To explore the role of the TNF-induced rapamycine-insensitive phosphorylation of 4E-BP1, we transfected cells with 4E-BP1μ, a non-phosphorylable mutant of the 4E-BP1. Overexpression of 4E-BP1μ significantly reduced the Rap-sensitive as well as Rap-insensitive part of the TNF-evoked increase in protein content.

**Conclusion:** Our data show that mTORC1 fully mediates the IGF-induced increase of protein content in cardiomyocytes. TNF induces cardiac hypertrophy via a Rap-insensitive pathway that involves phosphorylation of 4E-BP1. Our study brings new insights into the signaling pathways implicated in cardiac hypertrophy and may help to define new strategies against this disease.

# References

# 6. References

**1.** Gregorio CC, Antin PB. To the heart of myofibril assembly. *Trends Cell Biol.* 2000;10(9):355-362.

**2.** Hoffman JI. Incidence of congenital heart disease: II. Prenatal incidence. *Pediatr Cardiol.* 1995;16(4):155-165.

**3.** Vakili BA, Okin PM, Devereux RB. Prognostic implications of left ventricular hypertrophy. *Am Heart J.* 2001;141(3):334-341.

**4.** Olson EN. A decade of discoveries in cardiac biology. *Nat Med.* 2004;10(5):467-474.

**5.** Levy D, Garrison RJ, Savage DD, Kannel WB, Castelli WP. Prognostic implications of echocardiographically determined left ventricular mass in the Framingham Heart Study. *N Engl J Med.* 1990;322(22):1561-1566.

**6.** Ford LE. Heart size. *Circ Res.* 1976;39(3):297-303.

**7.** Sakata Y, Hoit BD, Liggett SB, Walsh RA, Dorn GW, 2nd. Decompensation of pressure-overload hypertrophy in G alpha q-overexpressing mice. *Circulation.* 1998;97(15):1488-1495.

**8.** Dorn GW, 2nd, Robbins J, Sugden PH. Phenotyping hypertrophy: eschew obfuscation. *Circ Res.* 2003;92(11):1171-1175.

**9.** Grossman W, Jones D, McLaurin LP. Wall stress and patterns of hypertrophy in the human left ventricle. *J Clin Invest.* 1975;56(1):56-64.

**10.** Opie LH, Commerford PJ, Gersh BJ, Pfeffer MA. Controversies in ventricular remodelling. *Lancet.* 2006;367(9507):356-367.

**11.** Meerson FZ. On the mechanism of compensatory hyperfunction and insufficiency of the heart. *Cor Vasa.* 1961;3:161-177.

**12.** Meerson FZ, Kapelko VI. The effect of cardiac hyperfunction on its automaticity and reactivity to the chronotropic effect of the vagus. *Cor Vasa.* 1965;7(4):264-272.

**13.** D'Angelo DD, Sakata Y, Lorenz JN, Boivin GP, Walsh RA, Liggett SB, Dorn GW, 2nd. Transgenic Galphaq overexpression induces cardiac contractile failure in mice. *Proc Natl Acad Sci U S A.* 1997;94(15):8121-8126.

**14.** Dorn GW, 2nd, Robbins J, Ball N, Walsh RA. Myosin heavy chain regulation and myocyte contractile depression after LV hypertrophy in aortic-banded mice. *Am J Physiol.* 1994;267(1 Pt 2):H400-405.

**15.** Gerdes AM, Kellerman SE, Moore JA, Muffly KE, Clark LC, Reaves PY, Malec KB, McKeown PP, Schocken DD. Structural remodeling of cardiac

myocytes in patients with ischemic cardiomyopathy. *Circulation.* 1992;86(2):426-430.

16.    Chien KR, Knowlton KU, Zhu H, Chien S. Regulation of cardiac gene expression during myocardial growth and hypertrophy: molecular studies of an adaptive physiologic response. *FASEB J.* 1991;5(15):3037-3046.

17.    Lowes BD, Gilbert EM, Abraham WT, Minobe WA, Larrabee P, Ferguson D, Wolfel EE, Lindenfeld J, Tsvetkova T, Robertson AD, Quaife RA, Bristow MR. Myocardial gene expression in dilated cardiomyopathy treated with beta-blocking agents. *N Engl J Med.* 2002;346(18):1357-1365.

18.    Arai M, Matsui H, Periasamy M. Sarcoplasmic reticulum gene expression in cardiac hypertrophy and heart failure. *Circ Res.* 1994;74(4):555-564.

19.    Yussman MG, Toyokawa T, Odley A, Lynch RA, Wu G, Colbert MC, Aronow BJ, Lorenz JN, Dorn GW, 2nd. Mitochondrial death protein Nix is induced in cardiac hypertrophy and triggers apoptotic cardiomyopathy. *Nat Med.* 2002;8(7):725-730.

20.    Maisel A. B-type natriuretic peptide levels: a potential novel "white count" for congestive heart failure. *J Card Fail.* 2001;7(2):183-193.

21.    Pluim BM, Zwinderman AH, van der Laarse A, van der Wall EE. The athlete's heart. A meta-analysis of cardiac structure and function. *Circulation.* 2000;101(3):336-344.

22.    Fagard RH. Impact of different sports and training on cardiac structure and function. *Cardiol Clin.* 1997;15(3):397-412.

23.    Eghbali M, Deva R, Alioua A, Minosyan TY, Ruan H, Wang Y, Toro L, Stefani E. Molecular and functional signature of heart hypertrophy during pregnancy. *Circ Res.* 2005;96(11):1208-1216.

24.    Kaplan ML, Cheslow Y, Vikstrom K, Malhotra A, Geenen DL, Nakouzi A, Leinwand LA, Buttrick PM. Cardiac adaptations to chronic exercise in mice. *Am J Physiol.* 1994;267(3 Pt 2):H1167-1173.

25.    Iemitsu M, Miyauchi T, Maeda S, Sakai S, Kobayashi T, Fujii N, Miyazaki H, Matsuda M, Yamaguchi I. Physiological and pathological cardiac hypertrophy induce different molecular phenotypes in the rat. *Am J Physiol Regul Integr Comp Physiol.* 2001;281(6):R2029-2036.

26.    McMullen JR, Shioi T, Zhang L, Tarnavski O, Sherwood MC, Kang PM, Izumo S. Phosphoinositide 3-kinase(p110alpha) plays a critical role for the induction of physiological, but not pathological, cardiac hypertrophy. *Proc Natl Acad Sci U S A.* 2003;100(21):12355-12360.

27.    McMullen JR, Jennings GL. Differences between pathological and physiological cardiac hypertrophy: novel therapeutic strategies to treat heart failure. *Clin Exp Pharmacol Physiol.* 2007;34(4):255-262.

28. Heineke J, Molkentin JD. Regulation of cardiac hypertrophy by intracellular signalling pathways. *Nat Rev Mol Cell Biol.* 2006;7(8):589-600.

29. Gutkind JS. Cell growth control by G protein-coupled receptors: from signal transduction to signal integration. *Oncogene.* 1998;17(11 Reviews):1331-1342.

30. Schlessinger J. Cell signaling by receptor tyrosine kinases. *Cell.* 2000;103(2):211-225.

31. Dorn GW, 2nd. The fuzzy logic of physiological cardiac hypertrophy. *Hypertension.* 2007;49(5):962-970.

32. Frey N, Olson EN. Cardiac hypertrophy: the good, the bad, and the ugly. *Annu Rev Physiol.* 2003;65:45-79.

33. Heitman J, Movva NR, Hall MN. Targets for cell cycle arrest by the immunosuppressant rapamycin in yeast. *Science.* 1991;253(5022):905-909.

34. Fingar DC, Blenis J. Target of rapamycin (TOR): an integrator of nutrient and growth factor signals and coordinator of cell growth and cell cycle progression. *Oncogene.* 2004;23(18):3151-3171.

35. Hay N, Sonenberg N. Upstream and downstream of mTOR. *Genes Dev.* 2004;18(16):1926-1945.

36. Wullschleger S, Loewith R, Hall MN. TOR signaling in growth and metabolism. *Cell.* 2006;124(3):471-484.

37. Yang Q, Guan KL. Expanding mTOR signaling. *Cell Res.* 2007;17(8):666-681.

38. Benjamin D, Colombi M, Moroni C, Hall MN. Rapamycin passes the torch: a new generation of mTOR inhibitors. *Nat Rev Drug Discov.* 2011;10(11):868-880.

39. Peterson RT, Beal PA, Comb MJ, Schreiber SL. FKBP12-rapamycin-associated protein (FRAP) autophosphorylates at serine 2481 under translationally repressive conditions. *J Biol Chem.* 2000;275(10):7416-7423.

40. Copp J, Manning G, Hunter T. TORC-specific phosphorylation of mammalian target of rapamycin (mTOR): phospho-Ser2481 is a marker for intact mTOR signaling complex 2. *Cancer Res.* 2009;69(5):1821-1827.

41. Chiang GG, Abraham RT. Phosphorylation of mammalian target of rapamycin (mTOR) at Ser-2448 is mediated by p70S6 kinase. *J Biol Chem.* 2005;280(27):25485-25490.

42. Holz MK, Blenis J. Identification of S6 kinase 1 as a novel mammalian target of rapamycin (mTOR)-phosphorylating kinase. *J Biol Chem.* 2005;280(28):26089-26093.

43. Cheng SW, Fryer LG, Carling D, Shepherd PR. Thr2446 is a novel mammalian target of rapamycin (mTOR) phosphorylation site regulated by nutrient status. *J Biol Chem.* 2004;279(16):15719-15722.

44. Acosta-Jaquez HA, Keller JA, Foster KG, Ekim B, Soliman GA, Feener EP, Ballif BA, Fingar DC. Site-specific mTOR phosphorylation promotes mTORC1-mediated signaling and cell growth. *Mol Cell Biol.* 2009;29(15):4308-4324.

45. Zoncu R, Efeyan A, Sabatini DM. mTOR: from growth signal integration to cancer, diabetes and ageing. *Nat Rev Mol Cell Biol.* 2011;12(1):21-35.

46. Kim DH, Sarbassov DD, Ali SM, King JE, Latek RR, Erdjument-Bromage H, Tempst P, Sabatini DM. mTOR interacts with raptor to form a nutrient-sensitive complex that signals to the cell growth machinery. *Cell.* 2002;110(2):163-175.

47. Sarbassov DD, Ali SM, Kim DH, Guertin DA, Latek RR, Erdjument-Bromage H, Tempst P, Sabatini DM. Rictor, a novel binding partner of mTOR, defines a rapamycin-insensitive and raptor-independent pathway that regulates the cytoskeleton. *Curr Biol.* 2004;14(14):1296-1302.

48. Yip CK, Murata K, Walz T, Sabatini DM, Kang SA. Structure of the human mTOR complex I and its implications for rapamycin inhibition. *Mol Cell.* 2010;38(5):768-774.

49. Wullschleger S, Loewith R, Oppliger W, Hall MN. Molecular organization of target of rapamycin complex 2. *J Biol Chem.* 2005;280(35):30697-30704.

50. Hara K, Maruki Y, Long X, Yoshino K, Oshiro N, Hidayat S, Tokunaga C, Avruch J, Yonezawa K. Raptor, a binding partner of target of rapamycin (TOR), mediates TOR action. *Cell.* 2002;110(2):177-189.

51. Balasubramanian S, Johnston RK, Moschella PC, Mani SK, Tuxworth WJ, Jr., Kuppuswamy D. mTOR in growth and protection of hypertrophying myocardium. *Cardiovasc Hematol Agents Med Chem.* 2009;7(1):52-63.

52. Murakami M, Ichisaka T, Maeda M, Oshiro N, Hara K, Edenhofer F, Kiyama H, Yonezawa K, Yamanaka S. mTOR is essential for growth and proliferation in early mouse embryos and embryonic stem cells. *Mol Cell Biol.* 2004;24(15):6710-6718.

53. Loewith R, Jacinto E, Wullschleger S, Lorberg A, Crespo JL, Bonenfant D, Oppliger W, Jenoe P, Hall MN. Two TOR complexes, only one of which is rapamycin sensitive, have distinct roles in cell growth control. *Mol Cell.* 2002;10(3):457-468.

54. Kim DH, Sarbassov DD, Ali SM, Latek RR, Guntur KV, Erdjument-Bromage H, Tempst P, Sabatini DM. GbetaL, a positive regulator of the rapamycin-sensitive pathway required for the nutrient-sensitive interaction between raptor and mTOR. *Mol Cell.* 2003;11(4):895-904.

55. Guertin DA, Stevens DM, Thoreen CC, Burds AA, Kalaany NY, Moffat J, Brown M, Fitzgerald KJ, Sabatini DM. Ablation in mice of the mTORC components raptor, rictor, or mLST8 reveals that mTORC2 is required for signaling to Akt-FOXO and PKCalpha, but not S6K1. *Dev Cell.* 2006;11(6):859-871.

56. Jacinto E, Loewith R, Schmidt A, Lin S, Ruegg MA, Hall A, Hall MN. Mammalian TOR complex 2 controls the actin cytoskeleton and is rapamycin insensitive. *Nat Cell Biol.* 2004;6(11):1122-U1130.

57. Shiota C, Woo JT, Lindner J, Shelton KD, Magnuson MA. Multiallelic disruption of the rictor gene in mice reveals that mTOR complex 2 is essential for fetal growth and viability. *Dev Cell.* 2006;11(4):583-589.

58. McDonald PC, Oloumi A, Mills J, Dobreva I, Maidan M, Gray V, Wederell ED, Bally MB, Foster LJ, Dedhar S. Rictor and integrin-linked kinase interact and regulate Akt phosphorylation and cancer cell survival. *Cancer Res.* 2008;68(6):1618-1624.

59. Hagan GN, Lin Y, Magnuson MA, Avruch J, Czech MP. A Rictor-Myo1c complex participates in dynamic cortical actin events in 3T3-L1 adipocytes. *Mol Cell Biol.* 2008;28(13):4215-4226.

60. Martin J, Masri J, Bernath A, Nishimura RN, Gera J. Hsp70 associates with Rictor and is required for mTORC2 formation and activity. *Biochem Biophys Res Commun.* 2008;372(4):578-583.

61. Jacinto E, Facchinetti V, Liu D, Soto N, Wei S, Jung SY, Huang Q, Qin J, Su B. SIN1/MIP1 maintains rictor-mTOR complex integrity and regulates Akt phosphorylation and substrate specificity. *Cell.* 2006;127(1):125-137.

62. Yang Q, Inoki K, Ikenoue T, Guan KL. Identification of Sin1 as an essential TORC2 component required for complex formation and kinase activity. *Genes Dev.* 2006;20(20):2820-2832.

63. Chen CH, Sarbassov DD. Integrity of mTORC2 is dependent on phosphorylation of SIN1 by mTOR. *J Biol Chem.* 2011.

64. Lu M, Wang J, Ives HE, Pearce D. mSIN1 protein mediates SGK1 protein interaction with mTORC2 protein complex and is required for selective activation of the epithelial sodium channel. *J Biol Chem.* 2011;286(35):30647-30654.

65. Leung AK, Robson WL. Tuberous sclerosis complex: a review. *J Pediatr Health Care.* 2007;21(2):108-114.

66. Mak BC, Yeung RS. The tuberous sclerosis complex genes in tumor development. *Cancer Invest.* 2004;22(4):588-603.

67. Saucedo LJ, Gao X, Chiarelli DA, Li L, Pan D, Edgar BA. Rheb promotes cell growth as a component of the insulin/TOR signalling network. *Nat Cell Biol.* 2003;5(6):566-571.

68. Stocker H, Radimerski T, Schindelholz B, Wittwer F, Belawat P, Daram P, Breuer S, Thomas G, Hafen E. Rheb is an essential regulator of S6K in controlling cell growth in Drosophila. *Nat Cell Biol.* 2003;5(6):559-565.

69. Garami A, Zwartkruis FJ, Nobukuni T, Joaquin M, Roccio M, Stocker H, Kozma SC, Hafen E, Bos JL, Thomas G. Insulin activation of Rheb, a mediator of mTOR/S6K/4E-BP signaling, is inhibited by TSC1 and 2. *Mol Cell.* 2003;11(6):1457-1466.

70. Bai X, Jiang Y. Key factors in mTOR regulation. *Cell Mol Life Sci.* 2010;67(2):239-253.

71. Inoki K, Li Y, Xu T, Guan KL. Rheb GTPase is a direct target of TSC2 GAP activity and regulates mTOR signaling. *Genes Dev.* 2003;17(15):1829-1834.

72. Long X, Ortiz-Vega S, Lin Y, Avruch J. Rheb binding to mammalian target of rapamycin (mTOR) is regulated by amino acid sufficiency. *J Biol Chem.* 2005;280(25):23433-23436.

73. Bai X, Ma D, Liu A, Shen X, Wang QJ, Liu Y, Jiang Y. Rheb activates mTOR by antagonizing its endogenous inhibitor, FKBP38. *Science.* 2007;318(5852):977-980.

74. Vander Haar E, Lee S, Bandhakavi S, Griffin TJ, Kim DH. Insulin signalling to mTOR mediated by the Akt/PKB substrate PRAS40. *Nat Cell Biol.* 2007;9(3):316-U126.

75. Oshiro N, Takahashi R, Yoshino KI, Tanimura K, Nakashima A, Eguchi S, Miyamoto T, Hara K, Takehana K, Avruch J, Kikkawa U, Yonezawa K. The proline-rich akt substrate of 40 kDa (PRAS40) is a physiological substrate of mammalian target of rapamycin complex 1. *Journal of Biological Chemistry.* 2007;282(28):20329-20339.

76. Wang X, Yue P, Kim YA, Fu H, Khuri FR, Sun SY. Enhancing mammalian target of rapamycin (mTOR)-targeted cancer therapy by preventing mTOR/raptor inhibition-initiated, mTOR/rictor-independent Akt activation. *Cancer Res.* 2008;68(18):7409-7418.

77. Zhang F, Beharry ZM, Harris TE, Lilly MB, Smith CD, Mahajan S, Kraft AS. PIM1 protein kinase regulates PRAS40 phosphorylation and mTOR activity in FDCP1 cells. *Cancer Biol Ther.* 2009;8(9):846-853.

78. Polak P, Hall MN. mTOR and the control of whole body metabolism. *Curr Opin Cell Biol.* 2009;21(2):209-218.

79. Ma L, Chen Z, Erdjument-Bromage H, Tempst P, Pandolfi PP. Phosphorylation and functional inactivation of TSC2 by Erk implications for tuberous sclerosis and cancer pathogenesis. *Cell.* 2005;121(2):179-193.

80. Inoki K, Ouyang H, Zhu T, Lindvall C, Wang Y, Zhang X, Yang Q, Bennett C, Harada Y, Stankunas K, Wang CY, He X, MacDougald OA, You M, Williams BO, Guan KL. TSC2 integrates Wnt and energy signals via a

coordinated phosphorylation by AMPK and GSK3 to regulate cell growth. *Cell.* 2006;126(5):955-968.

81. Fonseca BD, Smith EM, Lee VH, MacKintosh C, Proud CG. PRAS40 is a target for mammalian target of rapamycin complex 1 and is required for signaling downstream of this complex. *J Biol Chem.* 2007;282(34):24514-24524.

82. Wang X, Campbell LE, Miller CM, Proud CG. Amino acid availability regulates p70 S6 kinase and multiple translation factors. *Biochem J.* 1998;334 ( Pt 1):261-267.

83. Kim E, Goraksha-Hicks P, Li L, Neufeld TP, Guan KL. Regulation of TORC1 by Rag GTPases in nutrient response. *Nat Cell Biol.* 2008;10(8):935-945.

84. Sancak Y, Peterson TR, Shaul YD, Lindquist RA, Thoreen CC, Bar-Peled L, Sabatini DM. The Rag GTPases bind raptor and mediate amino acid signaling to mTORC1. *Science.* 2008;320(5882):1496-1501.

85. Findlay GM, Yan L, Procter J, Mieulet V, Lamb RF. A MAP4 kinase related to Ste20 is a nutrient-sensitive regulator of mTOR signalling. *Biochem J.* 2007;403(1):13-20.

86. Yan L, Mieulet V, Burgess D, Findlay GM, Sully K, Procter J, Goris J, Janssens V, Morrice NA, Lamb RF. PP2A T61 epsilon is an inhibitor of MAP4K3 in nutrient signaling to mTOR. *Mol Cell.* 2010;37(5):633-642.

87. Gulati P, Gaspers LD, Dann SG, Joaquin M, Nobukuni T, Natt F, Kozma SC, Thomas AP, Thomas G. Amino acids activate mTOR complex 1 via Ca2+/CaM signaling to hVps34. *Cell Metab.* 2008;7(5):456-465.

88. Nobukuni T, Joaquin M, Roccio M, Dann SG, Kim SY, Gulati P, Byfield MP, Backer JM, Natt F, Bos JL, Zwartkruis FJ, Thomas G. Amino acids mediate mTOR/raptor signaling through activation of class 3 phosphatidylinositol 3OH-kinase. *Proc Natl Acad Sci U S A.* 2005;102(40):14238-14243.

89. Sancak Y, Bar-Peled L, Zoncu R, Markhard AL, Nada S, Sabatini DM. Ragulator-Rag complex targets mTORC1 to the lysosomal surface and is necessary for its activation by amino acids. *Cell.* 2010;141(2):290-303.

90. Duran A, Amanchy R, Linares JF, Joshi J, Abu-Baker S, Porollo A, Hansen M, Moscat J, Diaz-Meco MT. p62 Is a Key Regulator of Nutrient Sensing in the mTORC1 Pathway. *Mol Cell.* 2011;44(1):134-146.

91. Dennis PB, Jaeschke A, Saitoh M, Fowler B, Kozma SC, Thomas G. Mammalian TOR: a homeostatic ATP sensor. *Science.* 2001;294(5544):1102-1105.

92. Hardie DG. AMP-activated/SNF1 protein kinases: conserved guardians of cellular energy. *Nat Rev Mol Cell Biol.* 2007;8(10):774-785.

93. Gwinn DM, Shackelford DB, Egan DF, Mihaylova MM, Mery A, Vasquez DS, Turk BE, Shaw RJ. AMPK phosphorylation of raptor mediates a metabolic checkpoint. *Mol Cell.* 2008;30(2):214-226.

94. Brugarolas J, Lei K, Hurley RL, Manning BD, Reiling JH, Hafen E, Witters LA, Ellisen LW, Kaelin WG, Jr. Regulation of mTOR function in response to hypoxia by REDD1 and the TSC1/TSC2 tumor suppressor complex. *Genes Dev.* 2004;18(23):2893-2904.

95. DeYoung MP, Horak P, Sofer A, Sgroi D, Ellisen LW. Hypoxia regulates TSC1/2-mTOR signaling and tumor suppression through REDD1-mediated 14-3-3 shuttling. *Genes Dev.* 2008;22(2):239-251.

96. Feng Z, Hu W, de Stanchina E, Teresky AK, Jin S, Lowe S, Levine AJ. The regulation of AMPK beta1, TSC2, and PTEN expression by p53: stress, cell and tissue specificity, and the role of these gene products in modulating the IGF-1-AKT-mTOR pathways. *Cancer Res.* 2007;67(7):3043-3053.

97. Budanov AV, Karin M. p53 target genes sestrin1 and sestrin2 connect genotoxic stress and mTOR signaling. *Cell.* 2008;134(3):451-460.

98. Frias MA, Thoreen CC, Jaffe JD, Schroder W, Sculley T, Carr SA, Sabatini DM. mSin1 is necessary for Akt/PKB phosphorylation, and its isoforms define three distinct mTORC2s. *Curr Biol.* 2006;16(18):1865-1870.

99. Sarbassov DD, Ali SM, Sengupta S, Sheen JH, Hsu PP, Bagley AF, Markhard AL, Sabatini DM. Prolonged rapamycin treatment inhibits mTORC2 assembly and Akt/PKB. *Mol Cell.* 2006;22(2):159-168.

100. Gan X, Wang J, Su B, Wu D. Evidence for direct activation of mTORC2 kinase activity by phosphatidylinositol 3,4,5-trisphosphate. *J Biol Chem.* 2011;286(13):10998-11002.

101. Oh WJ, Wu CC, Kim SJ, Facchinetti V, Julien LA, Finlan M, Roux PP, Su B, Jacinto E. mTORC2 can associate with ribosomes to promote cotranslational phosphorylation and stability of nascent Akt polypeptide. *EMBO J.* 2010;29(23):3939-3951.

102. Huang J, Dibble CC, Matsuzaki M, Manning BD. The TSC1-TSC2 complex is required for proper activation of mTOR complex 2. *Mol Cell Biol.* 2008;28(12):4104-4115.

103. Huang J, Wu S, Wu CL, Manning BD. Signaling events downstream of mammalian target of rapamycin complex 2 are attenuated in cells and tumors deficient for the tuberous sclerosis complex tumor suppressors. *Cancer Res.* 2009;69(15):6107-6114.

104. Schalm SS, Blenis J. Identification of a conserved motif required for mTOR signaling. *Curr Biol.* 2002;12(8):632-639.

105. Nojima H, Tokunaga C, Eguchi S, Oshiro N, Hidayat S, Yoshino K, Hara K, Tanaka N, Avruch J, Yonezawa K. The mammalian target of rapamycin

(mTOR) partner, raptor, binds the mTOR substrates p70 S6 kinase and 4E-BP1 through their TOR signaling (TOS) motif. *J Biol Chem.* 2003;278(18):15461-15464.

106. Thoreen CC, Kang SA, Chang JW, Liu Q, Zhang J, Gao Y, Reichling LJ, Sim T, Sabatini DM, Gray NS. An ATP-competitive mammalian target of rapamycin inhibitor reveals rapamycin-resistant functions of mTORC1. *J Biol Chem.* 2009;284(12):8023-8032.

107. Ma XM, Blenis J. Molecular mechanisms of mTOR-mediated translational control. *Nat Rev Mol Cell Biol.* 2009;10(5):307-318.

108. Sengupta S, Peterson TR, Sabatini DM. Regulation of the mTOR Complex 1 Pathway by Nutrients, Growth Factors, and Stress. *Molecular Cell.* 2010;40(2):310-322.

109. Ramirez-Valle F, Badura ML, Braunstein S, Narasimhan M, Schneider RJ. Mitotic raptor promotes mTORC1 activity, G(2)/M cell cycle progression, and internal ribosome entry site-mediated mRNA translation. *Mol Cell Biol.* 2010;30(13):3151-3164.

110. Mayer C, Zhao J, Yuan X, Grummt I. mTOR-dependent activation of the transcription factor TIF-IA links rRNA synthesis to nutrient availability. *Genes Dev.* 2004;18(4):423-434.

111. Martin DE, Hall MN. The expanding TOR signaling network. *Curr Opin Cell Biol.* 2005;17(2):158-166.

112. Michels AA. MAF1: a new target of mTORC1. *Biochem Soc Trans.* 2011;39(2):487-491.

113. Porstmann T, Santos CR, Griffiths B, Cully M, Wu M, Leevers S, Griffiths JR, Chung YL, Schulze A. SREBP activity is regulated by mTORC1 and contributes to Akt-dependent cell growth. *Cell Metab.* 2008;8(3):224-236.

114. Duvel K, Yecies JL, Menon S, Raman P, Lipovsky AI, Souza AL, Triantafellow E, Ma Q, Gorski R, Cleaver S, Vander Heiden MG, MacKeigan JP, Finan PM, Clish CB, Murphy LO, Manning BD. Activation of a metabolic gene regulatory network downstream of mTOR complex 1. *Mol Cell.* 2010;39(2):171-183.

115. Cunningham JT, Rodgers JT, Arlow DH, Vazquez F, Mootha VK, Puigserver P. mTOR controls mitochondrial oxidative function through a YY1-PGC-1alpha transcriptional complex. *Nature.* 2007;450(7170):736-740.

116. Majmundar AJ, Wong WJ, Simon MC. Hypoxia-inducible factors and the response to hypoxic stress. *Mol Cell.* 2010;40(2):294-309.

117. Neufeld TP. TOR-dependent control of autophagy: biting the hand that feeds. *Curr Opin Cell Biol.* 2010;22(2):157-168.

118. Kamada Y, Yoshino K, Kondo C, Kawamata T, Oshiro N, Yonezawa K, Ohsumi Y. Tor directly controls the Atg1 kinase complex to regulate autophagy. *Mol Cell Biol.* 2010;30(4):1049-1058.

119. Oh WJ, Jacinto E. mTOR complex 2 signaling and functions. *Cell Cycle.* 2011;10(14):2305-2316.

120. Facchinetti V, Ouyang W, Wei H, Soto N, Lazorchak A, Gould C, Lowry C, Newton AC, Mao Y, Miao RQ, Sessa WC, Qin J, Zhang P, Su B, Jacinto E. The mammalian target of rapamycin complex 2 controls folding and stability of Akt and protein kinase C. *EMBO J.* 2008;27(14):1932-1943.

121. Rosse C, Linch M, Kermorgant S, Cameron AJ, Boeckeler K, Parker PJ. PKC and the control of localized signal dynamics. *Nat Rev Mol Cell Biol.* 2010;11(2):103-112.

122. Ikenoue T, Inoki K, Yang Q, Zhou X, Guan KL. Essential function of TORC2 in PKC and Akt turn motif phosphorylation, maturation and signalling. *EMBO J.* 2008;27(14):1919-1931.

123. Lang F, Bohmer C, Palmada M, Seebohm G, Strutz-Seebohm N, Vallon V. (Patho)physiological significance of the serum- and glucocorticoid-inducible kinase isoforms. *Physiol Rev.* 2006;86(4):1151-1178.

124. Garcia-Martinez JM, Alessi DR. mTOR complex 2 (mTORC2) controls hydrophobic motif phosphorylation and activation of serum- and glucocorticoid-induced protein kinase 1 (SGK1). *Biochem J.* 2008;416(3):375-385.

125. Pearce LR, Sommer EM, Sakamoto K, Wullschleger S, Alessi DR. Protor-1 is required for efficient mTORC2-mediated activation of SGK1 in the kidney. *Biochem J.* 2011;436(1):169-179.

126. Lu M, Wang J, Jones KT, Ives HE, Feldman ME, Yao LJ, Shokat KM, Ashrafi K, Pearce D. mTOR complex-2 activates ENaC by phosphorylating SGK1. *J Am Soc Nephrol.* 2010;21(5):811-818.

127. Saci A, Cantley LC, Carpenter CL. Rac1 regulates the activity of mTORC1 and mTORC2 and controls cellular size. *Mol Cell.* 2011;42(1):50-61.

128. Zinzalla V, Stracka D, Oppliger W, Hall MN. Activation of mTORC2 by association with the ribosome. *Cell.* 2011;144(5):757-768.

129. Yu K, Toral-Barza L, Shi C, Zhang WG, Lucas J, Shor B, Kim J, Verheijen J, Curran K, Malwitz DJ, Cole DC, Ellingboe J, Ayral-Kaloustian S, Mansour TS, Gibbons JJ, Abraham RT, Nowak P, Zask A. Biochemical, Cellular, and In vivo Activity of Novel ATP-Competitive and Selective Inhibitors of the Mammalian Target of Rapamycin. *Cancer Research.* 2009;69(15):6232-6240.

130. Gulhati P, Bowen KA, Liu J, Stevens PD, Rychahou PG, Chen M, Lee EY, Weiss HL, O'Connor KL, Gao T, Evers BM. mTORC1 and mTORC2 regulate

EMT, motility, and metastasis of colorectal cancer via RhoA and Rac1 signaling pathways. *Cancer Res.* 2011;71(9):3246-3256.

131. Zhang F, Zhang X, Li M, Chen P, Zhang B, Guo H, Cao W, Wei X, Cao X, Hao X, Zhang N. mTOR complex component Rictor interacts with PKCzeta and regulates cancer cell metastasis. *Cancer Res.* 2010;70(22):9360-9370.

132. Liu L, Das S, Losert W, Parent CA. mTORC2 regulates neutrophil chemotaxis in a cAMP- and RhoA-dependent fashion. *Dev Cell.* 2010;19(6):845-857.

133. Gu Y, Lindner J, Kumar A, Yuan W, Magnuson MA. Rictor/mTORC2 is essential for maintaining a balance between beta-cell proliferation and cell size. *Diabetes.* 2011;60(3):827-837.

134. Goncharova EA, Goncharov DA, Li H, Pimtong W, Lu S, Khavin I, Krymskaya VP. mTORC2 is required for proliferation and survival of TSC2-null cells. *Mol Cell Biol.* 2011;31(12):2484-2498.

135. Wang RH, Kim HS, Xiao C, Xu X, Gavrilova O, Deng CX. Hepatic Sirt1 deficiency in mice impairs mTorc2/Akt signaling and results in hyperglycemia, oxidative damage, and insulin resistance. *J Clin Invest.* 2011.

136. Soukas AA, Kane EA, Carr CE, Melo JA, Ruvkun G. Rictor/TORC2 regulates fat metabolism, feeding, growth, and life span in Caenorhabditis elegans. *Genes Dev.* 2009;23(4):496-511.

137. Colombi M, Molle KD, Benjamin D, Rattenbacher-Kiser K, Schaefer C, Betz C, Thiemeyer A, Regenass U, Hall MN, Moroni C. Genome-wide shRNA screen reveals increased mitochondrial dependence upon mTORC2 addiction. *Oncogene.* 2011;30(13):1551-1565.

138. Chiang GG, Abraham RT. Targeting the mTOR signaling network in cancer. *Trends Mol Med.* 2007;13(10):433-442.

139. Moschella PC, Rao VU, McDermott PJ, Kuppuswamy D. Regulation of mTOR and S6K1 activation by the nPKC isoforms, PKCepsilon and PKCdelta, in adult cardiac muscle cells. *J Mol Cell Cardiol.* 2007;43(6):754-766.

140. Naga Prasad SV, Esposito G, Mao L, Koch WJ, Rockman HA. Gbetagamma-dependent phosphoinositide 3-kinase activation in hearts with in vivo pressure overload hypertrophy. *J Biol Chem.* 2000;275(7):4693-4698.

141. Yan Y, Backer JM. Regulation of class III (Vps34) PI3Ks. *Biochem Soc Trans.* 2007;35(Pt 2):239-241.

142. Mao K, Kobayashi S, Jaffer ZM, Huang Y, Volden P, Chernoff J, Liang Q. Regulation of Akt/PKB activity by P21-activated kinase in cardiomyocytes. *J Mol Cell Cardiol.* 2008;44(2):429-434.

143. Shiraishi I, Melendez J, Ahn Y, Skavdahl M, Murphy E, Welch S, Schaefer E, Walsh K, Rosenzweig A, Torella D, Nurzynska D, Kajstura J, Leri A, Anversa

P, Sussman MA. Nuclear targeting of Akt enhances kinase activity and survival of cardiomyocytes. *Circ Res.* 2004;94(7):884-891.

144. Shioi T, McMullen JR, Tarnavski O, Converso K, Sherwood MC, Manning WJ, Izumo S. Rapamycin attenuates load-induced cardiac hypertrophy in mice. *Circulation.* 2003;107(12):1664-1670.

145. Sadoshima J, Izumo S. Rapamycin selectively inhibits angiotensin II-induced increase in protein synthesis in cardiac myocytes in vitro. Potential role of 70-kD S6 kinase in angiotensin II-induced cardiac hypertrophy. *Circ Res.* 1995;77(6):1040-1052.

146. Simm A, Schluter K, Diez C, Piper HM, Hoppe J. Activation of p70(S6) kinase by beta-adrenoceptor agonists on adult cardiomyocytes. *J Mol Cell Cardiol.* 1998;30(10):2059-2067.

147. McMullen JR, Sherwood MC, Tarnavski O, Zhang L, Dorfman AL, Shioi T, Izumo S. Inhibition of mTOR signaling with rapamycin regresses established cardiac hypertrophy induced by pressure overload. *Circulation.* 2004;109(24):3050-3055.

148. Proud CG. Ras, PI3-kinase and mTOR signaling in cardiac hypertrophy. *Cardiovasc Res.* 2004;63(3):403-413.

149. Iijima Y, Laser M, Shiraishi H, Willey CD, Sundaravadivel B, Xu L, McDermott PJ, Kuppuswamy D. c-Raf/MEK/ERK pathway controls protein kinase C-mediated p70S6K activation in adult cardiac muscle cells. *J Biol Chem.* 2002;277(25):23065-23075.

150. Balasubramanian S, Kuppuswamy D. RGD-containing peptides activate S6K1 through beta3 integrin in adult cardiac muscle cells. *J Biol Chem.* 2003;278(43):42214-42224.

151. Shioi T, Matsumori A, Kakio T, Kihara Y, Sasayama S. Proinflammatory cytokine inhibitor prolongs the survival of rats with heart failure induced by pressure overload. *Jpn Circ J.* 2001;65(6):584-585.

152. Gao XM, Wong G, Wang B, Kiriazis H, Moore XL, Su YD, Dart A, Du XJ. Inhibition of mTOR reduces chronic pressure-overload cardiac hypertrophy and fibrosis. *J Hypertens.* 2006;24(8):1663-1670.

153. Soesanto W, Lin HY, Hu E, Lefler S, Litwin SE, Sena S, Abel ED, Symons JD, Jalili T. Mammalian target of rapamycin is a critical regulator of cardiac hypertrophy in spontaneously hypertensive rats. *Hypertension.* 2009;54(6):1321-1327.

154. Boluyt MO, Li ZB, Loyd AM, Scalia AF, Cirrincione GM, Jackson RR. The mTOR/p70S6K signal transduction pathway plays a role in cardiac hypertrophy and influences expression of myosin heavy chain genes in vivo. *Cardiovasc Drugs Ther.* 2004;18(4):257-267.

155. Kuzman JA, O'Connell TD, Gerdes AM. Rapamycin prevents thyroid hormone-induced cardiac hypertrophy. *Endocrinology.* 2007;148(7):3477-3484.

156. Siedlecki AM, Jin X, Muslin AJ. Uremic cardiac hypertrophy is reversed by rapamycin but not by lowering of blood pressure. *Kidney Int.* 2009;75(8):800-808.

157. Buss SJ, Muenz S, Riffel JH, Malekar P, Hagenmueller M, Weiss CS, Bea F, Bekeredjian R, Schinke-Braun M, Izumo S, Katus HA, Hardt SE. Beneficial effects of Mammalian target of rapamycin inhibition on left ventricular remodeling after myocardial infarction. *J Am Coll Cardiol.* 2009;54(25):2435-2446.

158. Shen WH, Chen Z, Shi S, Chen H, Zhu W, Penner A, Bu G, Li W, Boyle DW, Rubart M, Field LJ, Abraham R, Liechty EA, Shou W. Cardiac restricted overexpression of kinase-dead mammalian target of rapamycin (mTOR) mutant impairs the mTOR-mediated signaling and cardiac function. *J Biol Chem.* 2008;283(20):13842-13849.

159. Kemi OJ, Ceci M, Wisloff U, Grimaldi S, Gallo P, Smith GL, Condorelli G, Ellingsen O. Activation or inactivation of cardiac Akt/mTOR signaling diverges physiological from pathological hypertrophy. *J Cell Physiol.* 2008;214(2):316-321.

160. Zhu W, Soonpaa MH, Chen H, Shen W, Payne RM, Liechty EA, Caldwell RL, Shou W, Field LJ. Acute doxorubicin cardiotoxicity is associated with p53-induced inhibition of the mammalian target of rapamycin pathway. *Circulation.* 2009;119(1):99-106.

161. Zhang DH, Contu R, Latronico MVG, Zhang JAL, Rizzi R, Catalucci D, Miyamoto S, Huang K, Ceci M, Gu YS, Dalton ND, Peterson KL, Guan KL, Brown JH, Chen J, Sonenberg N, Condorelli G. MTORC1 regulates cardiac function and myocyte survival through 4E-BP1 inhibition in mice. *Journal of Clinical Investigation.* 2010;120(8):2805-2816.

162. Fujio Y, Nguyen T, Wencker D, Kitsis RN, Walsh K. Akt promotes survival of cardiomyocytes in vitro and protects against ischemia-reperfusion injury in mouse heart. *Circulation.* 2000;101(6):660-667.

163. Shioi T, McMullen JR, Kang PM, Douglas PS, Obata T, Franke TF, Cantley LC, Izumo S. Akt/protein kinase B promotes organ growth in transgenic mice. *Mol Cell Biol.* 2002;22(8):2799-2809.

164. Matsui T, Tao J, del Monte F, Lee KH, Li L, Picard M, Force TL, Franke TF, Hajjar RJ, Rosenzweig A. Akt activation preserves cardiac function and prevents injury after transient cardiac ischemia in vivo. *Circulation.* 2001;104(3):330-335.

165. Condorelli G, Drusco A, Stassi G, Bellacosa A, Roncarati R, Iaccarino G, Russo MA, Gu Y, Dalton N, Chung C, Latronico MV, Napoli C, Sadoshima J,

Croce CM, Ross J, Jr. Akt induces enhanced myocardial contractility and cell size in vivo in transgenic mice. *Proc Natl Acad Sci U S A.* 2002;99(19):12333-12338.

166. DeBosch B, Treskov I, Lupu TS, Weinheimer C, Kovacs A, Courtois M, Muslin AJ. Akt1 is required for physiological cardiac growth. *Circulation.* 2006;113(17):2097-2104.

167. Shiojima I, Walsh K. Regulation of cardiac growth and coronary angiogenesis by the Akt/PKB signaling pathway. *Genes Dev.* 2006;20(24):3347-3365.

168. Walsh K. Akt signaling and growth of the heart. *Circulation.* 2006;113(17):2032-2034.

169. Aoyama T, Matsui T, Novikov M, Park J, Hemmings B, Rosenzweig A. Serum and glucocorticoid-responsive kinase-1 regulates cardiomyocyte survival and hypertrophic response. *Circulation.* 2005;111(13):1652-1659.

170. Yang X, Cohen MV, Downey JM. Mechanism of cardioprotection by early ischemic preconditioning. *Cardiovasc Drugs Ther.* 2010;24(3):225-234.

171. Gurusamy N, Lekli I, Mukherjee S, Ray D, Ahsan MK, Gherghiceanu M, Popescu LM, Das DK. Cardioprotection by resveratrol: a novel mechanism via autophagy involving the mTORC2 pathway. *Cardiovasc Res.* 2010;86(1):103-112.

172. Gangloff YG, Mueller M, Dann SG, Svoboda P, Sticker M, Spetz JF, Um SH, Brown EJ, Cereghini S, Thomas G, Kozma SC. Disruption of the mouse mTOR gene leads to early postimplantation lethality and prohibits embryonic stem cell development. *Mol Cell Biol.* 2004;24(21):9508-9516.

173. Bentzinger CF, Romanino K, Cloetta D, Lin S, Mascarenhas JB, Oliveri F, Xia J, Casanova E, Costa CF, Brink M, Zorzato F, Hall MN, Ruegg MA. Skeletal muscle-specific ablation of raptor, but not of rictor, causes metabolic changes and results in muscle dystrophy. *Cell Metab.* 2008;8(5):411-424.

174. Kumar A, Harris TE, Keller SR, Choi KM, Magnuson MA, Lawrence JC, Jr. Muscle-specific deletion of rictor impairs insulin-stimulated glucose transport and enhances Basal glycogen synthase activity. *Mol Cell Biol.* 2008;28(1):61-70.

175. Polak P, Cybulski N, Feige JN, Auwerx J, Ruegg MA, Hall MN. Adipose-specific knockout of raptor results in lean mice with enhanced mitochondrial respiration. *Cell Metab.* 2008;8(5):399-410.

176. Cybulski N, Polak P, Auwerx J, Ruegg MA, Hall MN. mTOR complex 2 in adipose tissue negatively controls whole-body growth. *Proc Natl Acad Sci U S A.* 2009;106(24):9902-9907.

177. Kumar A, Lawrence JC, Jr., Jung DY, Ko HJ, Keller SR, Kim JK, Magnuson MA, Harris TE. Fat cell-specific ablation of rictor in mice impairs insulin-

regulated fat cell and whole-body glucose and lipid metabolism. *Diabetes.* 2010;59(6):1397-1406.

178. Dazert E, Hall MN. mTOR signaling in disease. *Curr Opin Cell Biol.* 2011.

179. Matsui T, Li L, Wu JC, Cook SA, Nagoshi T, Picard MH, Liao R, Rosenzweig A. Phenotypic spectrum caused by transgenic overexpression of activated Akt in the heart. *J Biol Chem.* 2002;277(25):22896-22901.

180. Shiojima I, Sato K, Izumiya Y, Schiekofer S, Ito M, Liao R, Colucci WS, Walsh K. Disruption of coordinated cardiac hypertrophy and angiogenesis contributes to the transition to heart failure. *J Clin Invest.* 2005;115(8):2108-2118.

181. Boluyt MO, Zheng JS, Younes A, Long X, O'Neill L, Silverman H, Lakatta EG, Crow MT. Rapamycin inhibits alpha 1-adrenergic receptor-stimulated cardiac myocyte hypertrophy but not activation of hypertrophy-associated genes. Evidence for involvement of p70 S6 kinase. *Circ Res.* 1997;81(2):176-186.

182. Schmelzle T, Hall MN. TOR, a central controller of cell growth. *Cell.* 2000;103(2):253-262.

183. Beretta L, Gingras AC, Svitkin YV, Hall MN, Sonenberg N. Rapamycin blocks the phosphorylation of 4E-BP1 and inhibits cap-dependent initiation of translation. *EMBO J.* 1996;15(3):658-664.

184. Sarbassov DD, Ali SM, Sabatini DM. Growing roles for the mTOR pathway. *Curr Opin Cell Biol.* 2005;17(6):596-603.

185. Choo AY, Yoon SO, Kim SG, Roux PP, Blenis J. Rapamycin differentially inhibits S6Ks and 4E-BP1 to mediate cell-type-specific repression of mRNA translation. *Proc Natl Acad Sci U S A.* 2008;105(45):17414-17419.

186. Sohal DS, Nghiem M, Crackower MA, Witt SA, Kimball TR, Tymitz KM, Penninger JM, Molkentin JD. Temporally regulated and tissue-specific gene manipulations in the adult and embryonic heart using a tamoxifen-inducible Cre protein. *Circ Res.* 2001;89(1):20-25.

187. Koitabashi N, Bedja D, Zaiman AL, Pinto YM, Zhang M, Gabrielson KL, Takimoto E, Kass DA. Avoidance of transient cardiomyopathy in cardiomyocyte-targeted tamoxifen-induced MerCreMer gene deletion models. *Circ Res.* 2009;105(1):12-15.

188. Taegtmeyer H. Energy metabolism of the heart: from basic concepts to clinical applications. *Curr Probl Cardiol.* 1994;19(2):59-113.

189. Stanley WC, Recchia FA, Lopaschuk GD. Myocardial substrate metabolism in the normal and failing heart. *Physiol Rev.* 2005;85(3):1093-1129.

190. Hall MN. mTOR-what does it do? *Transplant Proc.* 2008;40(10 Suppl):S5-8.

191. Huss JM, Torra IP, Staels B, Giguere V, Kelly DP. Estrogen-related receptor alpha directs peroxisome proliferator-activated receptor alpha signaling in the transcriptional control of energy metabolism in cardiac and skeletal muscle. *Mol Cell Biol.* 2004;24(20):9079-9091.

192. Campbell FM, Kozak R, Wagner A, Altarejos JY, Dyck JR, Belke DD, Severson DL, Kelly DP, Lopaschuk GD. A role for peroxisome proliferator-activated receptor alpha (PPARalpha ) in the control of cardiac malonyl-CoA levels: reduced fatty acid oxidation rates and increased glucose oxidation rates in the hearts of mice lacking PPARalpha are associated with higher concentrations of malonyl-CoA and reduced expression of malonyl-CoA decarboxylase. *J Biol Chem.* 2002;277(6):4098-4103.

193. Schieke SM, Phillips D, McCoy JP, Jr., Aponte AM, Shen RF, Balaban RS, Finkel T. The mammalian target of rapamycin (mTOR) pathway regulates mitochondrial oxygen consumption and oxidative capacity. *J Biol Chem.* 2006;281(37):27643-27652.

194. Sack MN, Rader TA, Park S, Bastin J, McCune SA, Kelly DP. Fatty acid oxidation enzyme gene expression is downregulated in the failing heart. *Circulation.* 1996;94(11):2837-2842.

195. Rosenblatt-Velin N, Montessuit C, Papageorgiou I, Terrand J, Lerch R. Postinfarction heart failure in rats is associated with upregulation of GLUT-1 and downregulation of genes of fatty acid metabolism. *Cardiovasc Res.* 2001;52(3):407-416.

196. Wright JJ, Kim J, Buchanan J, Boudina S, Sena S, Bakirtzi K, Ilkun O, Theobald HA, Cooksey RC, Kandror KV, Abel ED. Mechanisms for increased myocardial fatty acid utilization following short-term high-fat feeding. *Cardiovasc Res.* 2009;82(2):351-360.

197. Manning BD. Balancing Akt with S6K: implications for both metabolic diseases and tumorigenesis. *J Cell Biol.* 2004;167(3):399-403.

198. Krenz M, Robbins J. Impact of beta-myosin heavy chain expression on cardiac function during stress. *J Am Coll Cardiol.* 2004;44(12):2390-2397.

199. Fielitz J, Kim MS, Shelton JM, Latif S, Spencer JA, Glass DJ, Richardson JA, Bassel-Duby R, Olson EN. Myosin accumulation and striated muscle myopathy result from the loss of muscle RING finger 1 and 3. *J Clin Invest.* 2007;117(9):2486-2495.

200. Choo AY, Blenis J. Not all substrates are treated equally: implications for mTOR, rapamycin-resistance and cancer therapy. *Cell Cycle.* 2009;8(4):567-572.

201. Rockman HA, Wachhorst SP, Mao L, Ross J, Jr. ANG II receptor blockade prevents ventricular hypertrophy and ANF gene expression with pressure overload in mice. *Am J Physiol.* 1994;266(6 Pt 2):H2468-2475.

**202.** Blyszczuk P, Kania G, Dieterle T, Marty RR, Valaperti A, Berthonneche C, Pedrazzini T, Berger CT, Dirnhofer S, Matter CM, Penninger JM, Luscher TF, Eriksson U. Myeloid differentiation factor-88/interleukin-1 signaling controls cardiac fibrosis and heart failure progression in inflammatory dilated cardiomyopathy. *Circ Res.* 2009;105(9):912-920.

**203.** Pellieux C, Aasum E, Larsen TS, Montessuit C, Papageorgiou I, Pedrazzini T, Lerch R. Overexpression of angiotensinogen in the myocardium induces downregulation of the fatty acid oxidation pathway. *J Mol Cell Cardiol.* 2006;41(3):459-466.

**204.** How OJ, Aasum E, Severson DL, Chan WY, Essop MF, Larsen TS. Increased myocardial oxygen consumption reduces cardiac efficiency in diabetic mice. *Diabetes.* 2006;55(2):466-473.

**205.** Aasum E, Cooper M, Severson DL, Larsen TS. Effect of BM 17.0744, a PPARalpha ligand, on the metabolism of perfused hearts from control and diabetic mice. *Can J Physiol Pharmacol.* 2005;83(2):183-190.

**206.** Laplante M, Sabatini DM. mTOR signaling in growth control and disease. *Cell.* 2012;149(2):274-293.

**207.** Hagiwara A, Cornu M, Cybulski N, Polak P, Betz C, Trapani F, Terracciano L, Heim MH, Ruegg MA, Hall MN. Hepatic mTORC2 activates glycolysis and lipogenesis through Akt, glucokinase, and SREBP1c. *Cell Metab.* 2012;15(5):725-738.

**208.** Shende P, Plaisance I, Morandi C, Pellieux C, Berthonneche C, Zorzato F, Krishnan J, Lerch R, Hall MN, Ruegg MA, Pedrazzini T, Brink M. Cardiac raptor ablation impairs adaptive hypertrophy, alters metabolic gene expression, and causes heart failure in mice. *Circulation.* 2011;123(10):1073-1082.

**209.** Devereux RB, Casale PN, Kligfield P, Eisenberg RR, Miller D, Campo E, Alonso DR. Performance of primary and derived M-mode echocardiographic measurements for detection of left ventricular hypertrophy in necropsied subjects and in patients with systemic hypertension, mitral regurgitation and dilated cardiomyopathy. *Am J Cardiol.* 1986;57(15):1388-1393.

**210.** Hauselmann SP, Rosc-Schluter BI, Lorenz V, Plaisance I, Brink M, Pfister O, Kuster GM. beta1-Integrin is up-regulated via Rac1-dependent reactive oxygen species as part of the hypertrophic cardiomyocyte response. *Free Radic Biol Med.* 2011;51(3):609-618.

**211.** Nagata K, Liao R, Eberli FR, Satoh N, Chevalier B, Apstein CS, Suter TM. Early changes in excitation-contraction coupling: transition from compensated hypertrophy to failure in Dahl salt-sensitive rat myocytes. *Cardiovasc Res.* 1998;37(2):467-477.

212. Brink M, Erne P, de Gasparo M, Rogg H, Schmid A, Stulz P, Bullock G. Localization of the angiotensin II receptor subtypes in the human atrium. *J Mol Cell Cardiol.* 1996;28(8):1789-1799.

213. Costelli P, Almendro V, Figueras MT, Reffo P, Penna F, Aragno M, Mastrocola R, Boccuzzi G, Busquets S, Bonelli G, Lopez Soriano FJ, Argiles JM, Baccino FM. Modulations of the calcineurin/NF-AT pathway in skeletal muscle atrophy. *Biochim Biophys Acta.* 2007;1770(7):1028-1036.

214. Sussman MA, Volkers M, Fischer K, Bailey B, Cottage CT, Din S, Gude N, Avitabile D, Alvarez R, Sundararaman B, Quijada P, Mason M, Konstandin MH, Malhowski A, Cheng Z, Khan M, McGregor M. Myocardial AKT: the omnipresent nexus. *Physiol Rev.* 2011;91(3):1023-1070.

215. Chen W, Frangogiannis NG. The role of inflammatory and fibrogenic pathways in heart failure associated with aging. *Heart Fail Rev.* 2010;15(5):415-422.

216. Iadevaia V, Huo Y, Zhang Z, Foster LJ, Proud CG. Roles of the mammalian target of rapamycin, mTOR, in controlling ribosome biogenesis and protein synthesis. *Biochem Soc Trans.* 2012;40(1):168-172.

217. Thoreen CC, Chantranupong L, Keys HR, Wang T, Gray NS, Sabatini DM. A unifying model for mTORC1-mediated regulation of mRNA translation. *Nature.* 2012;485(7396):109-113.

218. Su B, Jacinto E. Mammalian TOR signaling to the AGC kinases. *Crit Rev Biochem Mol Biol.* 2011.

219. Liu QH, Molkentin JD. Protein kinase C alpha as a heart failure therapeutic target. *Journal of Molecular and Cellular Cardiology.* 2011;51(4):474-478.

220. Braz JC, Gregory K, Pathak A, Zhao W, Sahin B, Klevitsky R, Kimball TF, Lorenz JN, Nairn AC, Liggett SB, Bodi I, Wang S, Schwartz A, Lakatta EG, DePaoli-Roach AA, Robbins J, Hewett TE, Bibb JA, Westfall MV, Kranias EG, Molkentin JD. PKC-alpha regulates cardiac contractility and propensity toward heart failure. *Nat Med.* 2004;10(3):248-254.

221. Hahn HS, Marreez Y, Odley A, Sterbling A, Yussman MG, Hilty KC, Bodi I, Liggett SB, Schwartz A, Dorn GW, 2nd. Protein kinase Calpha negatively regulates systolic and diastolic function in pathological hypertrophy. *Circ Res.* 2003;93(11):1111-1119.

# **Acknowledgements**

# Acknowledgements

First of all, I am grateful to my supervisor Prof. Marijke Brink for giving the opportunity to carry out my PhD project in her lab. The project was really interesting and it was a great experience to work with Marijke as I learnt a lot from her. I am deeply indebted to Marijke for her constant encouragement and directional support all through my PhD.

I would like to express my sincere gratitude to Prof. Michael Hall for accepting to be the faculty supervisor for my dissertation. I thank him for his excellent advice and stimulating discussions despite his busy schedule. I want to thank Prof. Christophe Handschin for being the co-supervisor and for his suggestions during the course of PhD project. I would like to also deeply thank Prof. Markus Rüegg for the excellent collaboration and accepting to chair my PhD exam.

I am thankful to all the past and present members of the lab for keeping the lab environment enjoyable and most importantly supportive. I would like to thank especially Isabella Plaisance for her endless guidance in the beginning of my project. Special thanks to Christian Morandi for his excellent technical guidance and suggestions in the lab. I enjoyed a great amount of time with him while discussing on topics ranging from the great Indian culture to new Hollywood movies. I thank Lifen Xu for her great help with the mice work, and Laura Pentassuglia and Philip Heim for being supportive in the lab. I kindly appreciate the support that I got from Frederique Dubouloz, Silvia Meili-Burtz, Katherin Buheler, Vera Lorenz and especially, Stephanie Hauselmann for being a good friend during all these years.

The most important part of my life in Basel without whom my stay here was impossible, all my Dum-log friends including Kapil, Sudhir, Vijay, Vimal, Sanjay, Chanchal, Prasad, Varun, Satrajeet, Rishi, Pooja, Abhijeet, Manoj, Dheeraj, Kiran, and many more- their friendship meant to me a lot. I specially want to mention my

friend, my senior colleague Dr. Manjunath Joshi for his excellent advice and guidance, both in personal as well as in professional life.

Finally, I want to thank my family, my parents for their never-ending love and affection, especially my sisters for their constant support. Aba, I really miss you, "tumchya pathimbya-shivay he shakya navte". You have a lot to be proud of and I deeply thank you for your patience and understanding regardless of the long distance and few occasions that we managed to see each other. Last but not the least, I want to thank my love, for whom I was searching all these years and found her at the right time, my wife Madhuri. Thank you for being my friend and despite the distance and time we missed, you never faded away.

Pankaj

# Curriculum Vitae

## Pankaj S. Shende

Biozentrum, Klingelbergstrasse-50/70, Basel-4056, Switzerland
Email ID: pankaj.shende@unibas.ch

Educational qualifications:

2008-2012     **Ph.D. in Biomedicine (Cardiac Research)**
CardioBiology, Department of Biomedicine, University and university hospital Basel, Switzerland

2006-2007     **M.Sc. in Molecular Biology** with major in **Biotechnology**
University of Skovde, Sweden and Charite hospital, Berlin, Germany

2001-2005     **Bachelor of Pharmacy**,
Dr. D.Y. Patil Institute of Pharmaceutical Sciences, University of Pune, India

Publications:

1. **Shende, P**., Plaisance, I., Morandi, C., Pellieux, C., Berthonneche, C., Zorzato, F., Krishnan, J., Lerch, R., Hall, M.N., Ruegg, M.A., Pedrazzini, C. and Brink, M., Cardiac raptor ablation impairs adaptive hypertrophy, alters metabolic gene expression, and causes heart failure in mice. *Circulation* 123, 1073-1082, (2011), **IF 14.81** for 2010.

2. **Shende, P**., Xu, L., Morandi, C., Berthonneche, C., Pedrazzini, C. Kaufmann, B., Hall, M.N., Ruegg, M.A. and Brink, M., Rictor/mTORC2 regulates cardiac function under conditions of pressure overload but not during postnatal cardiac growth. (Ready for submission)

Awards & achievements:

- **Young Investigator Award** by the European Society of Cardiology, Annual meeting 2010, Stockholm, Sweden.

- Selected for Young Investigator **Spotlight interview**, *Circulation-European perspectives* for November 2010 issue.

- **Winner-poster prize** at annual meeting, Cardiovascular Biology and Clinical Implications meeting organized by Swiss-heart working group 2009, Murten, Switzerland.

Personal details:

- Date of Birth:       13th October 1983
- Gender:       Male
- Nationality:       Indian